

# Advanced Process Control and Relay Auto-tuning

RAIHANA FERDOUS

NATIONAL UNIVERSITY OF SINGAPORE

2005

# Advanced Process Control and Relay Auto-tuning

RAIHANA FERDOUS

A THESIS SUBMITTED  
FOR THE DEGREE OF DOCTOR OF PHILOSOPHY  
DEPARTMENT OF ELECTRICAL AND COMPUTER  
ENGINEERING  
NATIONAL UNIVERSITY OF SINGAPORE

2005

# Acknowledgments

During my years as a PhD student in National University of Singapore, I have benefited from interactions with many people for which I am deeply grateful. Among them firstly and mostly, I wish to express my utmost gratitude to my supervisor, Associate Professor Tan Kok Kiong for his astute guidance and encouragement in both the professional and personal aspects of my life. Without him, I would not have been able to complete this thesis so smoothly. Professor Tan's successive and endless enthusiasm in research arouse my interest in various aspects of control engineering. I have indeed benefited tremendously from all the discussions with him.

As a graduate student under Professor Tan, I have enjoyed the privilege of working with some of the finest colleagues in Mechatronics and Automation Laboratory. In particular, I have enjoyed many helpful discussions with Tang Kok Zuea, Tan Chee Siong, Goh Han Leong, Teo Chek Sing, Zhu Zhan, Zhao Shao and Dr. Huang Sunan. There were also many informal discussions with them which were very beneficial to me. All these while, they have made my postgraduate studies in NUS become an unforgettable and enjoyable experience. The second chapter of this thesis is a joint work with Chua Kok Yong, who is currently a PhD student under Professor Tan. I would like to express my utmost appreciation to him.

I would also like to thank my parents for their love and concern for me. Specially, I wish to express my deep appreciation to my husband Shaheen and daughter Samiha for their unconditional support, love and understanding all these moments. Finally, I would like to thank almighty Allah for everything !

# Summary

Process control industry has advanced in tandem with different advanced control technology, responding to the requirements from the control engineers. Advanced control schemes are necessary in many industrial control problems although the PID control remains a control strategy that has been successfully used over the years. Simplicity in use, robustness, a wide range of applicability and near-optimal achievable performance are some of the factors that have made PID control so attractive in both the academic and industry sectors. Automatic tuning and adaptation of PID controllers have been successfully applied to industrial process control systems in recent years. A particularly interesting technique in the automatic tuning of PID controllers is due to Astrom and co-workers who successfully used a relay feedback technique in the development of the so-called *auto-tuner* for the PID controller. Motivated by the Astrom and co-workers, in this thesis, particular attention is devoted to the relay feedback method and its application to several advanced control fields, such as identification of process critical point with an improved accuracy, assessment of robustness in the frequency domain, controller tuning method based on the assessment and finally for the control of nonlinear plant.

From the simplicity and practical viewpoints, this thesis has contributed to improve the original relay feedback method. Today, the use of the relay feedback technique for estimation of the critical point has been widely adopted in the process control industry. To this extent, the conventional relay feedback method is modified which expands the application scope of the conventional technique to the various fields of process control industries. In this thesis, a new technique is proposed to automatically estimate the critical point of a process frequency response. The method yields significantly and consistently improved accuracy over the relay feedback method, pioneered by Astrom and co-workers, at no significant incremental costs in terms of implementation resources and application complexities. The

proposed technique improves the accuracy of the conventional approach by boosting the fundamental frequency in the forced oscillations, using a preload relay which comprises of a normal relay in parallel with a gain. In addition, the new technique will show empirically the other benefits of the proposed method in terms of the extended classes of processes to which the method remains applicable, and the shorter time duration to attain stationary oscillations.

Robustness is one of the major design objective to achieve for control systems functioning under harsh practical conditions. In the frequency domain, the maximum sensitivity and stability margins provide assessment of the robustness of a compensated system. In this thesis, the basic relay feedback approach is modified for the assessment of robustness in control systems. The modification is done by adding a time delay element in series with the relay. The amount of time delay is swept over a range to automatically generate a number of sustained oscillations. From these oscillations, a systematic set of procedures is developed to yield estimates of the maximum sensitivity and stability margins. It is observed, in many cases, that the maximum sensitivity and stability margins of the compensated system may be unsatisfactory and, some means to automatically retune the controller would be necessary and useful. In this thesis, an approach for the design of the PI controller is proposed also to concurrently satisfy user specifications in terms of maximum sensitivity and stability margins.

Conventional controllers like PID and many advanced control method are useful to control linear processes. In practice, most processes are nonlinear and using only PID controller, it is very difficult to control a plant which is nonlinear to give good performance. In view of this, the thesis proposed two approaches for the tuning of PID controller for nonlinear system using relay feedback approach. The relay continues to be used in the control configuration, but in a new different way.

The results presented in the thesis have very practical values as well as sound theoretical contributions. This is evidenced by numerous simulation examples and successful results from the real-time experiments conducted

# Contents

<b>Acknowledgments</b>	<b>i</b>
<b>Summary</b>	<b>iv</b>
<b>1 Introduction</b>	<b>1</b>
1.1 Evolution of Advance Control System . . . . .	1
1.2 PID Control . . . . .	3
1.3 Advanced Process Control Using a Relay Feedback Approach . . . . .	4
1.3.1 Process identification . . . . .	7
1.3.2 Performance assessment . . . . .	8
1.3.3 Extension to nonlinear system . . . . .	9
1.4 Contributions . . . . .	11
1.5 Outline of Thesis . . . . .	14
<b>2 Preload Relay for Improved Critical Point Identification and PID Tuning</b>	<b>17</b>

2.1	Introduction . . . . .	17
2.2	Conventional Relay Feedback Technique . . . . .	19
2.3	Problems associated with conventional relay feedback estimation . . . . .	23
2.4	Preload relay feedback estimation technique . . . . .	24
2.4.1	Amplification of the fundamental oscillation frequency . . . . .	25
2.4.2	Choice of amplification factor . . . . .	26
2.5	Simulation Examples . . . . .	28
2.6	Real-time Experimental Results . . . . .	29
2.7	Additional benefits associated with the preload relay approach . . . . .	31
2.7.1	Control performance relative to specifications . . . . .	32
2.7.2	Improved robustness assessment . . . . .	34
2.7.3	Applicability to unstable processes . . . . .	37
2.7.4	Improvement in convergence rate . . . . .	41
2.7.5	Identification of other intersection points . . . . .	45
2.7.6	Comparison with another modified relay-based technique . . . . .	47
2.8	Conclusions . . . . .	48
<b>3</b>	<b>Robustness Assessment and Control Design Using a Relay Feedback Approach</b>	<b>49</b>
3.1	Introduction . . . . .	49



3.2	Control Robustness Assessment . . . . .	51
3.2.1	Maximum sensitivity . . . . .	52
3.2.2	Construction of $\lambda - \phi$ chart . . . . .	54
3.2.3	Stability margins assessment . . . . .	56
3.2.4	Simulation example . . . . .	58
3.3	Assessment Accuracy . . . . .	59
3.4	PI Control Design Based on Specifications of Maximum Sensitivity and Stability Margins . . . . .	60
3.4.1	Robust control design . . . . .	61
3.4.2	Simulation examples . . . . .	64
3.4.3	Meeting specifications . . . . .	67
3.5	Real-time Experiment . . . . .	69
3.6	Online Assessment . . . . .	70
3.6.1	Simulation example . . . . .	72
3.6.2	Assessment Accuracy . . . . .	74
3.7	Improved Robustness Assessment Using a Preload Relay . . . . .	75
3.8	Conclusion . . . . .	77
<b>4</b>	<b>Robust Control of Nonlinear Systems Using a Preload Relay</b>	<b>78</b>
4.1	Introduction . . . . .	78

4.2	Proposed Control Scheme . . . . .	81
4.2.1	PID control . . . . .	82
4.2.2	Preload relay . . . . .	83
4.3	Self-tuning PID Control . . . . .	83
4.3.1	Prototype frequency response approach . . . . .	84
4.3.2	Parametric approach . . . . .	85
4.4	Properties of Control Scheme . . . . .	87
4.5	Robustness Analysis . . . . .	90
4.6	Simulation Study . . . . .	94
4.6.1	Performance with different gain settings . . . . .	95
4.6.2	Comparison with a fixed PID controller . . . . .	97
4.7	Real-time Experiment . . . . .	98
4.8	Conclusion . . . . .	101
<b>5</b>	<b>Automatic Tuning of PID Controller for Nonlinear Systems</b>	<b>106</b>
5.1	Introduction . . . . .	106
5.2	Robustness Analysis . . . . .	107
5.3	Automatic Tuning of an Equivalent PID Controller . . . . .	111
5.4	Simulation Study . . . . .	113

5.5	Real-time Experiment . . . . .	115
5.6	Conclusion . . . . .	116
<b>6</b>	<b>Conclusions</b>	<b>120</b>
6.1	General Conclusions . . . . .	120
6.2	Suggestions for Further Work . . . . .	122
<b>A</b>	<b>AUTHOR'S PUBLICATIONS</b>	<b>131</b>

# List of Figures

2.1	Conventional relay feedback system. . . . .	20
2.2	Hysteretic relay. . . . .	22
2.3	Negative inverse describing function of the hysteretic relay. . . . .	23
2.4	Proposed configuration of P_Relay feedback system. . . . .	25
2.5	Negative inverse describing function of the P_Relay. . . . .	26
2.6	Limit cycle oscillation for different choice of $\alpha$ , (1) $\alpha = 0$ , conventional relay, (2) $\alpha = 0.2$ , (3) $\alpha = 0.3$ . . . . .	27
2.7	PE variation of $K_c$ with $\alpha$ . . . . .	33
2.8	PE variation of $\omega_c$ with $\alpha$ . . . . .	34
2.9	Photograph of experimental set-up. . . . .	35
2.10	Relay configuration for robustness assessment . . . . .	36
2.11	Relay tuning and control performance for a first-order unstable plant, (1)P_Relay feedback method, (2) Conventional relay feedback method. . . . .	38

2.12	Limit cycle oscillation for process $G_p = \frac{1}{(10s-1)}e^{-8s}$ using the P_Relay feedback method. . . . .	40
2.13	Limit cycle oscillation using (1) P_Relay, (2) conventional relay . . . . .	42
2.14	Limit cycle oscillation using (1) P_Relay, (2) conventional relay . . . . .	43
2.15	Nyquist plot of the process $G_p = \frac{s+0.2}{s^2+s+1}e^{-10s}$ , (1) critical point, (2) outermost point . . . . .	46
2.16	Nyquist plot of the process $G_p = \frac{s+0.2}{(s+1)^2}e^{-10s}$ , (1) critical point, (2) outermost point . . . . .	47
3.1	Feedback control system. . . . .	51
3.2	Definition of $M_s$ . . . . .	52
3.3	Relationship between $G_{ol}(j\omega_i)$ and $\lambda(\omega_i)$ . . . . .	53
3.4	Typical plot of $\lambda$ versus $\phi$ . . . . .	54
3.5	Proposed modified relay configuration. . . . .	55
3.6	Definition of $G_m$ and $\phi_m$ . . . . .	57
3.7	Identification of $G_m$ and $\phi_m$ from the $\lambda - \phi$ plot. . . . .	58
3.8	Identification of $M_s$ and stability margins for a high order system. . . . .	59
3.9	A plot of $ \lambda  - \phi$ for example 1. . . . .	66
3.10	Plot of $ \lambda  - \phi$ and $ \tilde{\lambda}  - \phi$ ; example 1. . . . .	67
3.11	Closed-loop response using the proposed tuning method; example 1. . . . .	67

3.12	Closed-loop response (1) proposed method, (2) Wang's method; example 2.	68
3.13	Identification of $M_s$ and the stability margins from the real-time experiment.	70
3.14	Plot of $ \lambda  - \phi$ and $ \tilde{\lambda}  - \phi$ ; real-time experiment. . . . .	71
3.15	Closed-loop response (1) before tuning, (2) after tuning; real-time experiment.	72
3.16	Online assessment . . . . .	73
3.17	Identification of $M_s$ and stability margins for a high order system. . . . .	74
3.18	Preload relay configuration for improved robustness assessment . . . . .	75
4.1	Schematic of the proposed control scheme. . . . .	81
4.2	Equivalent form of the proposed control scheme. . . . .	82
4.3	Variation of amplitude margin with $K$ . . . . .	90
4.4	Spherical tank. . . . .	96
4.5	Closed-loop performance based on proposed control system with $K = 0$ . . .	97
4.6	Amplified closed-loop performance based on proposed control system with $K = 0$ . . . . .	98
4.7	Closed-loop performance based on proposed control system with $K = 2$ . . .	99
4.8	Closed-loop performance based on proposed control system with $K = -2$ . .	100
4.9	Closed-loop performance based on a fixed PID setting. . . . .	101
4.10	Comparison of closed-loop performance (1) fixed gains PID controller, (2) proposed control system. . . . .	102

4.11	Schematic of the experiment setup of the spherical tank system. . . . .	102
4.12	Experimental setup. . . . .	103
4.13	Experimental result based on proposed control system with $K = 0$ . . . . .	103
4.14	Experimental result based on proposed control system with $K = 1$ . . . . .	104
4.15	Experimental result based on proposed control system with $K = -1$ . . . . .	104
4.16	Experimental result based on a fixed PID setting . . . . .	105
5.1	Configuration of the robust control scheme. . . . .	108
5.2	Equivalent PID controller. . . . .	112
5.3	Simulation results (a) control signal and (b) closed-loop performance (1) PID-Relay controller, (2) equivalent PID controller. . . . .	114
5.4	Simulation results (a) control signal (b) closed-loop performance at different operating level of the tank using the equivalent PID controller. . . . .	115
5.5	Closed-loop performance under the influence of measurement noise. . . . .	116
5.6	Closed-loop performance based on a fixed PID setting. . . . .	117
5.7	Comparison of closed-loop performance (1) fixed PID controller, (2) pro- posed control system. . . . .	117
5.8	Experimental result at different operating level of the tank using the PID- relay controller. . . . .	118
5.9	Experimental result at different operating level of the tank using the pro- posed equivalent PID controller. . . . .	118

5.10 Experimental result based on a fixed PID setting. . . . .	119
--	-----



# Chapter 1

## Introduction

The requirements of a control system may include many factors such as response to command signals, insensitivity to measurement noise and process variation, and rejection of load disturbances. The design of a control system also involves aspects of process dynamics, actuator saturation, and disturbance characteristics. Increased demand for process control has paved the way for advanced control solutions that can automatically and continuously adjust process controllers parameters on-line. In the past, the control of processes have relied on the expertise of operators who would periodically monitor by visual inspection of the product. These past methods are inadequate in today's demand for process control industries.

### 1.1 Evolution of Advance Control System

Advanced control methods have been proven to be more beneficial and profitable than elementary control methods although the PID control remains a control strategy that has been successfully used over the years [1]. Some claimed that applying advanced control

has resulted in cost savings or product quality improvements from 2% to 10%. As a class of control methods, advanced control is rather vague - not because of the large number of methods that can be included, but because of the indistinct classification criteria. The historical background that explains the variety of control methods that are today considered “advanced”, all started 60 years ago with simple but efficient PID control. Any method that evolved from PID control was considered as “advanced control” at the beginning of its invention.

Fundamentally, advanced control does not differ from any other control strategy in the sense that it is also based on feedback control. Yet, it is the intelligence behind advanced control that makes the difference when compared to conventional controllers. Typically, advanced control methods involve more complex calculations than the conventional PID controller algorithm. In short, it can be described by the following features:

- Process modelling and parameter identification (off-line or on-line);
- Prediction of process behavior using process model;
- Evaluation of performance criterion subject to process constraints;
- Optimization of performance criterion;
- Matrix calculations (multivariable control); and
- Feedback control

Often, advanced control is a high-level control procedure that takes care of subprocesses controlling low level unit control loops such as PID controllers. In this case, advanced control strategy aims to fulfill economic objectives by providing appropriate set points for the lower-level control loops to minimize a given performance criterion.

## 1.2 PID Control

Although advanced control schemes are necessary in many industrial control problems but the PID control remains a control strategy that has been successfully used over the years. Simplicity in use, robustness, a wide range of applicability and near-optimal achievable performance are some of the factors that have made PID control so attractive in both the academic and industry sectors. Despite the rapid evaluation in control hardware over past 60 years, the PID controller remains the workhorse in the process industries. It began with pneumatic control, through direct digital control to the distributed control system (DCS). Typically, logic function block, selector and sequence are combined with the PID controllers. Many sophisticated regulatory control strategies, override control, start-up and shut-down strategies can be designed around the classical PID control. The computing power of microprocessors provides additional features such as automatic tuning, gain scheduling and model switching to the PID controller. A lot of research work has been put into giving a higher level of operational autonomy to PID controllers. Many of these research works have already been translated into new and useful functions of industrial control products, such as those which enable automatic tuning and continuous retuning of PID control parameters. These features have been instrumental in reducing the reliance on long and tedious manual tuning procedures, thereby achieving cost savings in terms of manpower and product quality, and contributing to overall higher productivity in modern manufacturing and automation systems.

However, new possibilities and functionalities have become possible with a microprocessor-driven PID controller. Modern process controllers often contain much more than just the basic PID algorithm. Fault diagnosis, alarm handling, signals scaling, choice of type of output signal, filtering, simple logical and arithmetic operations are becoming common

functions to be expected in modern PID controllers. The physical size of the controller has shrunk significantly compared to the analog predecessors, and yet the functions and performance have greatly increased. Furthermore, riding on the advances in adaptive control and techniques, the modern PID controllers are becoming intelligent. Many high-end controllers are appearing in the market equipped with auto-tuning and self-tuning features. No longer is tedious manual tuning an inevitable part of process control. The role of operators in PID tuning has been very much reduced to simple specifications and decisions.

Different systematic methods for tuning of PID controllers are available. Regardless of the design method, the following three phases are applicable:

- The process is disturbed with specific control inputs or control inputs automatically generated in closed-loop.
- The response to the disturbance is analysed, yielding a model of the process which may be in a non-parametric or parametric form.
- Based on this model and certain operational specifications, the control parameters are determined.

### **1.3 Advanced Process Control Using a Relay Feedback Approach**

An interesting experiment for process frequency response analysis is the relay feedback system, first pioneered by Astrom and co-workers [1], who successfully used a relay feedback technique in the development of the so-called *auto-tuner* for the PID controller. This method has been subject of much interests in recent years and it has been field tested in a

wide range of applications. Actually, relay feedback is a classical configuration. The classical work by Weiss [2] and Tsypkin [3] was motivated by relays that were used as power amplifiers. The interest for relay systems has increased dramatically during the last few years after the successful application of Astrom's PID auto-tuner in process control. After Astrom's inaugural application of the method to tune simple three-term PID controllers, relay auto-tuning of controllers has been actively researched and since then, the method has been extended to advanced controllers such as the cascade controllers [4], Smith-predictor control [5], finite spectrum assignment controller [6], multiloop controllers [7], autotuning of full multivariable controllers for multivariable processes [8] etc. It has also been incorporated in knowledge-based and intelligent systems as integrated initialization and tuning modules [9], [10].

The main attraction of the pioneer method appears to be the viability of automation on a large scale for control tuning and this is particularly useful for the process control industry where the number of control loops in the order of several hundreds and thousands is commonly encountered. The another main features of the relay autotuning method, which probably accounts for its success more than any other associated features, is that it is a closed-loop method and therefore an on-off regulation of the process may be maintained even when the relay experiment is being conducted. However, the approach has several important practical constraints related to the structure which have remained, in large proportion, unresolved to-date. First, it has a sensitivity problem in the presence of disturbance signals, which may be real process perturbation signals or equivalent ones arising from varying process dynamics, nonlinearities and uncertainties present in the process. For small and constant disturbances, given that stationary conditions are known, an iterative solution has been proposed, essentially by adjusting the relay bias until symmetrical limit cycle oscillations are obtained. However, for general disturbance signals, there has been no effective solution to-date. Secondly, relating partly to the first problem, relay tuning

may only begin after stationary conditions are reached in the input and output signals, so that the relay switching levels may be determined with respect to these conditions and the static gain of the process. In practice, under open-loop conditions, it is difficult to determine when these conditions are satisfied, and therefore, when the relay experiment may begin. Thirdly, the relay autotuning method is not applicable to certain classes of processes which are not relay-stabilizable, such as the double integrator, runaway processes and some classes of unstable processes. For these processes, relay feedback is not able to effectively induce stable limit cycle oscillations. Finally, the basic relay method is an off-line tuning method, i.e. some information on the process is first extracted with the process under relay feedback and detached from the controller. The information is subsequently used to commission the controller. Off-line tuning has associated implications in the tuning-control transfer, affecting operational process regulation which may not be acceptable for certain critical applications. Indeed, in certain key process control areas (e.g. vacuum control, environment control, etc.) directly affecting downstream processes, it may be just too expensive or dangerous for the control loop to be broken for tuning purposes, and tuning under tight continuous closed-loop control (not the on-off type) is necessary. In particular, with the process model obtained, simple tuning rules should be developed which will only require the engineer to specify simple desired closed-loop properties.

Following the successful demonstration of the relay autotuning method in field tests and subsequent true industrial applications [11], there have been numerous attempts to improve on various aspects of the basic method [12], [13]. However, from simplicity and practicality viewpoints, it has remained to be seen whether a better configuration of the original recipe has been yet in place after these years. In this thesis, the basic relay feedback is modified which expand the application scope of the conventional technique to the various fields of process control industries, such as; critical point estimation, identification of robustness parameters and tuning of PID controller, and finally the method is also extended for the

nonlinear systems.

### 1.3.1 Process identification

While the relay feedback experiment design will yield sufficiently accurate results for many of the processes encountered in the process control industry, there are some potential problems associated with such techniques. These arise as a result of the approximations used in the development of the procedures for estimating the critical point, i.e. the ultimate frequency and ultimate gain. In particular, the basis of most existing relay-based procedures for critical point estimation is the describing function (DF) method. This method is approximate in nature, and under certain circumstances, the existing relay-based procedures could result in estimates of the critical point that are significantly different from their real values. Such problematic circumstances arise particularly in underdamped processes and processes with significant dead-time, and poorly tuned control loops would result if the critical point estimates were used for controller tuning. Many research works on modifying the relay feedback auto-tuning method have been reported in recent years. Improvement of the relay identification accuracy and efficiency have been proposed [14]-[16] by reducing high-order harmonic terms or using the Fourier analysis instead of the describing function method. The PID tuning formulae are refined to improve the controller performance for diverse processes such as long deadtime processes and oscillatory processes [17], [18]. An adaptive approach has been proposed by Lee et al. (1995) [14] to achieve near zero error in the estimation of the critical point. However, the improved accuracy is achieved at the expense of a more complicated implementation procedure over the basic relay method. The additional implementation cost may pose an obstacle to the acceptance of the improved method, since one key reason for the success of the relay feedback method in industrial applications has been the simple and direct approach it has adopted. Other known con-

straints of the conventional relay feedback method include inapplicability to certain classes of processes, and a long time duration to settle to stationary oscillations in some cases.

### 1.3.2 Performance assessment

More sophisticated control algorithms will produce better performance when fitted to a specific process, but poor performance results if the process changes. This sensitivity to process changes is called robustness, with more robust being less sensitive. The PID algorithm is an excellent trade-off between robustness and performance. Apart from control tuning, the relay feedback approach can also be used for control performance assessment purposes. Since the first systematic study on control loop performance assessment by Harris [19], it has now been widely recognized that performance assessment is very important in process industry. Research on control loop performance assessment has attracted significant interests from both academic and industry over the last 10 years. Many notable contributions can be found from, for example [20]–[22] and many others. From a pragmatic point of view, robustness problem in control systems can be considered as being consisted of two closely related aspects: stability robustness and performance robustness [21], with each focusing on a different side of the robustness problem. However, the two aspects of robustness issues are intrinsically related. It is intuitive that inevitably performance will be severely degraded before the closed-loop system goes to instability, if the plant is perturbed in a somewhat continuous way.

Maximum sensitivity ( $M_s$ ) fulfills the main requirements of a good design parameter for performance robustness. By imposing a bound on the maximum sensitivity, typically in the range from 1.3 to 2.0 [23], a satisfactory level of closed-loop performance can be achieved. Several PID tuning rules have been established, where the maximum sensitivity is used as a design parameter ([24]; [25]). On the other hand, stability margins in the specific forms



of gain and phase margins are traditional indicators of stability robustness. They have also been widely used as design specifications for the design of PID controllers ([26]; [27]). However, these two attributes of robustness (performance robustness and stability robustness) are intrinsically relevant, and to certain applications, they may be equally important, so that concurrent requirements, in terms of some fundamental levels of maximum sensitivity and stability margins, are necessary. If these parameters are assessed to be unsatisfactory, some means to automatically retune the controller would be necessary and useful.

### **1.3.3 Extension to nonlinear system**

It is already mentioned that the PID algorithm has been successfully used in the process industries since 1940s and remain the most often used algorithm today. But one of its major drawback is that the PID controller is a linear controller and it alone does not provide robust performance for nonlinear plants in some cases. All the physical systems are nonlinear and have time-varying parameters to some degree. Whether the nonlinearity is undesirable or intended, the objective of nonlinear analysis is to predict the behavior of the system. Linear analysis inherently cannot predict those features of behavior that are characteristics of nonlinear systems. While many PID controller design techniques for linear systems have been used extensively [1], there is no recognized, general nonlinear control theory that has been successfully and consistently applied in the process industry [28]. Control systems based on these linear methods are generally successful in the process industries because, (1) the control system maintains the process in a small range of operating variables, (2) many processes are not highly nonlinear, and (3) most control algorithms and designs are not sensitive to reasonable ( $\pm 20\%$ ) model errors due to nonlinearities. These three conditions are satisfied for many processes, but in certain cases, they are not satisfied.

For nonlinear systems, many have researched on adaptive control methods. However, its application is much more complicated than a fixed gain regulator, due to its inherent nonlinear characteristics. Many practical issues in the control environment make it difficult to satisfy the pre-requisites for an effective application of adaptive control, thus yielding results which are far from satisfactory, and in many cases, worse than that achievable by the good old PID control. This is despite the more significant effort and resources used in the implementation of adaptive control. A gain scheduling and robust high gain control should thus be considered as alternatives to adaptive control algorithms [29], [30]. Thus various approaches for tuning the PID controller for nonlinear systems have been proposed [31]-[34]. Relay-based tuning methods allow controller tuning to be done in closed loop. Using relay feedback, the process dynamics can be determined in several different ways. For robust control of nonlinear systems, a variable structure control scheme is usually necessary. While simple to use, this scheme induces chattering which is usually considered undesirable from a practical point of view. The amount of chattering can be reduced by a modification of the switching surface to include a hysteresis. Astrom [34], introduced a self-oscillating adaptive system (SOAS) using a relay for nonlinear systems. The idea of SOAS originated in work at Honeywell on adaptive flight control in the late 1950s. The inspiration came from work on nonlinear systems by Flugge-Lotze at Stanford Systems based on the idea were flight-tested in the F-94C, the F-101, and the X-15 aircraft. The idea has also been applied in process control, but the applicability of SOAS has been limited since it generates limit cycles which are acceptable only in particular applications. In [33], a modified SOAS, named Smooth Sliding Controller (SSC) was proposed to eliminate the limit cycle. Motivated by Astrom [34], the thesis presents two methods for the tuning of PID controller for nonlinear system using relay feedback approach. The relay continues to be used in the control configuration, but in a new different way. Chattering signal has introduced itself as a desirable feature and it is used as a naturally occurring signal for tuning and re-tuning the

PID controller as the operating regime digresses. No other explicit input signal is required for these new methods.

## 1.4 Contributions

The results from the thesis are useful as suitable modules within an advanced process controller described in Section 1.1. In particular, the thesis has investigated and contributed to the following main areas :

### **Preload Relay for Improved Critical Point Identification and PID Tuning**

This thesis provides, a new preload relay (abbreviated as P\_Relay) feedback technique to be applied to the process in the same manner as per the conventional relay feedback configuration. The method achieves improved estimation accuracy by boosting the fundamental frequency in a relay feedback loop via an additional gain. This allows the fundamental assumption of the relay estimation method to be better satisfied, and therefore deriving an estimate that is closer to the true value. As a result of a better estimate, the control and assessment performance which is based on this estimate is correspondingly enhanced as well. Apart from this primary objective, there are other benefits which can be achieved with regards to applicability to other classes of process when the present relay method fails, a shortened time to achieve stationary oscillations, and versatility to identify other points of the process frequency response. All these benefits are to be achieved at no further significant complexities over the present relay method.

### **Robustness Assessment and Control Design Using a Relay Feedback Approach**

The assessment of maximum sensitivity and stability margins of a control system usu-

ally requires a lengthy non-parametric frequency response identification. Motivated by the relay feedback method pioneered by Astrom [1] to efficiently identify key process parameters for the tuning of PID controllers, this thesis explores the use of a relay-type apparatus to automatically identify these robustness indicators from a control system. The experiment is a more elaborate one than the basic relay experiment to identify one critical point for PID tuning, since more information is clearly necessary for such an assessment. The apparatus uses a relay in series with a time delay element. The amount of time delay is swept over a range, generating a series of sustained oscillations. Based on the amplitude and frequency of the oscillations, a chart of the proximity (to the critical point) versus phase can be systematically plotted. The maximum sensitivity and stability margins can be directly identified from the chart. If these parameters are assessed to be unsatisfactory, some means to automatically retune the controller would be necessary and useful. In this thesis, an approach for the design of the PI controller is proposed also to concurrently satisfy user specifications in terms of maximum sensitivity and stability margins. Guidelines are given, in the chapter, to assist the user to select generally satisfactory parameters to meet robust design objectives. The PI control parameters are then obtained, via the minimization of objective functions, so that the robustness specifications can be met as closely as possible. A simulation study on commonly encountered processes and real-time experiment results are shown in the thesis to prove the effectiveness of the proposed design scheme.

### **Robust Control of Nonlinear Systems Using a Preload Relay**

In this thesis, a novel high gain feedback control system is provided, involving the use of a P-Relay) in series with the usual PID controller, for robust control of nonlinear systems which are possibly also time varying. The proposed system may be viewed as an extended and a more general form of the self-oscillating adaptive system (SOAS) first used

by Honeywell [34], in the flight control systems. The proposed control system, retains and extends on the nice stability property of the SOAS. The amplitude margin of two can still be achieved, and it is now adjustable so that a higher or lower closed-loop amplitude margin can be set via the proportional part of the preload relay, depending on the requirements. The chattering phenomenon is still inherently evident since a relay continues to be used in the control configuration. However, instead of viewing it as an undesirable feature, the chattering information is used to tune and re-tune the PID controller, as the operating regime digresses. The chattering signals are naturally occurring, thus no further explicit test signals are required. The PID gains will therefore change from one setpoint to another, exactly as an efficient gain scheduler with a very fine tabulation resolution will work, yet the gain adaptation will continue to take place, as long as the chattering exists. Thus, the method is applicable to time varying systems as well. Once the PID control is tuned to a new operating point, the relay part of the control system can be switched off and the chattering will cease consequently. It can be invoked again when another change in setpoint is initiated.

### **Automatic Tuning of PID Controller for Nonlinear Systems**

In the previous case, the controller comprises of PID controller with a preload relay. For the present case a robust control system, involving the use of a relay in parallel with a PID controller is proposed in this thesis, to provide a high gain feedback system which may be used for the robust control of nonlinear systems. The configuration may be viewed as PID control augmented with a sliding mode. The chattering signals, incurred as a consequence of the relay, are used in a recursive least squares (RLS) algorithm to autotune an equivalent robust PID controller which may then replace the parallel PID-Relay construct. The relay may be re-invoked for re-tuning purposes following changes in set-points or changes in the time-varying system dynamics, similar to the way an auto-tuning relay is used [34]. Ro-

bustness analysis will be provided in the thesis to illustrate the robust stability properties of the control scheme. Simulation and experimental results are provided to illustrate the effectiveness of the proposed control scheme when applied to the level control of fluid in a spherical tank.

## 1.5 Outline of Thesis

The thesis is organized as follows.

Chapter 2 presents a new technique to automatically estimate the critical point of a process frequency response. The technique proposed in the chapter improves the accuracy of the conventional relay feedback method, pioneered by Astrom and co-workers by boosting the fundamental frequency in the forced oscillations, using a preload relay which comprises a normal relay with a parallel gain. In addition, the chapter shows empirically the other benefits of the proposed approach in terms of the extended classes of processes to which the method remains applicable, and the shorter time duration to attain stationary oscillations. Simulation results on a variety classes of processes available in the process control industry is presented and a real-time experimental result in the critical point estimation of a coupled-tanks system is presented as well.

Chapter 3 proposes, a relay feedback approach for the assessment of robustness in control systems. The approach uses a relay in series with a time delay element, where the amount of time delay is swept over a range to automatically generate a number of sustained oscillations. From these oscillations, a systematic set of procedures is developed to yield estimates of the maximum sensitivity and stability margins. Following the identification of robustness parameters, the chapter also proposes the design of PI control based on specifications of maximum sensitivity and stability margins. The PI controller is tuned in such a way

that the desired and improved specifications can be met closely. Guidelines are given for a set of generally satisfactory specifications. The PI control parameters are obtained via the minimization of objective functions which are derived to fit these robustness characteristics of the compensated system as closely as possible to the user specifications. Simulation examples and results from a real-time experiment will show the effectiveness and assessment accuracy of the proposed approach.

Chapter 4 is focused on the development of the new robust self-tuning PID controller suitable for nonlinear systems. The control system employs a preload relay (P\_Relay) in series with a PID controller. The P\_Relay ensures a high gain to yield a robust performance. However, it also incurs a chattering phenomenon. In this chapter the chattering signal is viewed not as an undesirable yet inevitable feature rather than as a naturally occurring signal for tuning and re-tuning the PID controller as the operating point changes. No input signal is required as all the necessary information is available from the chattering signal. Once the PID controller is tuned for a particular operating point, the relay may be disabled and chattering ceases correspondingly. However, it is invoked when there is a change in setpoint to another operating regime. In this way, the approach is also applicable to time-varying systems as the PID tuning can be continuous, based on the latest set of chattering characteristics. Analysis is provided on the stability properties of the control scheme. Simulation and real-time experimental results are presented for the level control of fluid in a spherical tank using the proposed scheme.

In chapter 5, a robust control system is first proposed which is suitable for the control of a class of nonlinear systems. A parallel connection of a relay to a PID controller collectively forms the robust controller. The relay ensures robust control by providing a high feedback gain, but it also induces a control chattering phenomenon. Similarly as chapter 4, the chattering signals are used as natural excitation signals and it identifies an equivalent PID

controller using the recursive least squares (RLS) algorithm. Analysis is provided on the stability properties of the control scheme. Simulation and real-time experimental results for the level control of fluid in a spherical tank using the scheme are presented.

Finally in Chapter 6, general conclusions and suggestions for further work are documented.



# Chapter 2

## Preload Relay for Improved Critical Point Identification and PID Tuning

### 2.1 Introduction

Process model estimation is a fundamental and important component of industrial process control as the model, either in a non-parametric or parametric form, provides key input parameters to the control design. Traditional methods of process model estimation is, in general, a fairly time-consuming procedure, involving the injection of persistently exciting inputs and the application of various techniques [35], [36].

Fortunately, knowledge of an extensive full-fledged dynamical model is often not necessary in many of the controllers used in the process industry, and estimation of the critical point (*i.e.*, the critical frequency and gain) [37],[1] is sufficient. For example, in process control problems, this point has been effectively applied in controller tuning [37],[1], process modelling [38], [39], and process characterization [9]. Today, the use of the relay feedback

technique for estimation of the critical point has been widely adopted in the process control industry [40], [41]. This is an elegant yet simple experiment design for process estimation pioneered mainly by Astrom and co-workers [1] and now used in PID controller tuning [40]–[42]. The experiment design is based on the key observation that most industrial processes will exhibit stable limit cycle oscillations for the relay feedback system of Figure 2.1. Following the first successful applications of relay feedback to PID control tuning, a large number of research work to extend its application domain and to enhance various aspects of the conventional approach has been reported. Fundamental studies on the existence and stability of oscillations (e.g., [23], [43]) continue to be conducted. Modifications of the relay feedback method have also been reported [14], [44]–[46] to achieve different elements of improvement over the conventional relay feedback approach.

However, while the relay feedback experiment design will yield sufficiently accurate results for many of the processes encountered in the process control industry, there are some potential problems associated with such relay feedback-based estimation techniques, associated with the estimation accuracy. These arise as a result of the approximations used in the development of the procedures for estimating the critical point. In particular, the basis of most existing relay-based procedures of critical point estimation is the describing function method [47],[48]. This method is approximate in nature, and under certain circumstances, the existing relay-based procedures could result in estimates of the critical point that are significantly different from their real values. Such problematic circumstances arise particularly in underdamped processes and processes with significant time-delay, and poorly tuned control loops would result if the critical point estimates were used for controller tuning. An adaptive approach has been proposed by Lee [10] to achieve near zero error in the estimation of the critical point. However, the improved accuracy is achieved at the expense of a more complicated implementation procedure over the basic relay method. The additional implementation cost may pose an obstacle to the acceptance of the improved method, since

one key reason for the success of the relay feedback method in industrial applications has been the simple and direct approach it has adopted. Other known constraints of the conventional relay feedback method include inapplicability to certain classes of processes, and a long time duration to settle to stationary oscillations in some cases.

In this chapter, a new preload relay feedback to be applied to the process is presented in the same manner as per the conventional relay feedback configuration. The approach will yield significantly improved estimate of the critical point at no significant incremental implementation expenses. The key idea behind the modification is also motivated by describing function concepts, and the modification is designed to boost the fundamental frequency in the forced oscillations induced under a relay feedback configuration, such that compared to the conventional relay setup, the relative amplitude of the fundamental frequency over higher harmonics is increased. A benchmark of the accuracy attainable with the proposed approach against the conventional approach is provided, in the chapter, for rich classes of processes commonly encountered in the process control industry. In addition, other benefits associated with the proposed method are demonstrated via empirical simulation results. These benefits include improved control performance based on an improved estimate, applicability to other classes of processes when the conventional relay method fails, a shorter time duration to attain stationary oscillations, and possible application to extract other points of the process frequency response.

## 2.2 Conventional Relay Feedback Technique

Relay feedback system for process frequency response analysis is shown in Figure 2.1 and first pioneered by Astrom and co-workers [1].

Then ultimate frequency  $\omega_u$  of a process, where the phase lag is  $-\pi$ , can be determined

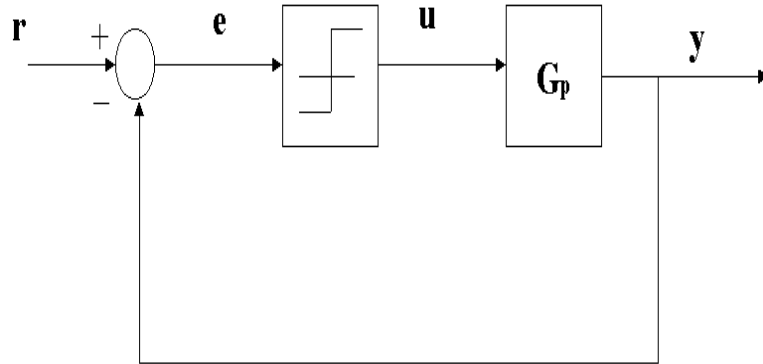


Figure 2.1: Conventional relay feedback system.

automatically from an experiment with relay feedback as shown in Figure 2.1. The usual method employed to analyze such systems is the describing function method which replaces the relay with an “equivalent” linear time invariant system. For estimation of the critical point (ultimate gain and ultimate frequency), the self-oscillation of the overall feedback system is of interest. Here, for the describing function analysis, a sinusoidal relay input,

$$e(t) = a \sin \omega t,$$

is considered, and the resulting signals in the overall system are analyzed. The relay output  $u(t)$  in response to  $e(t)$  would be a square wave having a frequency  $\omega$  and an amplitude equal to the relay output level  $\mu$ . Using a Fourier series expansion, the periodic output  $u(t)$  can be written as

$$u(t) = \frac{4\mu}{\pi} \sum_{k=1}^{\infty} \frac{\sin(2k-1)\omega t}{2k-1}$$

The describing function of the relay  $N(a)$  is simply the complex ratio of the fundamental component of  $u(t)$  to the input sinusoid, i.e.

$$N(a) = \frac{4\mu}{\pi a}.$$

Since the describing function analysis ignores harmonics beyond the fundamental component, define here the residual  $\varrho$  as the entire sinusoidally-forced relay output minus the fundamental component, i.e. the part of the output that is ignored in the describing function development,

$$\varrho = \frac{4\mu}{\pi} \sum_{k=1}^{\infty} \frac{\sin(2k-1)\omega t}{2k-1}. \quad (2.1)$$

In the describing function analysis of the relay feedback system, the relay is replaced with its quasi-linear equivalent DF, and a self-sustained oscillation of amplitude  $a$  and frequency,  $\omega_{osc}$  is assumed. Then, if  $G_p(s)$  denoted the transfer function of the process, the variables in the loop must satisfy the following relations,

$$e = -y, u = N(a)e, y = G_p(j\omega_{osc})u.$$

This implies that it must follow

$$G_p(j\omega_{osc}) = -\frac{1}{N(a)}. \quad (2.2)$$

Relay feedback estimation of the critical point for process control is thus based on the key observation that the intersection of the Nyquist curve of  $G_p(j\omega)$  and  $-\frac{1}{N(a)}$  in the complex plane gives the critical point of the linear process. Hence, if there is a sustained oscillation in the system of Figure 2.1 then the steady state, the oscillation must be at ultimate frequency, i.e.

$$\omega_u = \omega_{osc},$$

and the amplitude of the oscillation is related to the ultimate gain,  $k_u$  by

$$k_u = \frac{4\mu}{\pi a}.$$

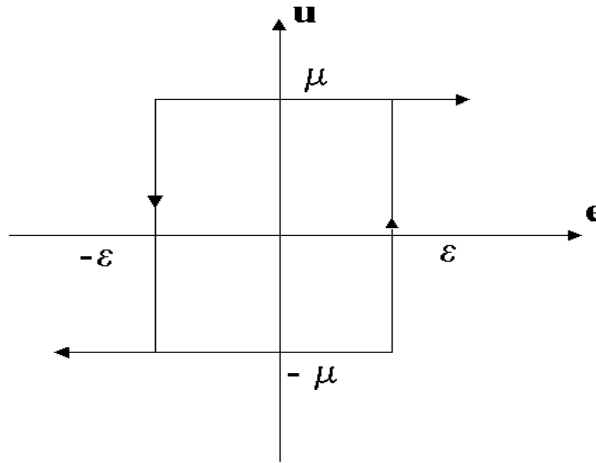


Figure 2.2: Hysteretic relay.

It may be advantageous to use a relay with hysteresis as shown in Figure 2.2 so that the resultant system is less sensitive to measurement noise. The inverse negative describing function of this relay is given by  $-\frac{1}{N(a)} = -\frac{\pi}{4u_m}(\sqrt{a^2 - \epsilon^2} + j\epsilon)$ . In this case, the oscillation corresponds to the point where the negative inverse describing function of the relay crosses the Nyquist curve of the process as shown in Figure 2.3. With hysteresis, there is an additional parameter  $\epsilon$  which can, however, be set automatically based on a pre-determination of the measurement noise level. In the presence of a constant load disturbance, a DC bias compensation can be introduced into the relay to prevent an asymmetrical oscillation [13]. In [49], a two step method using at one a PID controller, a relay and bias was proposed to improve the method developed in [13].

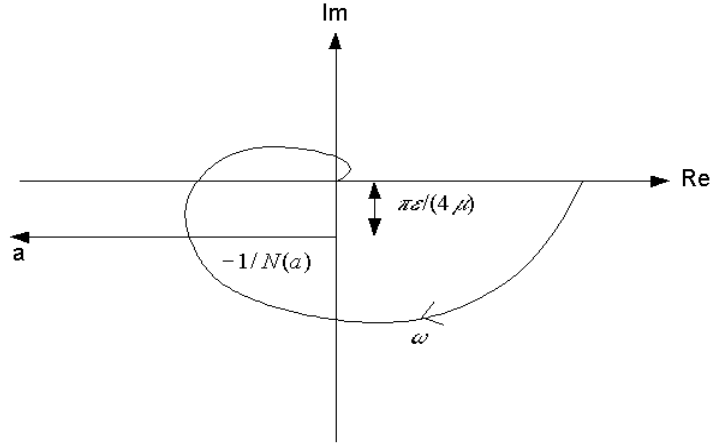


Figure 2.3: Negative inverse describing function of the hysteretic relay.

## 2.3 Problems associated with conventional relay feedback estimation

From the above discussion, it is evident that the accuracy of the relay feedback estimation depends on the relative magnitude of the residual  $\varrho$  (2.1) over the fundamental component which determines whether, and to what degree, the estimation of the critical point will be successful. For the relay,  $\varrho$  consists of all the harmonics in the relay output. The amplitude of the third and fifth harmonics are about 30% and 20% that of the fundamental component and they are not negligible if fairly accurate analysis results are desirable and therefore they limit the class of processes for which describing function analysis is adequate, *i.e.* the process must attenuate these signals sufficiently. This is the fundamental assumption of the describing function method which is also known as the *filtering hypothesis* [47]. Mathematically, the hypothesis requires that the process,  $G_p(s)$  must satisfy

$$|G_p(jk\omega_c)| \ll |G_p(j\omega_c)|, \quad k = 3, 5, 7, \dots, \quad (2.3)$$

and

$$|G_p(jk\omega_c)| \rightarrow 0, \quad k \rightarrow \infty. \quad (2.4)$$

Note that (2.3) and (2.4) require the process to be not simply low-pass, but rather low-pass at the critical frequency. This is essential as the delay-free portion of the process may be low-pass but the delay may still introduce higher harmonics within the bandwidth. Typical processes that fail the filtering hypothesis are processes with long dead-time and processes with resonant peaks in their frequency responses so that the undesirable frequencies are boosted instead of being attenuated. In fact, in simulation results shown later, it will be seen that fairly large errors can occur in critical point estimation for such processes when the conventional relay feedback technique is used.

Apart from the abovementioned problem relating to estimation accuracy, there are other constraints faced by the conventional relay method, such as inapplicability to certain classes of processes, a long time to attain steady state oscillations and inability to extract other points of the process frequency response.

## 2.4 Preload relay feedback estimation technique

Having observed the problems associated with conventional relay feedback estimation, the design of a modified relay feedback that addresses the issue of improved estimation accuracy is considered next. The modification of the basic relay feedback method is motivated by describing function concepts, and the modification is designed to boost the fundamental frequency in the forced oscillations induced under a modified relay feedback configuration. Figure 2.4 shows the proposed configuration using the preload relay (abbreviated as P\_Relay). The P\_Relay is equivalent to a parallel connection of the usual relay with a proportional gain  $K$ .

In this section, the operational principles and rationale for the proposed configuration and guidelines for the choice of gain  $K$  will be elaborated.



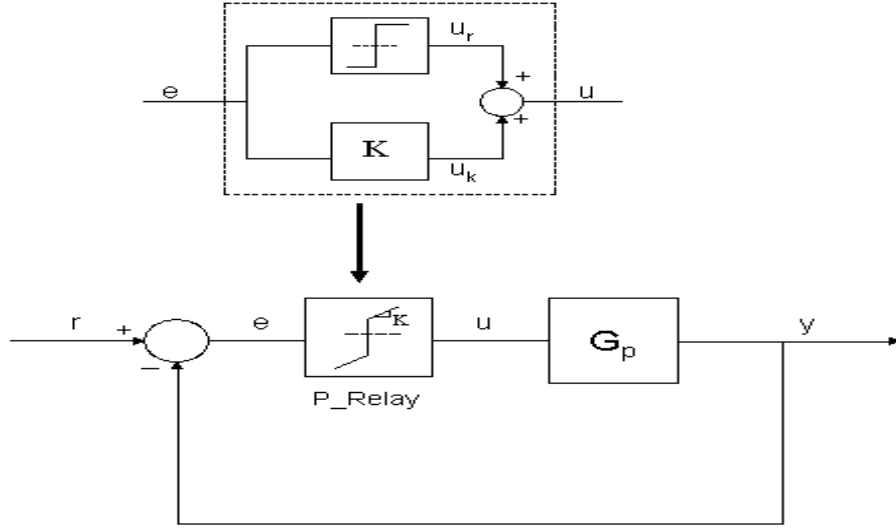


Figure 2.4: Proposed configuration of P\_Relay feedback system.

### 2.4.1 Amplification of the fundamental oscillation frequency

The key idea behind the proposed approach is to increase the amplitude of the fundamental frequency relative to the other harmonics via an additional periodic signal  $u_k$  added to the relay output signal  $u_r$  to form a moderated input signal  $u$  to the process, *i.e.*,

$$u = u_r + u_k.$$

With this moderation, the amplitude (denoted by  $u_1$ ) of the fundamental frequency at the output of the preload relay (given the input signal  $e(t) = a \sin \omega t$ ) is boosted from  $u_1 = \frac{4\mu}{\pi}$  to  $u_1 = \frac{4\mu}{\pi} + Ka$ , while the residual part  $\varrho$ , containing the higher harmonics, remains essentially unchanged.

The describing function of the P\_Relay is thus given by

$$N(a) = \left( \frac{4\mu}{\pi a} + K \right). \quad (2.5)$$

This implies that while the fundamental frequency has been boosted, the negative inverse describing function continues to lie on the negative real axis, albeit with a termination

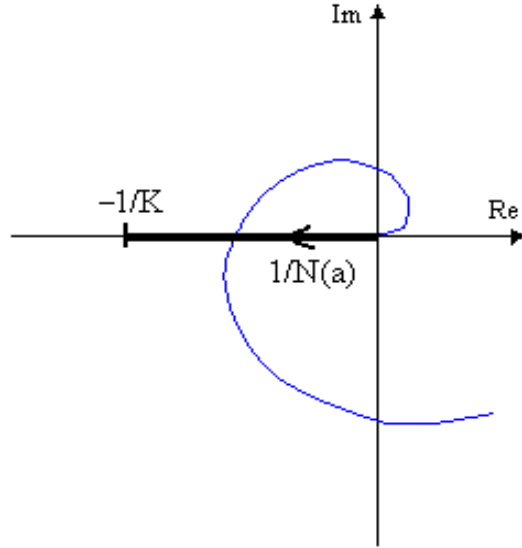


Figure 2.5: Negative inverse describing function of the P\_Relay.

point at  $-\frac{1}{K}$  as shown in Figure 2.5, such that if an intersection occurs between this locus and the process Nyquist curve, an oscillation is sustained and the critical frequency is still estimated as

$$\omega_c = \omega_{osc},$$

and the amplitude of the oscillation is related to the critical gain,  $K_c$  by

$$K_c = \frac{4\mu}{\pi a} + K.$$

For an intersection to occur under the describing function analysis, it is necessary that

$$K < K_c.$$

### 2.4.2 Choice of amplification factor

Compared to the original relay feedback configuration, the proposed method incurs the design of the additional parameter  $K$ . Intuitively, a larger  $K$  should lead to a more accurate

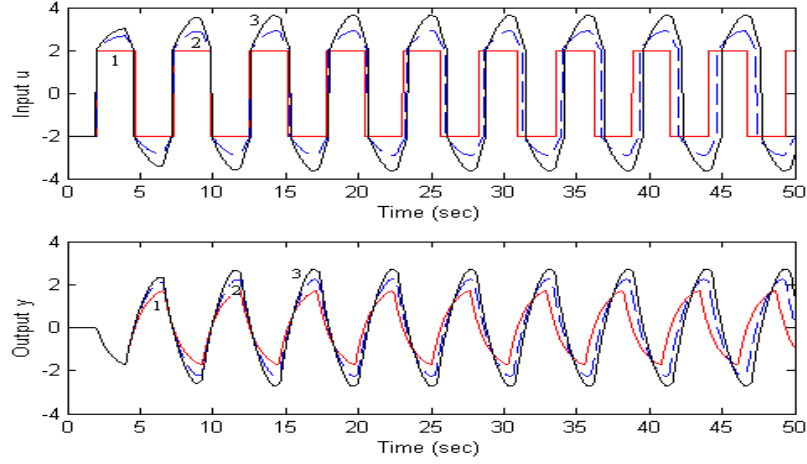


Figure 2.6: Limit cycle oscillation for different choice of  $\alpha$ , (1)  $\alpha = 0$ , conventional relay, (2)  $\alpha = 0.2$ , (3)  $\alpha = 0.3$ .

critical point estimate. It will be provided an empirical evidence for this conjecture in the next section. However, apart from the consideration of the termination point of the describing function, there are physical constraints and safety issues to be considered such as the magnitude of oscillation permissible and actuator saturation. These considerations are similar to those necessary for fixing the relay amplitude in a conventional relay feedback setup.

From extensive empirical studies, it is recommend that the gain can be fixed at 20% – 30% of the relay amplitude  $\mu$ , *i.e.*,

$$K = \alpha\mu,$$

where  $\alpha = 0.2 \sim 0.3$ . If this guideline is followed, essentially the method does not impose any additional and incremental requirements on the user over the original relay method. Figure 2.6 shows the limit cycle attained with different choice of  $\alpha$ . Although it may appear, from the figure, that the modified approach results in an increased overall amplitude of the limit cycle oscillation, the amplitude can be kept to the same tolerable level by varying  $\mu$  as well since it is the relative amplitude of  $K$  to  $\mu$  that is of key interest in this approach.

Note that as  $\alpha$  increases, the process output  $y$  becomes closer to a sinusoid, reflecting the relative smaller harmonics contents in the oscillations.

## 2.5 Simulation Examples

The use of the preload relay feedback for critical point estimation has been investigated in simulation, and the results are tabulated and compared with critical point estimation using conventional relay feedback in Tables 2.1–2.4. The same set of processes as reported in [14] is used in this simulation study. In the simulation study, the value of  $\alpha$  is fixed at  $\alpha = 0.3$  for all cases.

Table 2.1 shows the results for an overdamped process with different values for the time-delay. Tables 2.2 and 2.3 show the respective results for an underdamped process and an overdamped process, each with a (stable) process zero, with different values for the time-delay. Finally, the results for a non-minimum phase process with different values for the time-delay are shown in Table 2.4.

From the Tables, it can be seen that critical point estimation using the preload relay feedback consistently yields improved accuracy over the conventional relay feedback. The better accuracy is particularly marked in Tables 2.3 (overdamped process) and 2.4 (non-minimum phase process) and in the other Tables when the time-delay becomes significant.

The simulation results here have demonstrated the improved accuracy in critical point estimation achieved using the proposed P\_Relay feedback configuration. Further improvement can be obtained if a larger  $\alpha$  is admissible. Figure 2.7 and 2.8 show the variation in the estimate of the critical gain  $K_c$  and frequency  $\omega_c$  with different choice of  $\alpha$  for the process  $G_p = \frac{1}{s+1}e^{-5s}$ , verifying the conjecture that improved accuracy is achieved with a higher

Table 2.1: Process =  $\frac{1}{s+1}e^{-sL}$

	Real Process		Conventional Relay				Pre-load Relay				Improvement	
L	$K_c$	$\omega_c$	$\hat{K}_c$	PE	$\hat{\omega}_c$	PE	$\hat{K}_c$	PE	$\hat{\omega}_c$	PE	$K_c$	$\omega_c$
0.5	3.81	3.67	3.21	15.7	3.74	1.8	3.40	10.76	3.63	1.09	4.94	0.71
2.0	1.52	1.14	1.46	4.2	1.16	1.75	1.54	-1.31	1.14	0.0	2.89	1.75
5.0	1.13	0.53	1.28	13.2	0.55	3.7	1.2	7.01	0.524	1.13	7.01	2.57
10.0	1.04	0.29	1.27	22.4	0.29	2.3	1.16	10.86	0.29	1.03	10.86	1.27

PE : Percentage Error

gain  $K$ . It is possible to achieve very accurate estimates if a large  $K$  (relative to  $\mu$ ) is permissible

## 2.6 Real-time Experimental Results

The proposed P\_Relay relay feedback configuration described above has been applied to critical point estimation in a coupled-tanks system with transport delay, and the results are briefly described here. A photograph of the experimental set-up of the coupled-tanks system is shown in Figure 2.9. The pilot scale process consists of two rectangular tanks, Tank 1 and Tank 2, coupled to each other through an orifice at the bottom of the tank wall. The inflow (control input) is supplied by a variable speed pump which pumps water from a reservoir into Tank 1 through a long tube. The orifice between Tank 1 and Tank 2 allows the water to flow into Tank 2. In the experiments, it is chosen the process with the voltage to drive the pump as input, and the water level in Tank 2 as process output. This

Table 2.2: Process =  $\frac{s+0.2}{s^2+s+1}e^{-sL}$

	Real Process		Conventional Relay				Pre-load Relay				Improvement	
L	$K_c$	$\omega_c$	$\hat{K}_c$	PE	$\hat{\omega}_c$	PE	$\hat{K}_c$	PE	$\hat{\omega}_c$	PE	$K_c$	$\omega_c$
0.5	3.48	3.61	2.97	14.7	3.70	2.5	3.06	12.7	3.59	0.55	2.63	1.95
2.0	1.09	1.27	1.20	10.1	1.28	0.8	1.15	5.87	1.27	0.0	4.23	0.8
5.0	1.19	0.70	1.10	7.7	0.62	11.4	1.14	4.38	0.73	4.28	3.31	7.11
10.0	2.17	0.38	1.16	46.5	0.31	18.4	1.17	46.06	0.32	15.26	0.42	3.14

PE : Percentage Error

coupled-tanks pilot process has process dynamics that are representative of many fluid level control problems faced in the process control industry. A transport delay is present due to the extended tubing from the reservoir of water to the first tank. The coupled-tanks apparatus is connected to a PC via an A/D and D/A board. LabVIEW 7.0 from National Instruments is used as the control development platform.

In the real-time experiments, both the conventional relay feedback procedure and the proposed preload relay feedback procedure were used to estimate the critical point of the coupled-tanks process. For benchmarking of the accuracy in the estimates, an exhaustive spectrum analysis is also carried out with the process in the open-loop. It yields the actual  $K_c = 5.33$  and  $\omega_c = 3.9$ .

Table 2.5 shows the estimate obtained with the two approaches compared to the values from the frequency analysis experiment. Marked improvement of about 16% for the estimate of  $K_c$  and 13.5% for the estimate of  $\omega_c$  is achieved.

Table 2.3: Process =  $\frac{s+0.2}{(s+1)^2}e^{-sL}$

	Real Process		Conventional Relay				Pre-load Relay				Improvement	
L	$K_c$	$\omega_c$	$\hat{K}_c$	PE	$\hat{\omega}_c$	PE	$\hat{K}_c$	PE	$\hat{\omega}_c$	PE	$K_c$	$\omega_c$
0.5	4.26	4.02	3.81	10.6	4.16	3.5	4.07	4.46	4.14	3.16	6.14	0.34
2.0	2.07	1.35	2.37	15.0	1.38	2.2	2.14	3.38	1.33	1.48	11.62	0.72
5.0	2.09	0.65	1.98	5.3	0.61	6.2	2.05	1.91	0.647	0.46	3.39	5.74
10.0	2.78	0.35	1.93	30.6	0.31	11.4	2.13	23.38	0.34	2.81	7.22	8.55

PE : Percentage Error

## 2.7 Additional benefits associated with the preload relay approach

In the preceding sections, the improved critical point estimation accuracy achievable with the proposed configuration have shown at no significant incremental implementation costs. In this section, the benefits forthcoming from an improved estimate with regards to control performance will be shown, as well as other benefits which can be realised with the proposed configuration. The benefits will be illustrated via simulation study and supporting analysis where applicable, in this chapter, as more detailed work continues to be carried out along these directions.

Table 2.4: Process =  $\frac{-s+0.2}{(s+1)^2}e^{-sL}$

	Real Process		Conventional Relay				Pre-load Relay				Improvement	
L	$K_c$	$\omega_c$	$\hat{K}_c$	PE	$\hat{\omega}_c$	PE	$\hat{K}_c$	PE	$\hat{\omega}_c$	PE	$K_c$	$\omega_c$
0.5	1.97	0.83	1.64	17.0	0.72	13.3	1.95	1.01	0.843	1.56	15.98	11.74
2.0	2.31	0.51	1.54	33.0	0.53	3.9	2.10	9.09	0.502	1.57	11.62	0.72
5.0	2.97	0.31	1.51	49.2	0.35	13.0	1.87	37.07	0.34	9.67	12.13	3.33
10.0	3.69	0.20	1.51	59.1	0.23	15.0	1.87	49.32	0.22	10.0	9.78	5.0

PE : Percentage Error

### 2.7.1 Control performance relative to specifications

An improved critical point estimate will lead to improved control performance when the critical point is used as the basis for direct tuning of the controller, or for deriving a model to indirectly tune the controller. In this subsection, the better performance achieved with an improved critical point estimation will be illustrated in terms of how close the user specifications of gain and phase margins can be met.

Consider the following first-order process with time delay [14]

$$G_p = \frac{1}{s+1}e^{-5s}.$$

The desired gain margin is specified as  $G_m = 3$ . The PID controller is tuned via the method described in [11], based on the two different critical points estimates obtained with the conventional relay method and the preload relay method. The actual gain margin achieved is 2.65 and 2.83 respectively with the critical point estimate from the conventional relay method and the preload relay method respectively. The proposed method yields an



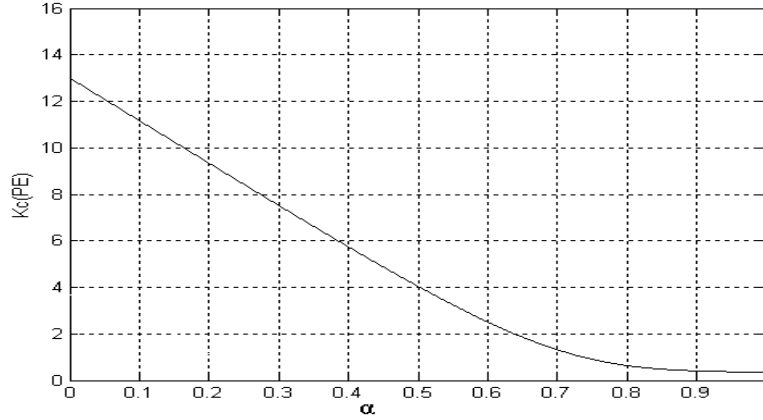


Figure 2.7: PE variation of  $K_c$  with  $\alpha$ .

Table 2.5: Estimates of the critical point for the coupled-tanks system

	Conventional Relay	Pre-load Relay
$K_c$	3.39	4.11
PE	36.39	22.88
$\omega_c$	2.51	3.14
PE	35.64	19.48

improvement of 5.76% in satisfying the specification.

The PID controller can be also tuned [11] based on a desired phase margin of  $\phi_m = 1.05$ . The actual phase margin achieved is 1.36 and 1.31 with the conventional relay method and the preload relay method respectively. An improvement of 4.66% is achieved in this case.

Finally, consider PI controller tuning based on a combined gain and phase margin specifications,  $G_m = 3$  and  $\phi_m = 1.05$  [18]. Table 2.6 shows the actual values obtained with the two approaches. An improvement of about 7% for the estimate of  $G_m$  and 0.4% for the estimate of  $\Phi_m$  is achieved.

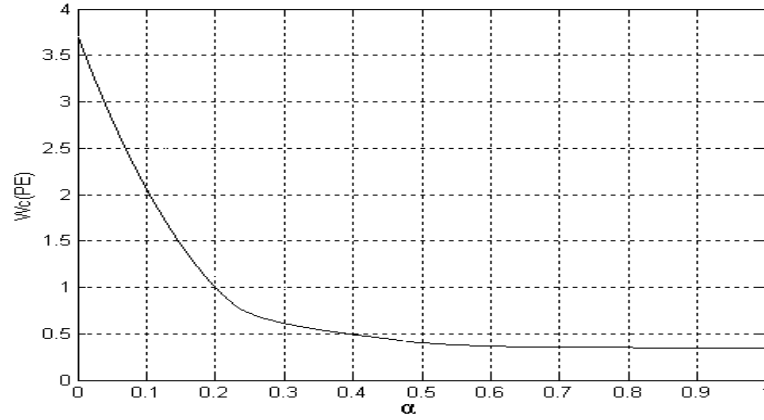


Figure 2.8: PE variation of  $\omega_c$  with  $\alpha$ .

Table 2.6: Actual gain and phase margins achieved

	Conventional Relay	Pre-load Relay
$G_m$	2.76	2.97
PE	8	1
$\Phi_m$	1.033	1.057
PE	1.34	0.95

## 2.7.2 Improved robustness assessment

The relay method has been applied to assess control robustness in terms of maximum sensitivity ( $M_s$ ), gain margin ( $G_m$ ) and phase margin ( $\Phi_m$ ). Using the configuration [50] as shown in Figure 2.10, where  $G_{ol} = G_c(s)G_p(s)$  is the compensated system comprising of the process  $G_p$  and the controller  $G_c$ , the preload relay can be applied here to replace the usual relay in Figure 3.18 to yield improved assessment accuracy. The method is simulated for various compensated systems in Table 2.7



Figure 2.9: Photograph of experimental set-up.

Table 2.7: Compensated systems for robustness assessment

Compensated process $G_{ol}$	Process $G_p$	Controller $G_c$
A	$G_{p1} = \frac{1}{(s+1)^4}$	$G_{c1} = 0.848 + \frac{0.297}{s}$
B	$G_{p2} = \frac{10}{(s+1)(1.5s+1)(2s+1)}e^{-2s}$	$G_{c2} = 0.0478 + \frac{0.0149}{s}$
C	$G_{p3} = \frac{(1-s)}{s(s+3)}$	$G_{c3} = 0.77 + \frac{0.09}{s}$

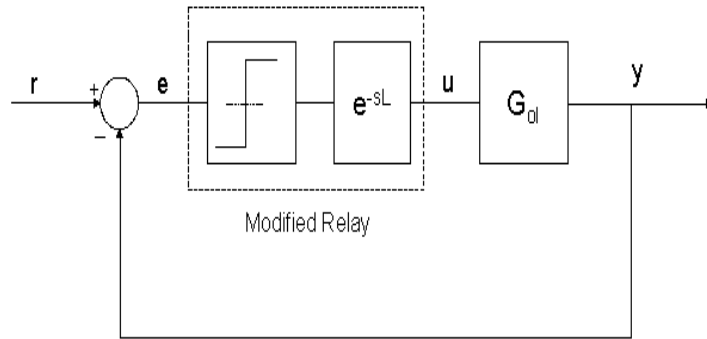


Figure 2.10: Relay configuration for robustness assessment

Table 2.8: Results of the modified relay feedback system

	Actual Value			Conventional Relay						P_Relay						Improvement		
	$M_s$	$G_m$	$\Phi_m$	$M_s$	PE	$G_m$	PE	$\Phi_m$	PE	$M_s$	PE	$G_m$	PE	$\Phi_m$	PE	$M_s$	$G_m$	$\Phi_m$
A	1.75	3	1.05	1.78	1.71	2.93	2.33	1.01	3.80	1.78	1.71	2.93	2.33	1.02	2.85	0	0	0.95
B	1.7	2.82	1.05	1.78	4.70	2.65	6.02	0.98	6.66	1.77	4.11	2.69	4.60	0.99	5.71	0.59	1.42	0.95
C	1.49	3.72	1.807	1.73	16.10	2.85	23.38	0.71	12.01	1.68	12.75	2.88	22.58	0.74	8.30	3.35	0.8	3.71

Table 2.8 shows the results and improvement in percentage errors for the two methods on the three compensated systems above. It is observed from the table that phase margin have improved for all the cases. The remarkable improvements can be observed specially for type B and type C systems.

### 2.7.3 Applicability to unstable processes

Unstable processes represent a class of processes for which the conventional relay feedback becomes inapplicable if the time-delay is long [51]. Furthermore, the control performance achievable for an unstable process is particularly sensitive to the accuracy of the process model. In simple cases of unstable processes with short time-delay, a stable limit cycle oscillation may exist, but if the estimate of the critical point is inaccurate and it is used as the basis for the tuning of the controller, the control performance may be very unsatisfactory or even unstable. The benefits with regards to the application of the preload relay method to unstable processes will be illustrated in this section.

#### Improved control performance

It is well-known that control of unstable processes is a difficult and challenging problem, with a low threshold for modelling errors to ensure a stable control performance. In this example, the difference in control performance will be elaborated, as a result of two different critical points obtained respectively via the conventional relay method and the proposed method.

Consider a first-order unstable plant with delay [52],

$$G_p = \frac{1}{10s - 1} e^{-2s}$$

Limit cycle oscillations can be sustained in both cases, but the proposed preload relay feedback yields improved estimation accuracy as evident in the results tabulated in Table 2.9 for the same process considered above, albeit with different time-delays.

With the critical point, PID controllers are tuned using the same method described in [53]. The controller, tuned using the estimate from the conventional relay feedback, is unable to yield a stable closed-loop response as shown in Figure 2.11, while the controller, tuned

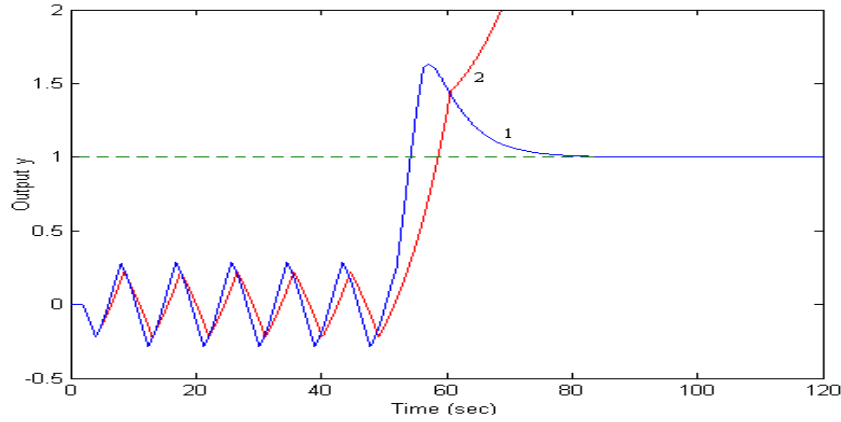


Figure 2.11: Relay tuning and control performance for a first-order unstable plant, (1)P\_Relay feedback method, (2) Conventional relay feedback method.

using the improved estimate from the preload relay feedback, yields a stable closed-loop response.

Table 2.9: Process =  $\frac{1}{(10s-1)}e^{-Ls}$

### Existence of sustained oscillations

Next, consider the same first-order unstable process but with a longer time delay, *i.e.*,  $G_p = \frac{1}{10s-1}e^{-8s}$ . As reported in [51], no stable limit cycle oscillation will result from the conventional relay feedback method. With the preload relay feedback, a stable limit cycle oscillation can still be obtained as shown in Figure 2.12. The same observation holds for the time-delay of  $L = 9$  as shown in Table 2.9.

### Supporting Analysis

In this sub-section, an analysis will be provided to show that the additional relay parameter  $K$  can help to provide a bound on the oscillation when the preload relay is applied to an unstable process. The following notations will be used in the analysis.

$\|M\|$  represents the norm of the matrix  $M$

Real Process			Conventional Relay				Pre-load Relay				Improvement	
L	$K_c$	$\omega_c$	$\hat{K}_c$	PE	$\hat{\omega}_c$	PE	$\hat{K}_c$	PE	$\hat{\omega}_c$	PE	$K_c$	$\omega_c$
2	7.24	0.71	5.78	20.23	0.75	5.03	6.47	10.75	0.73	3.35	9.48	1.67
5.0	2.53	0.234	1.95	22.92	0.196	16.24	2.16	14.62	0.209	10.68	8.30	5.56
8.0	1.38	0.095	–	–	–	–	1.309	5.14	0.084	11.57	–	–
9.0	1.17	0.06	–	–	–	–	1.127	3.22	0.05	16.66	–	–

$\lambda(M)$  denotes any eigenvalue of matrix  $M$

$\lambda_{max}(M)$  denotes the largest eigenvalue of  $M$

$\lambda_{min}(M)$  denotes the smallest eigenvalue of  $M$

Consider the following process

$$G_p : \dot{y} = ay + bu(t - h), \quad (2.6)$$

where  $h$  is time-delay. Given a reference signal  $y_d$ , the error equation can be generated as,

$$\dot{e} = ae - cu(t - h) + \dot{y}_d - ay_d. \quad (2.7)$$

This can be re-written as

$$\dot{X} = AX + Bu(t - h) + B\epsilon, \quad (2.8)$$

where  $X = [e]$ ,  $A = a$ ,  $B = -c$ , and  $\epsilon = \frac{\dot{y}_d - ay_d}{-c}$ . The control  $u$  is the same as in (2.23). The closed-loop system is thus given by

$$\dot{X} = AX + BKX(t - h) + BK_r \text{sgn}(e(t - h)) + B\epsilon \quad (2.9)$$

Consider the Lyapunov function  $V = X^T PX + \int_{t-h}^t X^T(\tau)QX(\tau)d\tau$ , where  $Q$  is a semi-

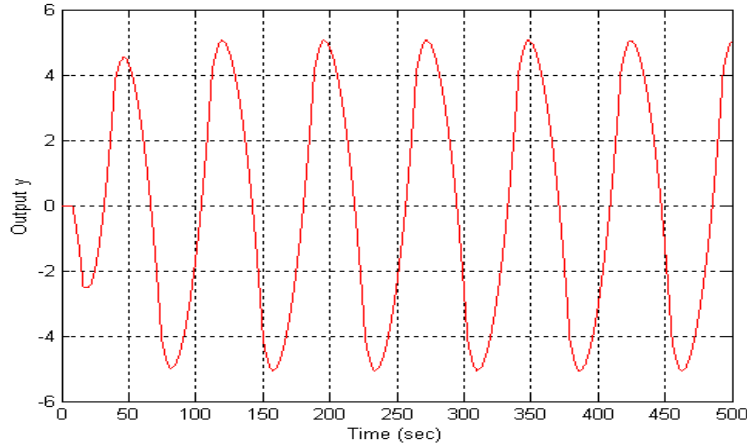


Figure 2.12: Limit cycle oscillation for process  $G_p = \frac{1}{(10s-1)}e^{-8s}$  using the P\_Relay feedback method.

positive definite matrix specified. The time derivative of  $V$  is given by

$$\begin{aligned}
\dot{V} &= X^T(A^T P + PA)X + X^T PBKX(t-h) + X^T(t-h)K^T B^T PX + X^T QX \\
&\quad - X^T(t-h)QX(t-h) + 2X^T PB[K_r \text{sgn}(e(t-h)) + \epsilon] \\
&\leq X^T(A^T P + PA)X + X^T PBKX(t-h) + X^T(t-h)K^T B^T PX + X^T QX \\
&\quad - X^T(t-h)QX(t-h) + X^T PBB^T PX + \|K_r + \epsilon_M\|^2 \\
&= \bar{X}^T \begin{bmatrix} A^T P + PA + PBB^T P + Q & PBK \\ K^T B^T P & -Q \end{bmatrix} \bar{X} + \|K_r + \epsilon_M\|^2, \tag{2.10}
\end{aligned}$$

where  $\bar{X} = [X^T, X(t-h)^T]^T$ . If the matrix

$$R = \begin{bmatrix} -A^T P - PA - PBB^T P - Q & -PBK \\ -K^T B^T P & Q \end{bmatrix} \tag{2.11}$$

is positive definite, then it has

$$\dot{V} \leq -\lambda_{\min}(R)\|\bar{X}\|^2 + \|K_r + \epsilon_M\|^2 \tag{2.12}$$

In order for (2.12) to satisfy  $\dot{V} < 0$ ,

$$\|\bar{X}\|^2 > \|K_r + \epsilon_M\|^2 / \lambda_{\min}(R). \tag{2.13}$$



Since  $\|X\| \leq \|\bar{X}\|$ , this condition is necessarily satisfied if

$$\|X\|^2 > \|K_r + \epsilon_M\|^2 / \lambda_{\min}(R). \quad (2.14)$$

Based on the results in [54],  $X$  is uniformly ultimately bounded (UUB) by  $\sqrt{\|K_r + \epsilon_M\|^2 / \lambda_{\min}(R)}$ .

It is observed that  $R$  can be determined by choosing the value of  $K$ . Thus, an appropriate value of  $K$  can make  $R$  positively definite and then the UUB is ensured. This property cannot be guaranteed for the conventional pure relay.

#### 2.7.4 Improvement in convergence rate

When the relay feedback approach is used to tune a PID controller, information from the steady state oscillations is extracted and used for this purpose. Thus, the tuning duration is directly dependent on how fast the oscillations settle to the steady state. To this end, a shorter duration is clearly desirable. Compared to the conventional relay, the preload relay effectively provides a higher feedback gain for the oscillating frequency, which can be adjustable by the user. With a higher gain threshold at the oscillating frequency, the limit cycle can settle into the stationary state at a faster rate, thus enabling a faster tuning time when the setup is used for control tuning purposes. In this section, this useful feature will be illustrated.

Consider the following process from [12],

$$G_p = \frac{4}{s^2 + s + 4} e^{-0.01}$$

In this example, steady state oscillations is deemed to have occurred when the amplitudes of two consecutive oscillations do not differ by more than 2%. Figure 2.13 shows the process output from the instant the relay (conventional or preload) is introduced into the loop. With the P\_Relay method, the system settles to steady state oscillations after 3.9s,

compared to the conventional relay feedback method, where the oscillations settles after 6.5s.

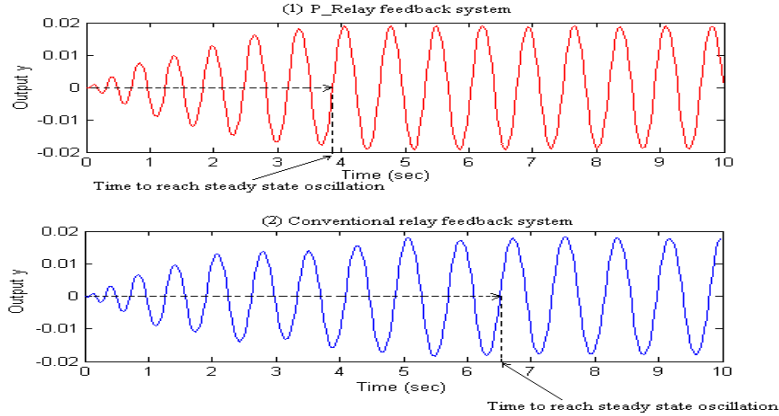


Figure 2.13: Limit cycle oscillation using (1) P\_Relay, (2) conventional relay

Next, consider an underdamped process with a long delay,

$$G_p = \frac{s + 0.2}{s^2 + 2s + 4} e^{-8s}.$$

With the P\_Relay method, the system settles to steady state oscillations after 42s, compared to the conventional relay feedback method, where the oscillation settles after 68.5s.

### Supporting Analysis

In this subsection, an analysis is provided to show that the proposed preload relay can achieve a faster convergence speed compared to the pure relay.

Consider a linear n-order plant

$$G_p(s) = \frac{1}{s^n + a_1 s^{n-1} + \dots + a_n}. \quad (2.15)$$

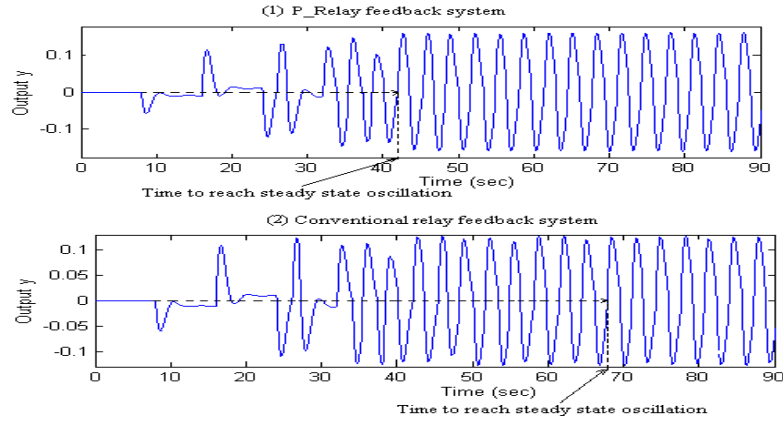


Figure 2.14: Limit cycle oscillation using (1) P\_Relay, (2) conventional relay

This can be re-written as in the state-space form :

$$\dot{z} = \begin{bmatrix} 0 & 1 & \dots & 0 \\ 0 & 0 & \dots & 0 \\ \vdots & \vdots & \dots & 0 \\ -a_n & -a_{n-1} & \dots & -a_1 \end{bmatrix} z + \begin{bmatrix} 0 \\ 0 \\ \vdots \\ 1 \end{bmatrix} u, \quad (2.16)$$

$$y = z_1, \quad (2.17)$$

where  $z = [z_1, z_2, \dots, z_n]^T \in R^n$  represents the states of the system,  $u \in R$  is the control input of the system, and  $y$  is the output of the system. For a reference  $y_d$  which is assumed to be smooth and bounded, the tracking error as  $e = y_d - y$  is defined. Thus, the following error equation have formed

$$\dot{x} = Ax + Bu + B\epsilon, \quad (2.18)$$

where

$$x = [e, \dot{e}, \dots, e^{(n-1)}]^T, \quad (2.19)$$

$$A = \begin{bmatrix} 0 & 1 & \dots & 0 \\ 0 & 0 & \dots & 0 \\ \vdots & \vdots & \dots & 0 \\ -a_n & -a_{n-1} & \dots & -a_1 \end{bmatrix}, \quad (2.20)$$

$$B = \begin{bmatrix} 0 \\ 0 \\ \vdots \\ -1 \end{bmatrix}, \quad (2.21)$$

$$\epsilon = y_d^{(n)} - a_n \dot{y}_d \dots - a_1 y_d^{(n-1)}, \quad (2.22)$$

where  $\dot{y}_d$  is the time derivative of  $y_d$  and  $y_d^{(k)}$  is the  $k$ th time derivative of  $y_d$ .

Since the reference  $y_d$  is assumed to be smooth and bounded,  $\epsilon$  is also bounded, i.e.,  $|\epsilon| \leq \epsilon_M$ . The control  $u$  can be written as

$$u = Ke + K_r \text{sgn}(e) \quad (2.23)$$

where  $K$  is the proportional gain of the preload part of the relay and  $K_r$  is the amplitude of the relay.

Applying the control  $u$ , the following closed-loop system can be formed

$$\dot{x} = (A + B\bar{K})x + BK_r \text{sgn}(e) + B\epsilon = \bar{A}x + BK_r \text{sgn}(e) + B\epsilon, \quad (2.24)$$

where  $\bar{K} = [K, 0, \dots, 0]$  and  $\bar{A} = A + B\bar{K}$ . Consider a Lyapunov function  $V = x^T P x$ , where  $P$  is the solution of the following equation

$$\bar{A}^T P + P\bar{A} + PBB^T P + Q = 0, \quad (2.25)$$

where  $Q$  is a semi-positive definite matrix. This equation has a solution if  $\bar{A}$  is a stable matrix. The time derivative of  $V$  is given by

$$\dot{V} = x^T (\bar{A}^T P + P\bar{A})x + 2x^T PBK_r \text{sgn}(e) + 2x^T PB\epsilon. \quad (2.26)$$

By using the inequality  $2\alpha^T\beta \leq \alpha^T\alpha + \beta^T\beta$ , it has

$$\begin{aligned} 2x^T PB(K_r \text{sgn}(e) + \epsilon) &\leq x^T PBB^T Px + (K_r \text{sgn}(e) + \epsilon)^2 \\ &\leq x^T PBB^T Px + (\|K_r\| + \epsilon_M)^2. \end{aligned} \quad (2.27)$$

Substituting the above equation into (2.26) and using (2.25), it follows

$$\begin{aligned} \dot{V} &\leq x^T (\bar{A}^T P + P\bar{A} + PBB^T P)x + (\|K_r\| + \epsilon_M)^2 \\ &= -\lambda_{\min}(Q)\|x\|^2 + (\|K_r\| + \epsilon_M)^2. \end{aligned} \quad (2.28)$$

Since  $\lambda_{\min}(P)\|x\|^2 \leq V \leq \lambda_{\max}(P)\|x\|^2$ , it has

$$\dot{V} \leq -\frac{\lambda_{\min}(Q)}{\lambda_{\max}(P)}V + (\|K_r\| + \epsilon_M)^2. \quad (2.29)$$

For the above inequality, using Lemma 3.2.4 of [55], it will obtain

$$\lambda_{\min}(P)\|x\|^2 \leq V \leq \frac{\lambda_{\max}(P)}{\lambda_{\min}(Q)}(\|K_r\| + \epsilon_M)^2 + [V(0) - \frac{\lambda_{\max}(P)}{\lambda_{\min}(Q)}(\|K_r\| + \epsilon_M)^2] e^{-\frac{\lambda_{\min}(Q)}{\lambda_{\max}(P)}t}. \quad (2.30)$$

Note that the convergence speed is influenced by the function  $e^{-\frac{\lambda_{\min}(Q)}{\lambda_{\max}(P)}t}$ . Thus, by choosing the value of  $K$  appropriately, the value of  $\frac{\lambda_{\min}(Q)}{\lambda_{\max}(P)}$  can be changed, while in the pure relay this term is fixed. This implies that a faster convergence speed can be achieved compared to the pure relay case, when an appropriate value of  $K$  is chosen.

### 2.7.5 Identification of other intersection points

For a process with long delay, there can be several intersection points between its Nyquist plot and the negative real axis of the complex plane. The critical point is usually defined as the first intersection point as the frequency increases. It is observed that the conventional relay feedback yields the critical point, but not the outermost point although the outermost

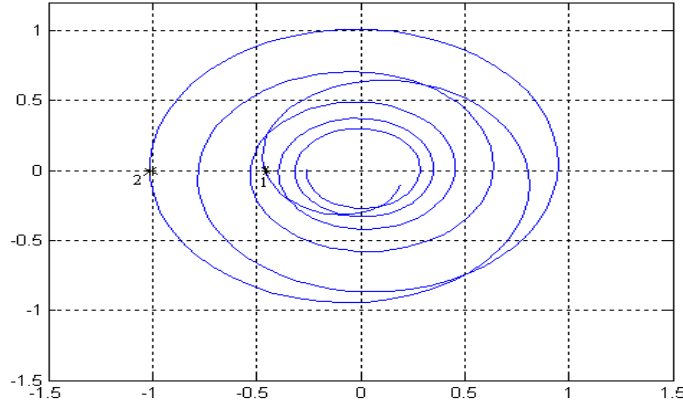


Figure 2.15: Nyquist plot of the process  $G_p = \frac{s+0.2}{s^2+s+1}e^{-10s}$ , (1) critical point, (2) outermost point

point can be a more crucial point to consider during the controller design phase. In this section, it will be demonstrated that outermost point may be obtained with the preload relay by appropriately adjusting the gain  $K$ .

Consider the following underdamped process with long delay [14]

$$G_p = \frac{s + 0.2}{s^2 + s + 1}e^{-10s}.$$

Figure 2.15 shows the Nyquist plot of the above process, the critical point and outermost point are located at (2.17,0.38) and (0.987,0.935) respectively (the first argument refers to the inverse gain and the second refers to the frequency). Note that the outermost intersection point is associated with a higher frequency. This is due to the resonance in the frequency response of this process. The P\_Relay feedback method identifies these two points as (1.17,0.32) and (0.992,0.897) respectively, when the gain of P\_Relay is selected to be 20% and 60% of the relay amplitude. The conventional relay identifies only the critical point at (1.16,0.31). Next, consider a overdamped process with long delay [14]

$$G_p = \frac{s + 0.2}{(s + 1)^2}e^{-10s}.$$

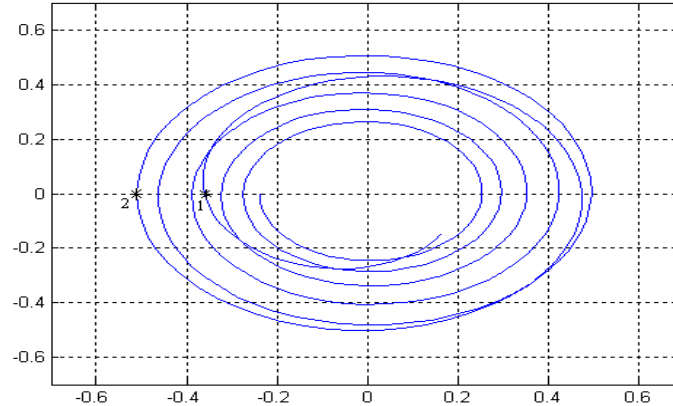


Figure 2.16: Nyquist plot of the process  $G_p = \frac{s+0.2}{(s+1)^2}e^{-10s}$ , (1) critical point, (2) outermost point

Figure 2.16 shows the Nyquist plot of the overdamped process, the critical point and the outermost point are located at  $(2.78,0.35)$  and  $(1.96,0.928)$  respectively. This process also exhibits a resonance in the frequency response due to its zero. The P\_ReIay feedback method identifies these two points as  $(2.13,0.34)$  and  $(1.98,0.897)$  respectively, when the gain of P\_ReIay is selected at 20% and 65% of the relay amplitude. The conventional relay identifies only the critical point at  $(1.51,0.23)$ .

### 2.7.6 Comparison with another modified relay-based technique

The proposed P\_ReIay feedback method can be compared with the method proposed in [14]. The method proposed in [14] addressed the accuracy of the conventional relay feedback approach by eliminating the errors introduced in the usual describing function analysis. By using this method [14], theoretically it is possible to obtain an exact estimate of the process critical point under ideal conditions. Except an accurate critical point identification, the method in [14] failed to show the other benefits of the P\_ReIay feedback method, such as, identification of other intersection points of the process frequency response, applicability

to unstable process if time-delay is long and a shorter time duration to attain stationary oscillations.

## 2.8 Conclusions

In this chapter, a modified relay feedback method named as P\_Relay feedback method is presented for estimating the critical point in process control systems with improved accuracy over the conventional relay feedback method pioneered by Astrom and co-workers. Empirical evidence is also provided to show other benefits of the proposed approach with respect to improved control performance based on an improved estimate, applicability to other classes of processes when the conventional relay method fails, a shorter time duration to attain stationary oscillations, and possible application to extract other points of the process frequency response. In the next chapter, the proposed method will be applied for an improved robustness assessment.



# Chapter 3

## Robustness Assessment and Control Design Using a Relay Feedback Approach

### 3.1 Introduction

Robustness has always been an important design objective to achieve for control systems functioning under harsh practical conditions. A good control system is expected to be sufficiently robust to unmodelled dynamics as well as extraneous signals arising from time to time during the system operations, including noise and load disturbances. Control robustness is also commonly used as an indication of how well the controller has been tuned, and whether re-tuning should be initiated. In the frequency domain, the maximum sensitivity and stability margins provide assessment of the robustness of a compensated system.

The maximum sensitivity ( $M_s$ ) fulfills the main requirements of a good design parameter for robustness [56]. Robustness can usually be guaranteed by imposing a bound on the maximum sensitivity, typically in the range from 1.3 to 2.0. Lower values give better robustness at the expense of a slower reaction [23]. Several PID tuning rules have been established, where the maximum sensitivity is used as a design parameter [57], [23]. For a quick assessment of robustness, stability margins (the gain and phase margins) are classical performance indicators which have been existent for a long time, and have found affinity among most practising engineers. They have also been widely used as design specifications for the design of PID controllers [11], [26].

The assessment of maximum sensitivity and stability margins of a control system usually requires a lengthy non-parametric frequency response identification [36]. Motivated by the relay feedback method by [1] to efficiently identify key process parameters for the tuning of PID controllers, this chapter explores the use of a relay-type apparatus to automatically identify these robustness indicators from a control system. The experiment is a more elaborate one than the basic relay experiment to identify one critical point for PID tuning, since more information is clearly necessary for such an assessment. The apparatus uses a relay in series with a time delay element. The amount of time delay is swept over a range (which can be determined), in the process, generating a series of sustained oscillations. Based on the amplitude and frequency of the oscillations, a chart of the proximity (to the critical point) versus phase (to be explained later in the chapter) can be systematically plotted. The maximum sensitivity and stability margins can be directly identified from the chart. Simulation examples on a group of processes, representative of a wide range of process dynamics, is presented in the chapter to show the effectiveness and assessment accuracy of the proposed approach. In addition, real-time experiments will be conducted to identify these robustness parameters from a coupled-tanks apparatus, and the identification results will be furnished in the chapter. By this way, a relay-based approach is proposed in this

chapter which provides a systematic way to enable the estimation of all the aforementioned robustness indicators, i.e., the maximum stability and stability margins of a compensated system. If these parameters are assessed to be unsatisfactory, some means to automatically retune the controller would be necessary and useful. In this chapter, an approach for the design of the PI controller is subsequently proposed also to concurrently satisfy user specifications in terms of maximum sensitivity and stability margins. Guidelines are provided, in the chapter, to assist the user to select generally satisfactory parameters to meet robust design objectives. The PI control parameters are then obtained, via the minimization of objective functions, so that the robustness specifications can be met as closely as possible. A simulation study on commonly encountered processes will show the effectiveness of the proposed design scheme.

## 3.2 Control Robustness Assessment

Figure 3.1 shows a feedback control system comprising of a controller  $G_c$  and the plant  $G_p$ .  $G_{ol} = G_c(s)G_p(s)$  denotes the compensated system, otherwise known as the loop transfer function.

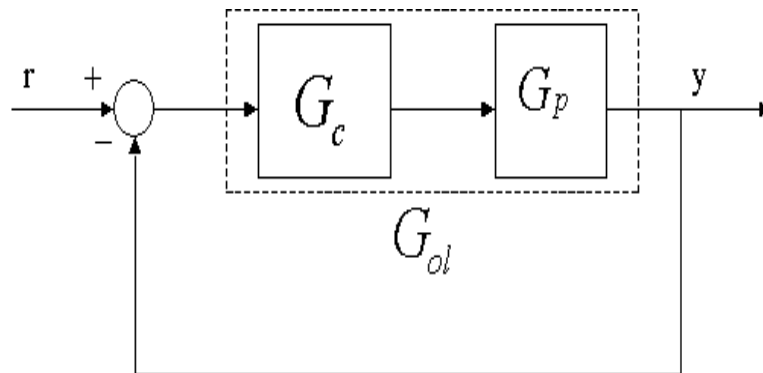


Figure 3.1: Feedback control system.

### 3.2.1 Maximum sensitivity

The maximum sensitivity  $M_s$  is defined as the maximum value of the sensitivity function, i.e.,

$$M_s = \max_{\omega} \left| \frac{1}{1 + G_{ol}(j\omega)} \right| = \max_{\omega} |S(j\omega)|, \quad (3.1)$$

where  $S$  denotes the sensitivity function and it has many useful physical interpretations [58], [59]. Figure 3.2 shows  $M_s$  defined graphically and equivalently as the inverse of the shortest distance from the locus of  $G_{ol}(j\omega)$  to the critical point  $s = -1$ . The distance from other points on  $G_{ol}(j\omega)$  to the critical point is thus always larger than  $1/M_s$ . Figure 3.3

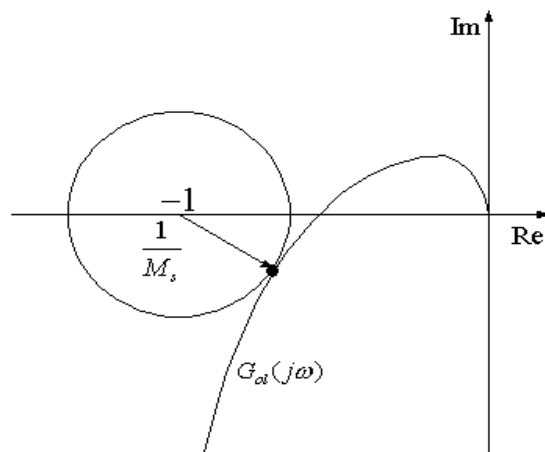


Figure 3.2: Definition of  $M_s$ .

shows two points on  $G_{ol}(j\omega_i)$ ,  $i = 1, 2$ , at the respective phase lags of  $-\pi + \phi(\omega_i)$ ,  $i = 1, 2$ , i.e.,  $\phi(\omega_i) = \pi + \arg G_{ol}(j\omega_i)$ ,  $i = 1, 2$ . Both points are at a distance of  $\lambda(\omega_1) = \lambda(\omega_2)$  from the critical point  $s = -1$ . They can thus be viewed as the intersection points with the circle centered at  $s = -1$  with a radius of  $\lambda(\omega_i)$ . Direct vector manipulation will give

$$\lambda(\omega) = |G_{ol}(j\omega) + 1|. \quad (3.2)$$

Consider a series of circles all centered at  $s = -1$  with different radii  $\lambda$ . Following the definition of  $M_s$ , the circle at  $s = -1$  with radius  $\lambda(\omega^*) = 1/M_s$  will intersect the fre-

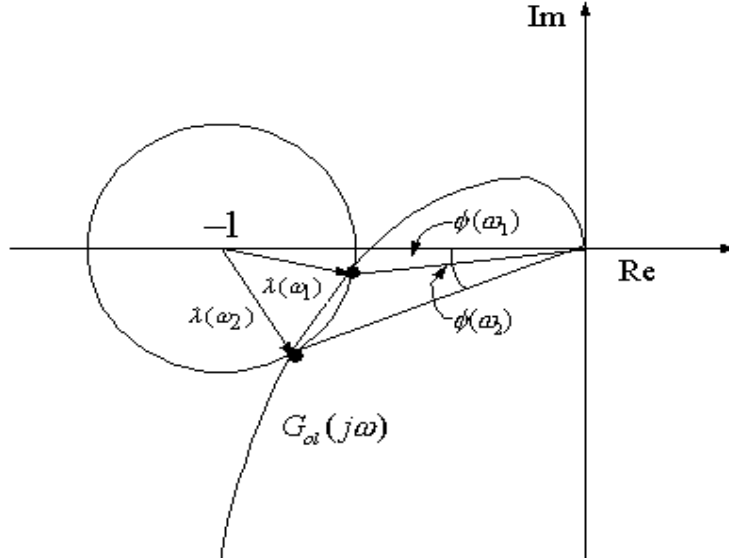


Figure 3.3: Relationship between  $G_{ol}(j\omega_i)$  and  $\lambda(\omega_i)$ .

quency response  $G_{ol}(j\omega)$  at only one point ( $\omega = \omega^*$ ) (Figure 3.2). If the radius is larger than  $1/M_s$ , i.e.,  $\lambda > 1/M_s$ , intersection will occur at more points, typically two. On the other hand, if the radius is smaller than  $1/M_s$ , i.e.,  $\lambda < 1/M_s$ , there will be no intersection. Herein this observation, lies the main idea for the identification of the maximum sensitivity.

Assume for now  $G_{ol}(j\omega)$  is available. A plot of  $\lambda(\omega) = |G_{ol}(j\omega) + 1|$  versus  $\phi(\omega)$  will typically exhibit characteristics as shown in Figure 3.4. From this plot, the turning point, where there is a one-to-one mapping from  $\lambda(\omega)$  to  $\phi(\omega)$ , can be located. This is the minimum point on the plot in Figure 3.4, which corresponds to  $\omega = \omega^*$  (i.e., where there is only one intersection). Denoting this specific value of  $\lambda(\omega^*)$  as  $\lambda^*$ , the maximum sensitivity can thus be obtained as

$$M_s = \frac{1}{\lambda^*}. \quad (3.3)$$

In the next subsection, we will elaborate how this  $\lambda$ - $\phi$  chart can be generated automatically and efficiently via a modified relay experiment.

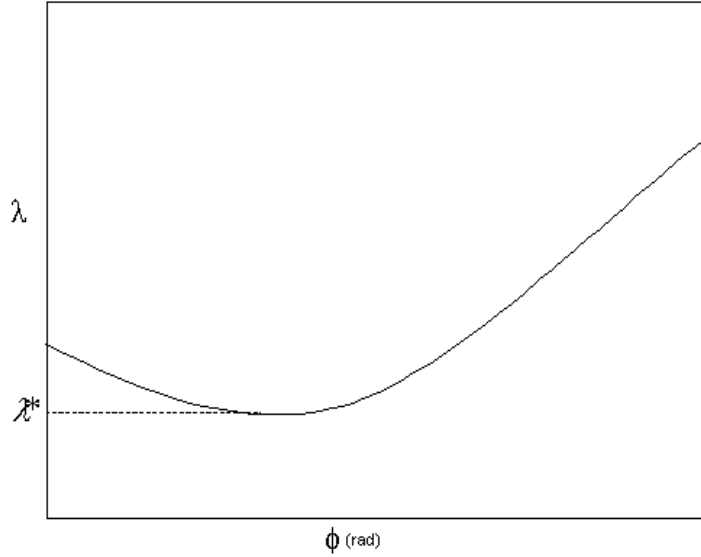


Figure 3.4: Typical plot of  $\lambda$  versus  $\phi$ .

### 3.2.2 Construction of $\lambda - \phi$ chart

Consider a modified relay feedback configuration as shown in Figure 3.5. The modified relay comprises of a normal relay in series with a time delay element which simply delay the action of the relay by  $L$  time units. As shown in [50], under this configuration, sustained oscillation at frequency  $\omega_L$  can be usually attained from which the point at a phase lag of  $-\pi + \omega_L L$  can be obtained. Then, by sweeping the time delay over a suitable range,  $G_{ol}(j\omega)$  in the third and fourth quadrants of the complex plane can be obtained.

Assume for a specific time delay  $L$  and a relay amplitude  $d$ , a sustained oscillation with amplitude  $a$  and frequency  $\omega_L$  is obtained. Suppose  $G_{ol}(j\omega_L) = \alpha_L + j\beta_L$ , then  $\alpha_L$  and  $\beta_L$  can be computed from the oscillations using the following equations which are obtained from a describing function analysis,

$$\alpha_L = \frac{\pi a \cos(\omega_L L - \pi)}{4d}, \quad (3.4)$$

$$\beta_L = \frac{\pi a \sin(\omega_L L - \pi)}{4d}. \quad (3.5)$$

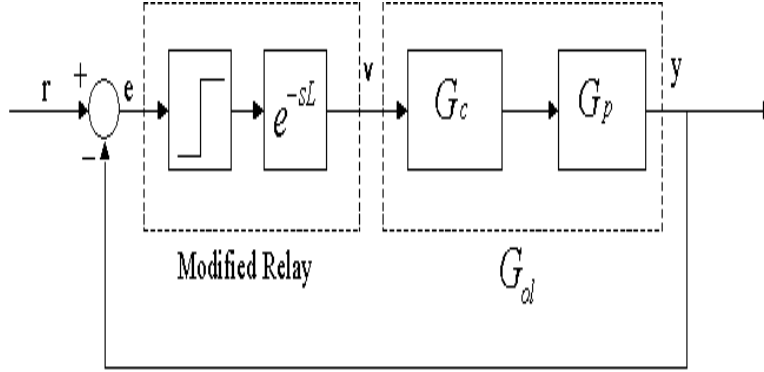


Figure 3.5: Proposed modified relay configuration.

The describing function analysis is an approximation method, thus there is some inevitable tolerance to be expected with these estimates. Alternatively, since the oscillations are periodic, Fourier or Spectral analysis may be efficiently applied to the signals  $v$  and  $y$  (Figure 3.5) to yield a good estimate of  $G_{ol}(j\omega_L)$  at  $\omega = \omega_L$  as :

$$G_{ol}(j\omega_L) = \frac{\int_0^{T_L} y(t)e^{-j\omega_L t} dt}{\int_0^{T_L} v(t)e^{-j\omega_L t} dt}, \quad (3.6)$$

where  $T_L = \frac{2\pi}{\omega_L}$ . In this way,  $G_{ol}(j\omega_L)$  is obtained and thus the corresponding  $\lambda(\omega_L)$  can be computed. By sweeping  $L$  over a range, the plot of  $\lambda - \phi$  can be generated using describing function analysis or Fourier analysis method.

It may be of concern, especially to potential users of the approach, on the range of  $L$  to be used, since this range will determine the duration of the identification experiment. To this end, it may be noted that the parameters to be determined ( $M_s$  and also the stability margins to be addressed in Section 3.2.3) can typically be derived from  $G_{ol}(j\omega)$  in the third quadrant of the complex plane. The experiment can thus be terminated when  $\phi(\omega_L)$  is close to  $\pi/2$ , i.e.,

$$L\omega_L \geq \gamma \frac{\pi}{2},$$

where empirically,  $\gamma$  (a user selectable parameter) can range from 0.8 to 1. Alternatively, the experiment can also terminate once all the required parameters (maximum sensitivity and stability margins) are obtained. It is also possible, in certain cases, to pre-determine an upper bound for  $L$  (denoted as  $L_{upp}$ ) by identifying the frequency  $\tilde{\omega}$ , where  $G_{ol}(j\tilde{\omega})$  lies on the negative imaginary axis. This can be done by adding an integrator to the compensated system  $G_{ol}(s)$  [23], in addition to the modified relay. Then, it is straightforward to pre-determine  $L_{upp}$  as

$$L_{upp} = \frac{\pi}{2\tilde{\omega}}.$$

### 3.2.3 Stability margins assessment

The gain and phase margins of a compensated system are classical stability indicators which are familiar to most control engineers. In fact, many PID design rules are formulated to achieve desired stability margins which are specified by the users.

The gain margin ( $G_m$ ) and phase margin ( $\phi_m$ ) of a compensated system are defined as follows:

$$G_m = \frac{1}{|G_{ol}(j\omega_u)|}, \quad (3.7)$$

$$\phi_m = \phi(\omega_g) = \pi + \arg G_{ol}(j\omega_g), \quad (3.8)$$

where  $\omega_u$  is the phase-crossover frequency, i.e.,  $\arg G_{ol}(j\omega_u) = -\pi$  and  $\omega_g$  is the gain-crossover frequency, i.e.,  $|G_{ol}(j\omega_g)| = 1$  (Figure 3.6). Typical desired values of  $G_m$  and  $\phi_m$  can range from 2 to 5, and  $\pi/6$  to  $\pi/3$  respectively. Following [23], it may be noted that the following relations hold:

$$G_m > \frac{M_s}{M_s - 1},$$

$$\phi_m > 2 \sin^{-1} \frac{1}{2M_s}.$$



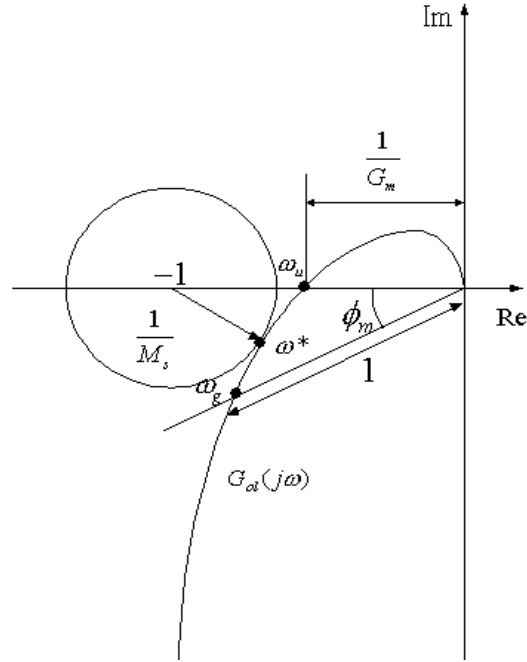


Figure 3.6: Definition of  $G_m$  and  $\phi_m$ .

This implies that typically  $\omega_g < \omega^* < \omega_u$ . The gain and phase margins can be simultaneously identified from the same  $\lambda - \phi$  chart generated earlier without additional experimentation. Referring to Figure 3.7, based on their definitions, it can be shown that the gain margin of the compensated system can be obtained as

$$G_m = \frac{1}{1 - \lambda(\omega_u)},$$

where  $\lambda(\omega_u)$  corresponds to  $\phi = 0$ . Identification of the phase margin  $\phi_m$  is slightly more elaborate. It requires the equivalent point on the chart to be located where  $|G_{ol}(j\omega)| = 1$ . This can be done by substituting  $|G_{ol}(j\omega)| = 1$  into (3.2), thus obtaining the locus of  $|G_{ol}(j\omega)| = 1$  which can be shown to be described by:

$$\lambda = \sqrt{2(1 - \cos \phi)}.$$

The intersection between this locus and the earlier plotted  $\lambda - \phi$  curve will yield  $\phi_m$ .

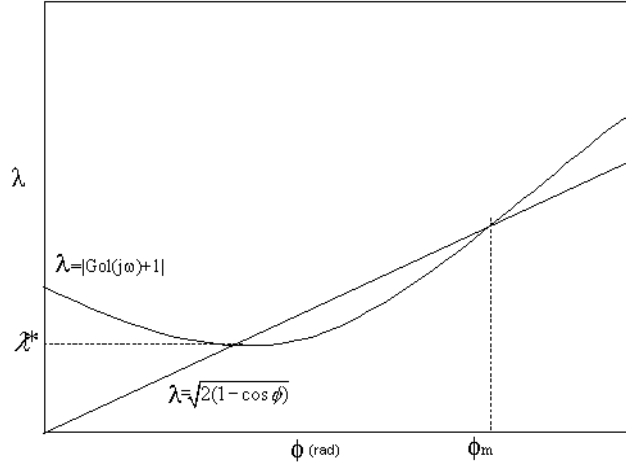


Figure 3.7: Identification of  $G_m$  and  $\phi_m$  from the  $\lambda - \phi$  plot.

### 3.2.4 Simulation example

Consider a high-order system [60] described by:

$$G_p(s) = \frac{1}{(s + 1)^4}.$$

The PI controller used to control the system is described by:

$$G_c(s) = 0.848 + \frac{0.297}{s}.$$

Following the procedures described in Section 3.2.2,  $L$  is varied from 0.01 to 3.5. Table 3.1 shows the variation of  $\lambda$  and  $\phi$  with  $L$ .

Table 3.1: (Relation between  $\lambda$ ,  $\phi$  and  $L$ )

$L$	0.01	0.1	0.3	0.5	0.8	1.00	1.20	1.50	2.0	2.5	3	3.5
$\phi$	0.008	0.075	0.21	0.33	0.45	0.54	0.62	0.70	0.86	1.03	1.15	1.30
$\lambda$	0.67	0.61	0.58	0.55	0.55	0.58	0.60	0.65	0.78	0.93	1.06	1.21

Figure 3.17 shows the  $\lambda - \phi$  plot, from which the maximum sensitivity is identified as  $M_s = 1.82$  and the stability margins as 3.22 ( $G_m$ ) and 1.13 ( $\phi_m$ ).

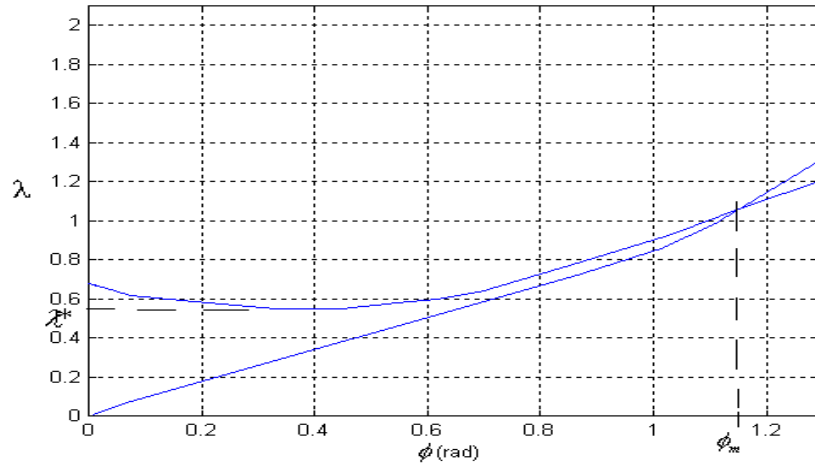


Figure 3.8: Identification of  $M_s$  and stability margins for a high order system.

### 3.3 Assessment Accuracy

Since the main objective of the proposed method is to assess the maximum sensitivity and stability margins of a compensated system, it is useful to investigate the assessment accuracy achievable with the method. To this end, a group of processes with dynamics representing a wide range of those encountered in the process industry [60], [61], is used in a simulation study to assess the accuracy of the parameters thus identified.

A summary of the results is presented in Table 3.2. Using the proposed configuration, it is clearly observed that maximum sensitivity and stability margins can be identified with an acceptable error for all the three cases.

Table 3.2: Assessment accuracy

C ompensated process $G_w = G_p G_c$	Actual			Identified (DF)			Identified (Fourier)			Error(%) (DF)			Error(%) (Fourier)		
	$M_s$	$G_m$	$\phi_m$	$M_s$	$G_m$	$\phi_m$	$M_s$	$G_m$	$\phi_m$	$M_s$	$G_m$	$\phi_m$	$M_s$	$G_m$	$\phi_m$
$G_{p1} = \frac{1}{(s+1)^4}$ $G_{c1} = 0.848 + \frac{0.297}{s}$	1.7	3	1.05	1.82	3.22	.99	1.73	3.03	.98	6.59	6.83	5.26	1.7	.99	6.66
$G_{p2} = \frac{10e^{-2s}}{(s+1)(1.5s+1)(2s+1)}$ $G_{c2} = 0.0478 + \frac{0.0149}{s}$	1.7	2.66	1.05	1.85	2.65	1.09	1.76	2.66	1.04	8.10	.37	3.66	3.4	.37	.96
$G_{p3} = \frac{(1-s)}{s(s+3)}$ $G_{c3} = 0.77 + \frac{0.09}{s}$	1.9	3.72	.807	1.75	3.6	.722	1.8	3.65	.795	7.89	3.22	10.5	5.26	1.88	1.5

### 3.4 PI Control Design Based on Specifications of Maximum Sensitivity and Stability Margins

In this Section, an approach for the design of the PI controller is proposed to concurrently satisfy user specifications in terms of maximum sensitivity and stability margins. Guidelines are given, in the chapter, to assist the user to select generally satisfactory parameters to meet robust design objectives. The PI control parameters are then obtained, via the minimization of objective functions, so that the robustness specifications can be met as closely as possible. A simulation study on commonly encountered processes will show the effectiveness of the proposed design scheme.

### 3.4.1 Robust control design

The newly designed PI controller may be defined as  $\bar{G}_c(s)=G_c(s) + \Delta G_c(s)$ , where  $\Delta G_c(s)$  may be viewed as the incremental adjustment to the original controller  $G_c$  to allow the subsequently compensated system to meet the desired robustness specifications. The robustness function  $\lambda$  can be defined as

$$\lambda(\omega) = G_{ol}(j\omega) + 1. \quad (3.9)$$

Following Section 3.2, the desired (ideal)  $\tilde{\lambda}(\omega)$  is defined as

$$\tilde{\lambda}(\omega) = \tilde{G}_{ol}(j\omega) + 1, \quad (3.10)$$

where  $\tilde{G}_{ol}$  will represent the desired compensated system. In the later part of the chapter, guidelines will be provided on the specifications of  $\tilde{\lambda}(\omega)$ .

Since the actual  $\lambda$  and the ideal  $\tilde{\lambda}$  are both complex, to facilitate subsequent developments, the following relationship is assumed

$$\tilde{\lambda} = k(\omega)\lambda, \quad (3.11)$$

where  $k$  represents a real gain parameter which varies with frequency. This assumption will lead to  $\tilde{\lambda}$  and  $\lambda$  differing only in amplitude and consistent in phase. Now, we may define the ideal controller (based on the specifications) as  $\tilde{G}_c(s)=G_c(s) + \Delta\tilde{G}_c(s)$ , it follows from (3.10) and (3.9) that

$$\tilde{\lambda} = \lambda + \Delta\tilde{G}_c(\omega)G_p(\omega). \quad (3.12)$$

From (3.9),

$$G_p(\omega) = \frac{\lambda - 1}{G_c(\omega)}. \quad (3.13)$$

Therefore,

$$\Delta\tilde{G}_c(\omega) = \frac{(k(\omega) - 1)\lambda}{(\lambda - 1)}G_c(\omega). \quad (3.14)$$

Note that, in this way, the design specifications in terms of  $\tilde{\lambda}(\omega)$  have been translated directly to an objective frequency response for the ideal incremental controller  $\Delta\tilde{G}_c$ . It remains to fit the actual incremental control  $\Delta G_c$  to the ideal control  $\Delta\tilde{G}_c$ , an optimisation effort which will be addressed in later part of this chapter.

### Specification of $\tilde{\lambda}$

Using the assessment method as proposed in Section 3.2, the actual  $|\lambda| - \phi$  plot (Figure 3.7) will be generated which enables the identification of the three robustness indicators ( $M_s$ ,  $G_m$  and  $\phi_m$ ). This plot may serve as the basis for the desired  $|\tilde{\lambda}| - \phi$  plot which will provide for the necessary adjustments to yield the incremental margin for robustness. The user may provide a new ideal plot  $|\tilde{\lambda}| - \phi$ , or he may adjust the current one by specifying the new and improved robustness indicators  $\tilde{M}_s$ ,  $\tilde{G}_m$  and  $\tilde{\phi}_m$ . Combining (3.3), (3.7) and (3.8), where  $\lambda = |\lambda|$ , the desired indicators will translate to three objective points on the  $|\tilde{\lambda}| - \phi$  plot.

$$|\tilde{\lambda}| = \begin{cases} \left(1 - \frac{1}{\tilde{G}_m}\right), & \phi = 0, \\ \frac{1}{\tilde{M}_s}, & \phi = \phi_{\lambda^*}, \\ \sqrt{2(1 - \cos \tilde{\phi}_m)}, & \phi = \phi_m, \end{cases} \quad (3.15)$$

With these three points and possibly existing points on the  $|\lambda| - \phi$  plot, a data interpolation technique (such as the interpolation function available in MATLAB) can be used to generate the  $|\tilde{\lambda}| - \phi$  plot over the frequency range of concern. Then, from this generated

plot and the assumed amplitude scaling relationship between  $\lambda$  and  $\tilde{\lambda}$ , the ideal control frequency response  $\Delta\tilde{G}_c$  can be derived as explained earlier.

### Optimal PI parameters

The incremental controller is also of the PI type and can be represented with the following transfer function

$$\Delta G_c(s) = \Delta K_p + \frac{\Delta K_i}{s}.$$

By separating the real and imaginary part of the incremental controller, the above equation can be written in a matrix form as,

$$\begin{bmatrix} Re\Delta G_c(\omega) \\ Im\Delta G_c(\omega) \end{bmatrix} = \begin{bmatrix} 1 & 0 \\ 0 & -\frac{1}{\omega} \end{bmatrix} \begin{bmatrix} \Delta K_p \\ \Delta K_i \end{bmatrix} \quad (3.16)$$

(3.16) can be written in the linear-in-the parameters form as:

$$Y(\omega) = \theta(\omega)\Phi^T,$$

where  $Y(\omega) = \begin{bmatrix} Re\Delta G_c(\omega) \\ Im\Delta G_c(\omega) \end{bmatrix}$ ,  $\theta(\omega) = \begin{bmatrix} \Delta K_p \\ \Delta K_i \end{bmatrix}$  and  $\Phi^T = \begin{bmatrix} 1 & 0 \\ 0 & -\frac{1}{\omega} \end{bmatrix}$ . Thus, after the incremental controller is designed, the final PI control gains will be  $\bar{K}_p = K_p + \Delta K_p$  and  $\bar{K}_i = K_i + \Delta K_i$ .

The tuning objective is to determine  $\Delta K_p$  and  $\Delta K_i$  such that the frequency response of  $\Delta G_c$  is as close as possible to that of  $\Delta\tilde{G}_c$ . To this end, two objective functions  $J_1$  and  $J_2$  are defined respectively as

$$J_1 = \sum_{i=1}^n \left| (Re(\Delta\tilde{G}_c(\omega_i)) - Re(\Delta G_c(\omega_i))) \right|^2, \quad (3.17)$$

and

$$J_2 = \sum_{i=1}^n \left| (Im(\Delta\tilde{G}_c(\omega_i)) - Im(\Delta G_c(\omega_i))) \right|^2, \quad (3.18)$$

where  $Re$  and  $Im$  denotes the real and imaginary parts of the complex number respectively. These are cost functions in terms of the least squares error for both the real and imaginary part of the designed and ideal control frequency response. The least squares solution to the cost functions is given by

$$\theta = \left( \sum_{i=1}^n \Phi(\omega_i)^T \Phi(\omega_i) \right)^{-1} \left( \sum_{i=1}^n \Phi(\omega_i)^T \tilde{Y}(\omega_i) \right), \quad (3.19)$$

where  $\tilde{Y}(\omega_i) = \begin{bmatrix} Re \Delta \tilde{G}_c(\omega_i) \\ Im \Delta \tilde{G}_c(\omega_i) \end{bmatrix}$ , that is the desired incremental controller found from (3.14)

The tuning procedure is summarized as follows:

- For a given compensated system  $G_{ol}(s)$ , plot  $|\lambda| - \phi$  curve and identify  $M_s$ ,  $G_m$  and  $\phi_m$  as described in Section 3.2. The user may assess if the current robustness indicators are fine. If not, we will proceed to the next steps.
- Obtain the desired  $\tilde{\lambda}$  function from the user, either directly, or generating the function via his specifications of new and desired robust indicators based on the existing plot.
- The desired frequency response for the incremental controller  $\Delta \tilde{G}_c$  can now be obtained via (3.14).
- The incremental controller parameters  $\Delta K_p$  and  $\Delta K_i$  can be determined using the least squares approach via (3.19).

### 3.4.2 Simulation examples

Several examples will be provided in this section to demonstrate the use of the proposed method. The first example will provide the details of proposed tuning method systematically. The other examples will provide a performance comparison study with other relevant



methods. The comparison is made with the PI tuning method proposed in [25] and [27]. The former [25] is based on a sensitivity function under several practical performance constraints. The latter [27] is a method which is designed to meet user-specified gain and phase margins.

**Example 3.8.1:**

Consider a high order process with delay [60],

$$G_p(s) = \frac{10}{(s+1)(1.5s+1)(2s+1)}e^{-2s}.$$

The PI controller used to control the system is described by:

$$G_c(s) = 0.0478 + \frac{0.0149}{s}.$$

Following the procedures adopted Section 3.2, a  $|\lambda| - \phi$  curve is generated (Figure 3.9) and the maximum sensitivity ( $M_s$ ), gain margin ( $G_m$ ) and phase margin ( $\phi_m$ ) are identified as 1.85, 2.65 and 1.09 respectively. The desired maximum sensitivity ( $\tilde{M}_s$ ), gain margin ( $\tilde{G}_m$ ) and phase margin ( $\tilde{\phi}_m$ ) are specified as 1.5, 4 and 1.047 respectively. These specifications are translated to

$$\tilde{\lambda}(\omega) = \begin{cases} 0.750, & \phi = 0, \\ 0.666, & \phi = 0.5464, \\ 0.999, & \phi = 0.722. \end{cases} \quad (3.20)$$

Figure 3.10 shows a plot of  $|\lambda|$  and  $|\tilde{\lambda}|$  versus  $\phi$ . Based on the new plot, the new PI controller is designed as

$$\tilde{G}_c(s) = 0.0255 + \frac{0.0115}{s}.$$

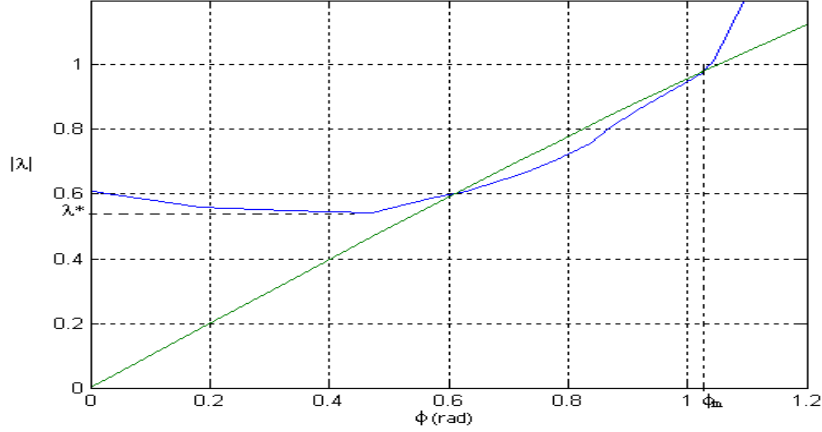


Figure 3.9: A plot of  $|\lambda| - \phi$  for example 1.

The resultant compensated system yields  $M_s = 1.61$ ,  $G_m = 3.84$  and  $\phi_m = 1.086$  respectively. Figure 3.10 shows the closed-loop set-point response under these control settings.

### Example 3.8.2:

Consider a high order and oscillatory process reported in [25]:

$$G_p(s) = \frac{1}{(s^2 + s + 1)(s + 2)} e^{-0.1s}.$$

The PI controller used is described by

$$G_c(s) = 0.7851 + \frac{0.7968}{s}.$$

The desired  $\tilde{M}_s$ ,  $\tilde{G}_m$  and  $\tilde{\phi}_m$  are specified as 1.414, 3.5 and 1.134 respectively. Following the proposed tuning method, the new PI controller is

$$\tilde{G}_c(s) = 0.235 + \frac{0.535}{s}.$$

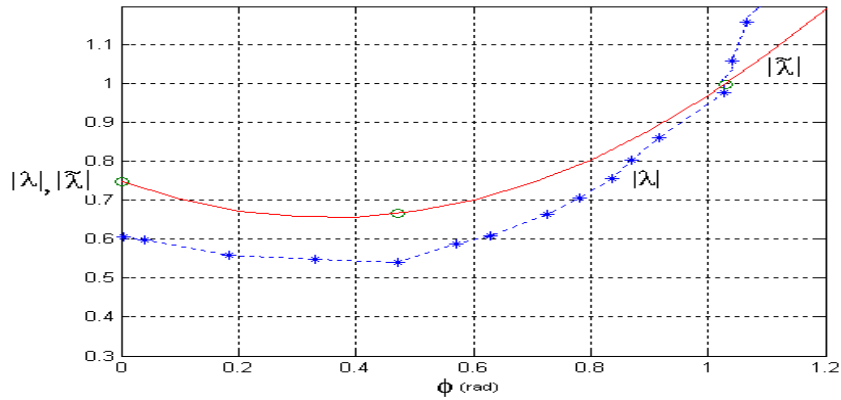


Figure 3.10: Plot of  $|\lambda| - \phi$  and  $|\tilde{\lambda}| - \phi$ ; example 1.

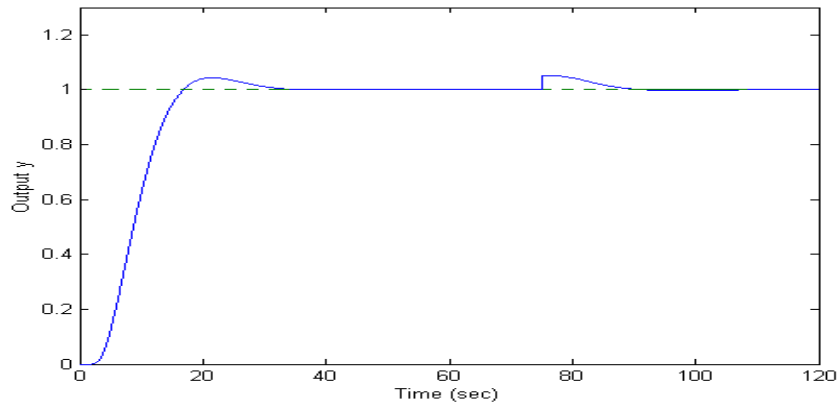


Figure 3.11: Closed-loop response using the proposed tuning method; example 1.

The compensated system achieves  $M_s = 1.47$ ,  $G_m = 3.34$  and  $\phi_m = 1.221$ . Figure 3.12 compares the closed-loop response under the proposed method with the method of Wang [25] with a specification of  $M_s = 1.414$ .

### 3.4.3 Meeting specifications

With the desired values of robustness indicators specified by the user requirement, it is useful to investigate how closely the specifications can be met with the proposed tuning method. To this end, a summary of the results is presented in Table 3.3. The table verifies

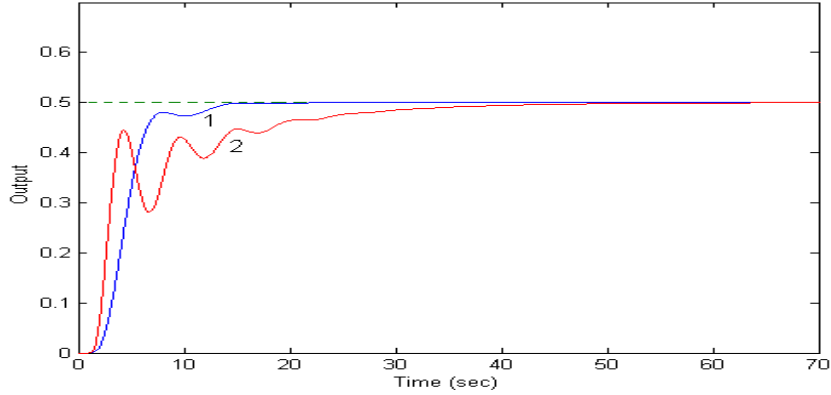


Figure 3.12: Closed-loop response (1) proposed method, (2) Wang’s method; example 2.

that the achieved maximum sensitivity, gain margin and phase margin are rather close to the desired ones.

Since the proposed tuning method makes use of three desired points, there may be some cases where the error of achieved parameters and desired specified parameters are too large. To avoid such incidents, an acceptable range of error is defined in this chapter that is 10%. If for any parameters the error exceeds this range, it is necessary to make some adjustment (by respecifying the desired parameters) so that all three parameters are within the range.

Table 3.3: Comparison of desired and achieved parameters

Compensated Process $G_{ol}(s)$	Desired Parameters			Achieved Parameters			Error(%)		
	$M_s$	$G_m$	$\phi_m$	$M_s$	$G_m$	$\phi_m$	$M_s$	$G_m$	$\phi_m$
$G_P = \frac{10e^{-2s}}{(s+1)(1.5s+1)(2s+1)}$ $G_c = 0.0255 + 0.0115/s$	1.5	4	1.047	1.61	3.84	1.085	6.83	4.16	3.48
$G_P = \frac{e^{-0.1s}}{(s^2 + s + 1)(s + 2)}$ $G_c = 0.235 + 0.535/s$	1.414	3.5	1.134	1.47	3.34	1.221	3.8	4.79	7.125

### 3.5 Real-time Experiment

The proposed modified relay feedback approach for the assessment of robustness is applied to a real-time experiment on water level control in a coupled-tanks apparatus. The apparatus consists of two small tower-type tanks mounted above a reservoir which functions as storage for the water. Water is pumped into the first tank which is then fed through to the second tank and subsequently discharged via gravity back to the reservoir. The level of water in the second tank is controlled by manipulating the speed of the pump. The manipulated variable is therefore the voltage applied to the pump and the process variable is the water level in the second tank. The coupled-tanks apparatus is connected to a PC via an A/D and D/A board. LabVIEW 6.0 from National Instruments is used as the control development platform. A photograph of the experimental set-up is given in Figure 2.9.

Using the basic relay experiment, a PI controller is chosen from a first-order with deadtime model which gives a stable response for the real time experiment and is described as:

$$G_c(s) = 25 + \frac{0.5}{s}.$$

Following the procedures described in Section 3.2,  $L$  is varied from 0.5 to 2.5. Table 3.4 shows the variation of  $\lambda$  and  $\phi$  with  $L$ .

Table 3.4: (Relation between  $\lambda$ ,  $\phi$  and  $L$ )

$L$	0.5	0.6	0.8	1	1.1	1.2	1.3	1.4	1.5	2	2.2	2.5
$\phi$	0.12	0.16	0.24	0.35	0.38	0.42	0.45	0.49	0.55	0.78	1.1	1.31
$\lambda$	0.84	0.81	0.77	0.75	0.72	0.69	0.68	0.68	0.70	0.73	0.96	1.15

Figure 3.13 shows the  $\lambda - \phi$  plot, from which the maximum sensitivity can be identified as  $M_s = 1.47$  and the stability margins as 7.142 ( $G_m$ ) and 0.75 ( $\phi_m$ ).

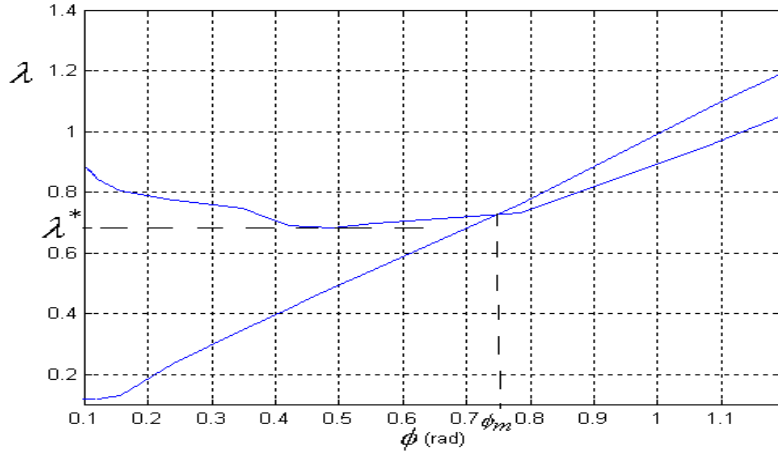


Figure 3.13: Identification of  $M_s$  and the stability margins from the real-time experiment.

The desired  $\tilde{M}_s$ ,  $\tilde{G}_m$  and  $\tilde{\phi}_m$  are specified as 1.47, 4 and 1.047 respectively. Figure 3.14 shows a plot of  $|\lambda|$  and  $|\tilde{\lambda}|$  versus  $\phi$ . Based on this plot, the new PI controller is designed, according to the prescribed procedures, as

$$\bar{G}_c(s) = 19.55 + \frac{0.612}{s}.$$

The resultant compensated system has stability margins of  $M_s = 1.525$ ,  $G_m = 4.435$  and  $\phi_m = 0.973$ , which are close to the specifications. Figure 3.15 shows the closed-loop set-point response under the new tuned controller settings, compared to the response before the controller is adjusted towards the tighter robustness specifications. The figure shows clearly that an improved closed-loop response is achieved with the new specifications and re-tuning.

## 3.6 Online Assessment

The proposed configuration uses the relay within the loop. One disadvantage with such a configuration is that the assessment experiment will affect closed-loop operations since

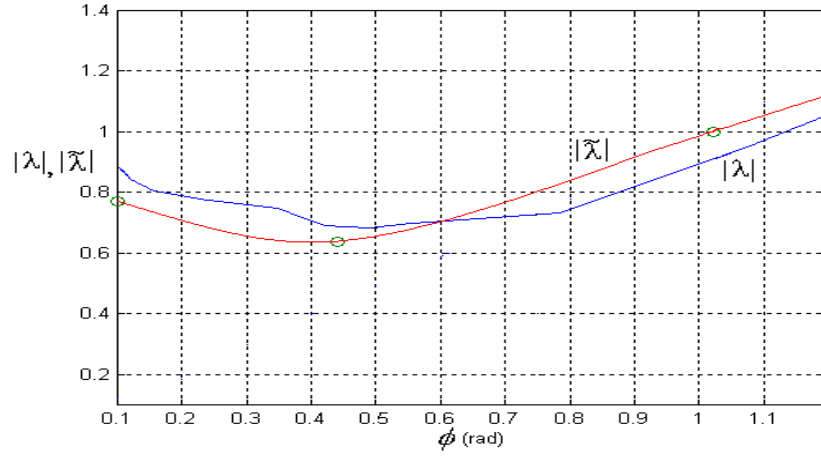


Figure 3.14: Plot of  $|\lambda| - \phi$  and  $|\tilde{\lambda}| - \phi$ ; real-time experiment.

the control loop is disrupted inevitably. The configuration may also be inappropriate when there exists significant disturbances during the experiment as these will distort the oscillations [13], or when a double integrator exists in the loop, in which case no stable oscillations will occur. To this end, it should be mentioned that it is also possible to apply the modified relay outside of the core control loop in the configuration as shown in Figure 3.16. The advantages of using such a configuration are described duly in [12]. Under this configuration, the closed-loop frequency response  $G_{cl}(j\omega)$  is obtained instead, where  $G_{cl} = \frac{G_c G_p}{1 + G_c G_p}$ . However, it is straightforward to obtain  $G_{ol}(j\omega)$  from  $G_{cl}(j\omega)$  via the following equation:

$$G_{ol}(j\omega_u) = \frac{G_{cl}(j\omega_u)}{1 - G_{cl}(j\omega_u)}. \quad (3.21)$$

The procedures prescribed to identify the maximum sensitivity and stability margins remain applicable. Next subsection will illustrate the effectiveness of the online assessment by the similar example that have shown in the Section 3.2.4.

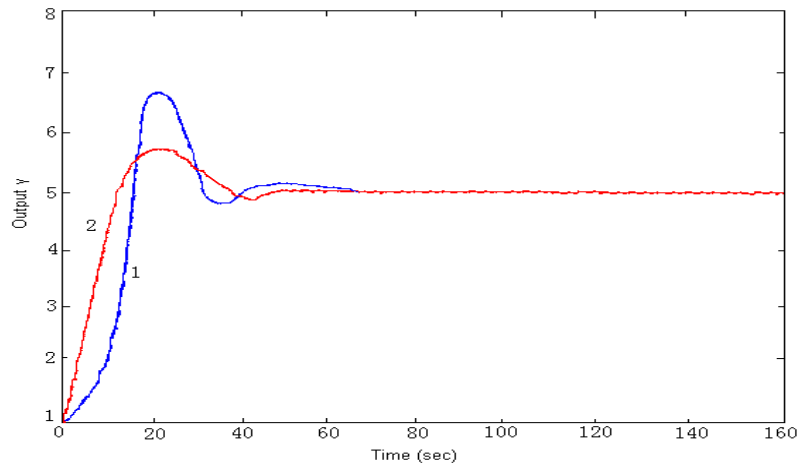


Figure 3.15: Closed-loop response (1) before tuning, (2) after tuning; real-time experiment.

### 3.6.1 Simulation example

Consider the similar high-order system described by:

$$G_p(s) = \frac{1}{(s + 1)^4}.$$

The PI controller used to control the system is described by:

$$G_c(s) = 0.848 + \frac{0.297}{s}.$$

Following the procedures described in Section 3.2.2,  $L$  is varied from 0.01 to 7.5. Table 3.5 shows the variation of  $\lambda$  and  $\phi$  with  $L$ .



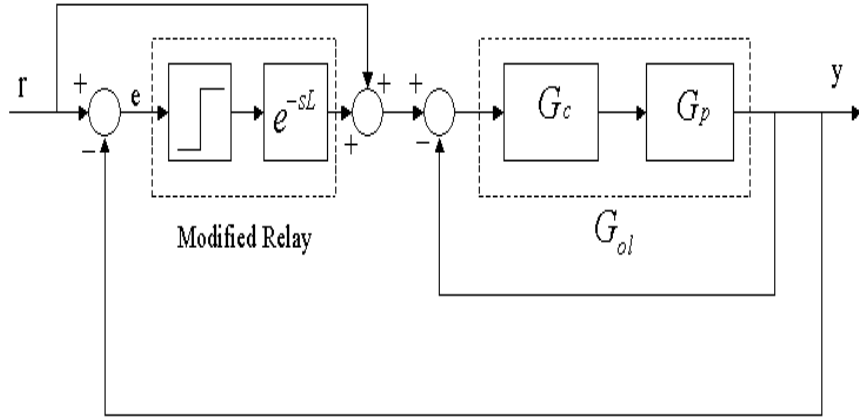


Figure 3.16: Online assessment

Table 3.5: (Relation between  $\lambda$ ,  $\phi$  and  $L$ )

$L$	0.01	0.1	0.5	1.0	1.5	2.00	2.50	3.50	4.0	5.0	6	7.0	7.5
$\phi$	0.005	0.052	0.21	0.35	0.46	0.56	0.65	0.81	0.88	0.97	1.10	1.15	1.153
$\lambda$	0.66	0.64	0.59	0.56	0.57	0.59	0.62	0.72	0.87	0.92	1.00	1.03	1.11

Figure 3.17 shows the  $\lambda - \phi$  plot, from which the maximum sensitivity is identified as  $M_s = 1.75$  and the stability margins as 2.94 ( $G_m$ ) and 1.12 ( $\phi_m$ ). The second intersection point identifies the phase margin ( $\phi_m$ ) as  $|G_{ol}(j\omega)| = 1$  there.

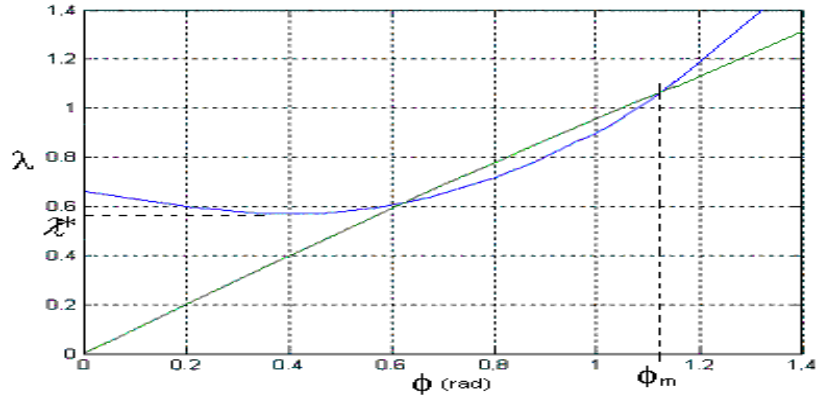


Figure 3.17: Identification of  $M_s$  and stability margins for a high order system.

### 3.6.2 Assessment Accuracy

A summary of the results is presented in Table 3.6. Using the online configuration, it is clearly observed that maximum sensitivity and stability margins can be identified with an acceptable error for all the three cases.

Table 3.6: Assessment accuracy from the on-line configuration

C compensated process $G_{cl} = G_c G_e$	Actual			Identified (DF)			Identified (Fourier)			Error(%) (DF)			Error(%) (Fourier)		
	$M_s$	$G_m$	$\phi_m$	$M_s$	$G_m$	$\phi_m$	$M_s$	$G_m$	$\phi_m$	$M_s$	$G_m$	$\phi_m$	$M_s$	$G_m$	$\phi_m$
$G_{p1} = \frac{1}{(s+1)^4}$ $G_{c1} = 0.848 + \frac{0.297}{s}$	1.7	3	1.05	1.75	2.94	1.12	1.73	3.03	.98	2.86	2.04	6.25	1.7	.99	7.14
$G_{p2} = \frac{10e^{-2s}}{(s+1)(1.5s+1)(2s+1)}$ $G_{c2} = 0.0478 + \frac{0.0149}{s}$	1.7	2.66	1.05	1.72	2.78	1.16	1.76	2.66	1.04	1.16	4.32	9.72	3.4	0.0	.96
$G_{p3} = \frac{(1-s)}{s(s+3)}$ $G_{c3} = 0.77 + \frac{0.09}{s}$	1.9	3.72	.807	1.75	3.45	0.74	1.8	3.65	.795	8.57	7.82	9.05	5.55	1.92	1.5

### 3.7 Improved Robustness Assessment Using a Preload Relay

A modification on the relay is proposed here to increase accuracy on the results. In the new system, the preload relay configuration from Chapter 2 is used with another time delay element. The input to the relay,  $e(t)$  is fed through this time delay element and adds up to the output of the modified relay. The main idea is similar to the Preload relay, by adding a sinusoidal wave to the square wave, it will increase the amplitude of the fundamental frequency component since they share the same frequency. The new time delay element is configured identically as the time delay element in the modified relay block to ensure both signals are in the same phase. In this configuration, a sustained sinusoidal oscillation can be obtained at the output of the compensated process. However, as the time delay increases to a level, the system becomes unstable. Sustained oscillation cannot be obtained at the output. A gain control circuitry is introduced in Figure 3.18 to overcome this flaw.

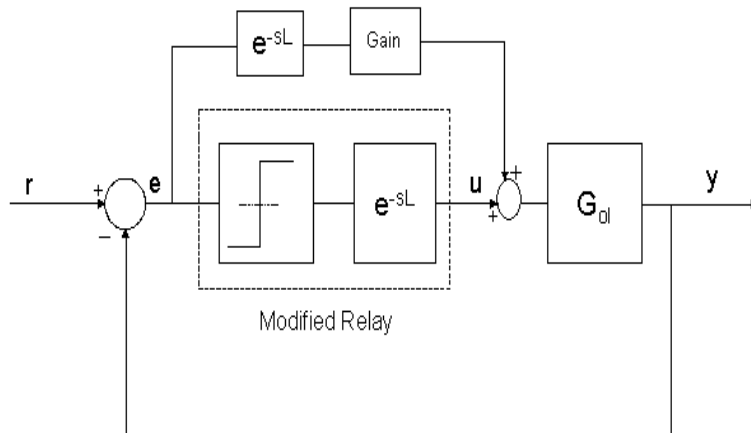


Figure 3.18: Preload relay configuration for improved robustness assessment

Under this configuration (3.4) and (3.5) is changed to the following form,

$$\alpha_L = \frac{\pi a \cos(\omega_L L - \pi)}{4d + \pi a K}, \quad (3.22)$$

$$\beta_L = \frac{\pi a \sin(\omega_L L - \pi)}{4d + \pi a K}. \quad (3.23)$$

The same procedure described in Section 3.2.2 is applied to yield improved assessment accuracy. The method is simulated for similar compensated systems and have shown in Table 3.7.

Table 3.7: Compensated systems for robustness assessment

Compensated process $G_{ol}$	Process $G_p$	Controller $G_c$
A	$G_{p1} = \frac{1}{(s+1)^4}$	$G_{c1} = 0.848 + \frac{0.297}{s}$
B	$G_{p2} = \frac{10}{(s+1)(1.5s+1)(2s+1)}e^{-2s}$	$G_{c2} = 0.0478 + \frac{0.0149}{s}$
C	$G_{p3} = \frac{(1-s)}{s(s+3)}$	$G_{c3} = 0.77 + \frac{0.09}{s}$

Table 3.8: Results of the modified relay feedback system

	Actual Value			Conventional Relay						P_Relay						Improvement		
	$M_s$	$G_m$	$\varphi_m$	$M_s$	PE	$G_m$	PE	$\varphi_m$	PE	$M_s$	PE	$G_m$	PE	$\varphi_m$	PE	$M_s$	$G_m$	$\varphi_m$
A	1.75	3	1.05	1.78	1.71	2.93	2.33	1.01	3.80	1.78	1.71	2.93	2.33	1.02	2.85	0	0	0.95
B	1.7	2.82	1.05	1.78	4.70	2.65	6.02	0.98	6.66	1.77	4.11	2.69	4.60	0.99	5.71	0.59	1.42	0.95
C	1.49	3.72	1.807	1.73	16.10	2.85	23.38	0.71	12.01	1.68	12.75	2.88	22.58	0.74	8.30	3.35	0.8	3.71

Table 3.8 shows the results and improvement in percentage errors for the two methods on the three compensated systems above. The remarkable improvements can be observed specially for type B and type C systems. In general it is observed that phase margin have improved for all the cases.

## 3.8 Conclusion

The chapter has presented a relay feedback approach for the assessment of sensitivity in control systems. The approach uses a relay in series with a time delay element, where the amount of time delay is swept over a range to automatically generate a number of sustained oscillations. From the oscillations, a systematic set of procedures is developed to yield estimates of the maximum sensitivity and stability margins. Simulation examples on a group of processes and a real-time experiment on a coupled-tanks apparatus have verified the effectiveness and assessment accuracy of the proposed approach. Based on the proposed method an approach has been proposed for the design of PI control based on specifications of maximum sensitivity and stability margins. The PI controller is tuned in such a way that the desired and improved specifications can be met closely. Guidelines have been given for a set of generally acceptable specifications. The PI control parameters are obtained via the minimization of objective functions which are derived to fit these robustness characteristics of the compensated system as closely as possible to the user specifications. A simulation study of the control design on commonly encountered processes has verified the effectiveness of the proposed scheme.

# Chapter 4

## Robust Control of Nonlinear Systems Using a Preload Relay

### 4.1 Introduction

The PID controller has remained arguably the top performing industrial controller since its inauguration, both in terms of sales and applications. This phenomenon is remarkable, since research and development in both the theoretical and application aspects of advanced and complex control systems has been persistently striving, judging by the greatly increased number of academic journals devoted to this area in the past two decades. The continued success of this controller provides a strong testimony to the rule-of-thumb in engineering practice, the TSTF (Try Simple Things First) principle. Indeed, the PID controller has probably the most impressive record in terms of the number of successful industrial applications. It is simple to use, to the extent that almost everyone with some basic knowledge in control engineering can commission it satisfactorily. To some, however, it has become uninteresting, the incremental reward from doing more work to a controller as established

as this has been deemed not worth the while. However, the irony remains that this “simple and uninteresting controller” still provides the driving force to the millions of automation and manufacturing systems operating every day, in almost all industries where a control system is needed.

A multitude of approaches towards the design of PID control for linear systems has been reported over the years [1], [23], [31]. For nonlinear systems, adaptive control methods are rampantly suggested and used in the literature [62], [63]. However, one should be careful of the possible abuse of adaptive schemes, which being inherently nonlinear, is much more complicated than a fixed gain regulator. Under the harsh realities of a practical control environment, the pre-requisites for an effective application of adaptive control can be easily breached, yielding results which are far from satisfactory, and in many cases, worse than that achievable by the good old PID control. This is despite of the more significant effort and resources used in the implementation of adaptive control schemes.

A gain scheduling and robust high gain control should thus be considered as alternatives to adaptive control algorithms [29], [30]. The gain schedule is typically a tabulation of setpoint versus control parameters. Essentially, this approach views a nonlinear system as a collection of linear ones throughout the operating range. Thus, it requires good and sound knowledge about the system and also that some auxiliary variables can be measured. Ultimately, the achievable performance with such a scheme depends on the resolution of the tabulation. A finer resolution is accompanied by a more than proportional amount of work to derive the linear models necessary to yield the control gains at the various operational levels where calibration is done. In between these levels, linear interpolation is usually applied to derive intermediate gains. If the system parameters are uncertain and changes with time, the scheme rapidly becomes less attractive, as the validity of the gain schedule is time limited and the amount of work necessary to initiate and update the gain schedule

can be tremendous.

In this chapter, a novel high gain feedback control system is proposed, involving the use of a preload relay (P\_Relay) in series with the usual PID controller, for robust control of nonlinear systems which are possibly also time varying. The proposed system may be viewed as an extended and a more general form of the self-oscillating adaptive system (SOAS) first used by Honeywell [34] in the flight control systems. The SOAS has a very desirable property: it tracks automatically an amplitude margin of two in the closed loop, by using an on-off element. However, this desirable property is inherited along with inevitable chattering in the control signal, although the amplitude of which can be adjusted via a lead-lag compensator. This greatly limits its applications, since the inevitable chattering phenomenon implies that SOAS will not be suitable when valves or other mechanical parts are used as actuators, due to the potential wear and tear problems it will bring about.

The proposed control system, in this chapter, retains and extends on the nice stability property of the SOAS. The amplitude margin of two can still be achieved, and it is now adjustable so that a higher or lower closed-loop amplitude margin can be set via the proportional part of the preload relay, depending on the requirements. The chattering phenomenon is still inherently evident since a relay continues to be used in the control configuration. However, in the chapter, instead of viewing it as an undesirable feature, the chattering information will be used to tune and re-tune the PID controller, as the operating regime digresses. The chattering signals are naturally occurring, thus no further explicit test signals are required. The PID gains will therefore change from one setpoint to another, exactly as an efficient gain scheduler with a very fine tabulation resolution will work, yet the gain adaptation will continue to take place, as long as the chattering exists. Thus, the method is applicable to time varying systems as well. Once the PID control is tuned to a new operating point, the relay part of the control system can be switched off and



the chattering will cease consequently. It can be invoked again when another change in setpoint is initiated. Theoretical analysis will be provided in the chapter to illustrate the nice stability properties of the control scheme, with respect to closed-loop stability margins and robustness. The effectiveness of this control scheme will be illustrated via a simulation study and real-time experiment on the level control of fluid in a spherical tank.

## 4.2 Proposed Control Scheme

The proposed control scheme comprises of a preload relay in series with a PID controller as shown in Figure 5.1.

The control scheme of Figure 5.1 may be posed equivalently in the configuration of

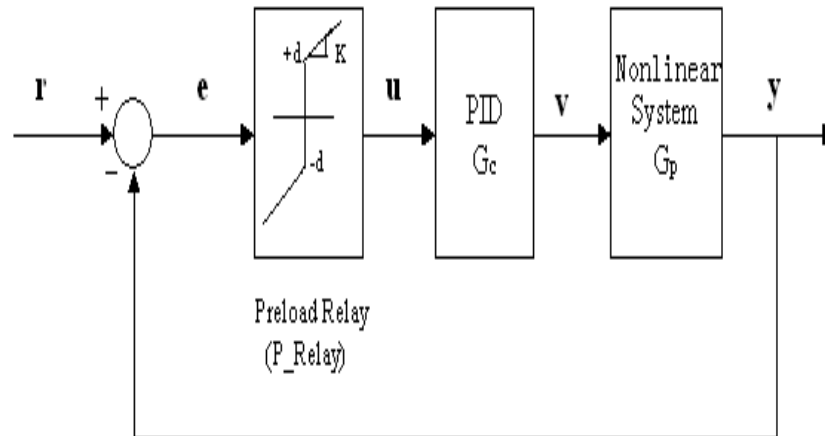


Figure 4.1: Schematic of the proposed control scheme.

Figure 5.2, since the preload relay (P\_Relay, described in chapter 2) is equivalent to a parallel connection of the usual relay with a proportional gain. The PID compensated system, comprising of the PID controller and the nonlinear system, may be considered as

the equivalent system under the control of the P\_Relay. This equivalent form of the control configuration holds certain useful features in the analysis and design of the controller as will be illustrated in due course.

In the following sub-sections, the function of each component of the overall control scheme will be briefly described.

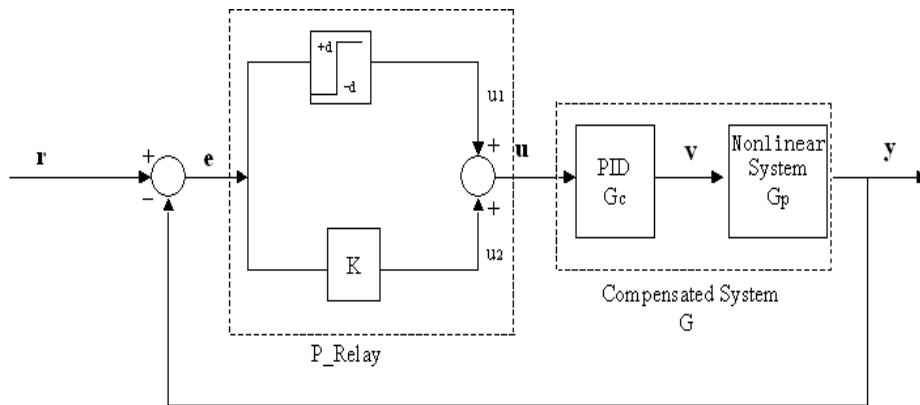


Figure 4.2: Equivalent form of the proposed control scheme.

### 4.2.1 PID control

PID control remains a core component of the proposed control scheme. However, since the system, considered in this chapter is nonlinear and possibly time varying, PID control with a fixed set of parameters does not suffice to yield good consistent performance. To this end, some way to automatically adjust PID gains to adapt the controller to changes in the operating setpoint is highly desirable. While it is indeed possible to re-tune the controller to perform at a new setpoint via an independent tuning experiment (such as a step or relay test), the focus of the chapter is to use naturally occurring signals in the closed-loop for

the PID self-tuning purposes. Thus, there is no need to incur additional resources or to break the loop for additional identification experiments. The preload relay (`P_Relay`), to be described in the next subsection, will fulfill this requirement.

### 4.2.2 Preload relay

The `P_Relay` is introduced in this chapter to maintain robust performance as the dynamics of the system changes with time, or changes in response to a change in operating point. This interesting property will be elaborated in Section 4.4.

While the use of an on-off element is useful for robust control, it also induces chattering. Most control practitioners dislike the chattering phenomenon as it greatly limits practical applications, due to the potential wear and tear problems it causes when mechanical actuators are used. In this chapter, it is attempted to use the limit cycle oscillations induced in the steady state, over a limited time span, to tune and re-tune the PID controller, as the operating point changes. Thus, no other explicit input signal is required. Once tuned for the new operating point, the `P_Relay` can be switched off and chattering will also cease correspondingly. It is invoked again to fulfill the robust performance requirement when the next change in operating point/setpoint is commanded.

## 4.3 Self-tuning PID Control

In this section, the self-tuning of the PID control from the limit cycle oscillations naturally induced by the `P_Relay` will be elaborated. Two possible approaches are highlighted, one is a non-parametric approach based on a prototype frequency response specified by the user, and the other is a parametric approach where the PID control is tuned based on a

low-order rational transfer function model.

### 4.3.1 Prototype frequency response approach

In the prototype frequency response approach, the controller is tuned based directly on the frequency response information of the system obtained from the chattering signal. No structural assumption is made of the system. When the closed-loop system settles in a steady-state limit cycle oscillation at frequency  $\omega_c$ ,  $G_p(j\omega_c)$  can be obtained from a Fourier or frequency analysis of the signals  $v$  and  $y$  in the usual manner.

Denote the prototype frequency response at this point as  $\bar{G}_{yr}(j\omega_c)$ . This point may be obtained directly from the user specification of a desirable closed-loop transfer function [12]. The desired frequency response of the controller at the oscillating frequency  $\omega_c$  denoted by  $\bar{G}_c(j\omega_c)$  may then be derived from  $G_p(j\omega_c)$  and prototype frequency response  $\bar{G}_{yr}(j\omega_c)$  at the oscillating frequency  $\omega_c$ , i.e.,

$$\bar{G}_c(j\omega_c) = \frac{\bar{G}_{yr}(j\omega_c)}{G_p(j\omega_c)(1 - \bar{G}_{yr}(j\omega_c))}. \quad (4.1)$$

Suppose  $G_c(s)$  is a PI controller given by:

$$G_c(s) = K_c \left( 1 + \frac{1}{T_i s} \right).$$

$K_c$  and  $T_i$ , may thus be chosen so that  $G_c(j\omega) = \bar{G}_c(j\omega)$  for  $\omega = \omega_c$ . Denoting  $\bar{G}_c(j\omega_c)$  explicitly as  $\bar{G}_c(j\omega_c) = g_{c,r} + jg_{c,i}$ , and matching  $G_c(j\omega_c)$  to  $\bar{G}_c(j\omega_c)$ , the control parameters can thus be obtained as:

$$K_c = g_{c,r},$$

and

$$T_i = -\frac{g_{c,r}}{g_{c,i}\omega_c}.$$

If a full PID controller is to be used, i.e.,

$$G_c(s) = K_c \left( 1 + \frac{1}{T_i s} + T_d s \right),$$

$T_d$  can be chosen according to the heuristic rule  $T_d = 0.25T_i$  of [1].

### 4.3.2 Parametric approach

The parametric approach will attempt to fit a low-order transfer function model, based on the chattering signals already prevalent in the loop. The PID controller can then be tuned based on the parametric model. In this section, a first order rational transfer function model with deadtime is considered as:

$$\hat{G}_p(s) = \frac{K_p}{T_s + 1} e^{-Ls}.$$

This model is simple in structure, with only three model parameters. Yet, it is one of the most common and adequate ones used, especially in the process control industries.

The describing function of the P\_Relay is given by:

$$N(a) = \left( \frac{4d}{\pi a} + K \right),$$

where  $d$  is the relay amplitude,  $K$  is the proportional gain part of the P\_Relay, and  $a$  is the amplitude of the limit cycle oscillation. The PID compensated system  $G$ , comprising of the PID controller  $G_c$  and the actual system  $G_p$ , is denoted as:

$$G(s) = G_c(s)G_p(s).$$

It should be clarified and reinforced here that although the system concerned is a nonlinear one, our approach is to view the nonlinear dynamics as a variation of linear ones along the operational range, thus the use of transfer function representation at individual operating points.

Under the relay feedback, the amplitude ( $a$ ) and oscillation frequency ( $\omega_c$ ) of the limit cycle is thus given approximately by the solution to:

$$G(j\omega_c) = -\frac{1}{N(a)}. \quad (4.2)$$

The complex equation (4.2) will generate the following two equations:

$$|G(j\omega_c)| = \left| \frac{1}{N(a)} \right|,$$

$$\arg G(j\omega_c) + \arg(N(a)) = -\pi.$$

$K_p$  can be determined from  $K_p = \frac{\Delta y_{ss}}{\Delta u_{ss}}$  following a change in setpoint, where  $\Delta y_{ss}$  and  $\Delta u_{ss}$  denotes the steady state change in the output and input of the system respectively. The remaining two unknown parameters  $T$  and  $L$  of the model can be obtained from the solution of these equations as:

$$T = \frac{1}{\omega_c} \sqrt{\left( \frac{K_p(4d + \pi a K)}{\gamma \pi a} \right)^2 - 1}, \quad (4.3)$$

$$L = \frac{(\pi + \arg G_c(j\omega_c) - \tan^{-1} T \omega_c)}{\omega_c}, \quad (4.4)$$

where  $\gamma = \left| \frac{1}{G_c(j\omega_c)} \right|$ .

Based on this model, many approaches to tune the PID controller have been proposed

[12]. In this chapter, without prejudice, the tuning method proposed by [64] is used, where the PID parameters are given by:

$$K_c = \frac{T}{K_p(L + T_c)},$$

$$T_i = T,$$

$$T_d = \frac{L}{2}.$$

$T_c$  is the desired closed-loop time constant.

## 4.4 Properties of Control Scheme

The use of a relay in the proposed control structure induces control chattering which is utilized positively in the tuning and re-tuning of the PID controllers as shown in Section 4.3. This stability property of P\_Relay will be illustrated in this section. The motivation for having a proportional gain in parallel with the normal relay (i.e., the P\_Relay) to achieve an adjustable margin will be further elaborated.

For an analysis of the closed-loop properties, the propagation of a signal in the closed-loop is considered, comprising of a sinusoidal component representative of the chattering phenomenon and a slowly changing and small component arising due to setpoint changes or the presence of disturbances. Correspondingly, the error signal  $e(t)$  can be expressed in the form:

$$e(t) = a \sin \omega t + b(t),$$

where  $a \sin \omega t$  is the high frequency component and  $b(t)$  is the low frequency (almost d.c.) component. It is assumed that  $b(t)$  varies so slowly that it can be approximated by a constant. This assumption is reasonable especially when the system is near steady state

condition, so that  $e = r - y$  is small and almost constant.

It is considered first the propagation of  $e(t)$  through the P\_Relay. The output of the P\_Relay ( $u$ ) is thus a combination of the signals  $u_1$  and  $u_2$ , which are the outputs from the relay and the proportional gain respectively.

Clearly,

$$u_2 = Kb + Ka \sin \omega t.$$

Following [34], a describing function analysis yields:

$$u_1 = N_B b + N_A a \sin \omega t,$$

where

$$N_B = \frac{2d}{\pi b} \sin^{-1} \left( \frac{b}{a} \right),$$

and

$$N_A = \frac{4d}{\pi a} \sqrt{1 - \left( \frac{b}{a} \right)^2}.$$

The describing function analysis considers only the d.c. and first harmonic component in the output of the relay, since the higher harmonics are likely to be attenuated by the linear parts of the system.  $N_B$  which describes the propagation of a constant signal is called the dual-input describing function.

Since  $b$  is small compared to  $a$ ,

$$N_B \approx \frac{2d}{\pi a},$$

and

$$N_A \approx \frac{4d}{\pi a}.$$



Therefore,  $u = u_1 + u_2$  can be expressed in terms of the equivalent describing functions of the P\_Relay  $\tilde{N}_A$  and  $\tilde{N}_B$  as

$$u = \tilde{N}_B b + \tilde{N}_A a \sin \omega t,$$

where  $\tilde{N}_B = N_B + K$  and  $\tilde{N}_A = N_A + K$ .

The ratio,

$$\frac{\tilde{N}_B}{\tilde{N}_A} = \frac{4d + \pi a K}{2d + \pi a K},$$

as it will be illustrated shortly, relates to the closed-loop amplitude margin.

The tools for explaining the properties of the closed-loop are now available. Applying the describing function analysis to the system of Figure 4.2 for the transmission of the sinusoidal signal, it follows that

$$\tilde{N}_A |G(j\omega_c)| = 1. \quad (4.5)$$

The amplitude of oscillation thus automatically adjusts so that the loop gain is unity at the oscillating frequency  $\omega_c$  of the chattering signal. Now consider the propagation of slowly varying signals superimposed on the chattering signals. The propagation of the signals through the linear parts of the system is described by  $\tilde{N}_B$ . The propagation of slowly varying signals is thus approximately described by the loop transfer function:

$$G_0(s) = \tilde{N}_B(a)G(s).$$

It follows from (4) and (5) that

$$|G_0(j\omega_c)| = \tilde{N}_B(a)|G(j\omega_c)| = \frac{\tilde{N}_B}{\tilde{N}_A} \tilde{N}_A |G(j\omega_c)| = \frac{\tilde{N}_B}{\tilde{N}_A} = \frac{2d + \pi a K}{4d + \pi a K}. \quad (4.6)$$

Choosing  $K = 0$ , the system reduces to the basic SOAS as,

$$|G_0(j\omega_c)| = 0.5,$$

i.e., an amplitude margin of two is achieved. However, more general than the SOAS, the amplitude margin can be varied by using a non-zero gain  $K$ . Figure 4.3 illustrates how the amplitude margin varies with different choice of  $K$  for a certain chattering amplitude  $a$ . Depending on the actual requirements, a faster response (but less stable) can be achieved with a small positive  $K$ , and a slower (but more stable) response can be achieved with a small negative  $K$ . However, one should be careful when choosing a negative  $K$  that the conditions  $\tilde{N}_A, \tilde{N}_B > 0$  are preserved. In the next section, a robustness analysis of the

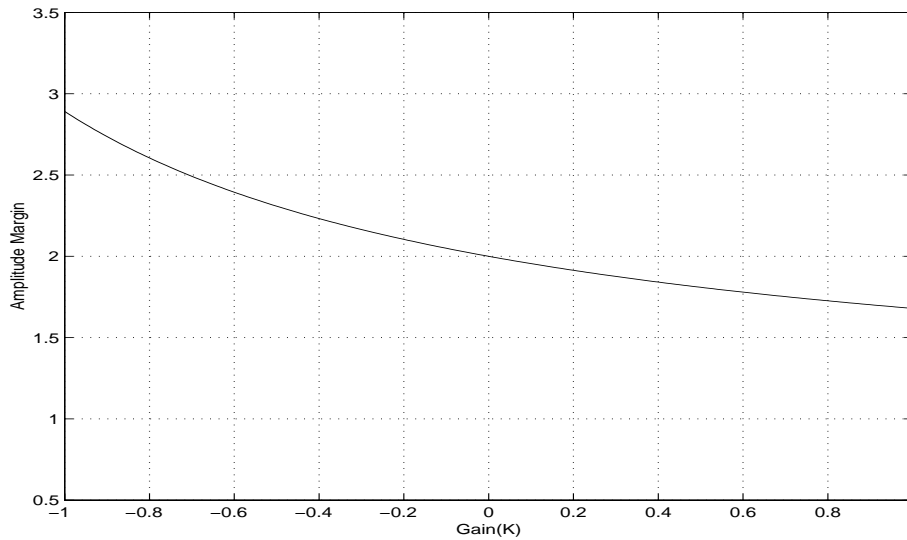


Figure 4.3: Variation of amplitude margin with  $K$ .

control scheme will be provided with respect to a dominant linear model with a possibly nonlinear and uncertain part.

## 4.5 Robustness Analysis

Consider a class of nonlinear systems described by:

$$\ddot{y} = a\dot{y} + by + cv + f(y, \dot{y}), \quad (4.7)$$

where the nonlinear part described by  $f(y, \dot{y})$  is assumed to be bounded, i.e.,  $\|f(y, \dot{y})\| \leq f_M$ .

Define the error between the desired trajectory  $r$  and the system output  $y$ :

$$e = r - y. \quad (4.8)$$

Under the proposed structure,

$$u = d \operatorname{sgn}(e) + Ke, \quad (4.9)$$

where  $\operatorname{sgn}(\cdot)$  is the usual sign operator. The control  $v$  is given by:

$$v = k_p u + k_i \int_0^t u d\tau + k_d \dot{u}, \quad (4.10)$$

where  $k_p = K_c$ ,  $k_i = \frac{K_c}{T_i}$  and  $k_d = K_c T_d$ , directly relating to the earlier set of PID notations used. Substituting  $u$  into  $v$  yields

$$v = k_p Ke + k_i K \int_0^t e d\tau + k_d K \dot{e} + k_p d \operatorname{sgn}(e) + k_i d \int_0^t \operatorname{sgn}(e) d\tau + k_d d \operatorname{sgn}(\dot{e}). \quad (4.11)$$

For closed-loop control based on the model (5.1) under the control (5.3), it follows that

$$\begin{aligned} \ddot{e} = & a\dot{e} + be - ck_p Ke - ck_i K \int_0^t e d\tau - ck_d K \dot{e} - ck_p d \operatorname{sgn}(e) - ck_i d \int_0^t \operatorname{sgn}(e) d\tau \\ & - ck_d d \operatorname{sgn}(\dot{e}) - f(y, \dot{y}) + f_d. \end{aligned} \quad (4.12)$$

Letting

$$z = \left[ \int_0^t e d\tau \quad e \quad \dot{e} \right]^T, \quad (4.13)$$

and it shows

$$\dot{z} = Az + B[D(t) - f(y, \dot{y}) + f_d], \quad (4.14)$$

where

$$A = \begin{bmatrix} 0 & 1 & 0 \\ 0 & 0 & 1 \\ -ck_iK & b - ck_pK & a - ck_dK \end{bmatrix}, \quad (4.15)$$

$$B = \begin{bmatrix} 0 \\ 0 \\ 1 \end{bmatrix}, \quad (4.16)$$

$$D(t) = -ck_p d \operatorname{sgn}(e) - ck_i d \int_0^t \operatorname{sgn}(e) d\tau - ck_d d \operatorname{sgn}(\dot{e}), \quad (4.17)$$

$$f_d = \ddot{r} - a\dot{r} - br. \quad (4.18)$$

Note that the PID parameters  $k_p, k_i, k_d$  with  $K$  can be tuned to ensure the dominant system is stable. This implies that  $A$  is a stable matrix. Thus, the following Lyapunov equation holds:

$$A^T P + PA = -I, \quad (4.19)$$

where  $I$  is the unit matrix.

**Theorem 4.1.** Assume that system (4.7) admits a symmetric relay-induced oscillation under the setup proposed. Then, if the PID parameters with  $K$  are tuned properly, the state  $y$  is uniformly bounded.

**Proof.**

Define the Lyapunov function

$$V = z^T P z. \quad (4.20)$$

The derivative of  $V$  is given by:

$$\begin{aligned} \dot{V} &= z^T (A^T P + PA) z + 2z^T P B D(t) - 2z^T P B f(y, \dot{y}) + 2z^T P B f_d \\ &= -\|z\|^2 + 2z^T P B D(t) - 2z^T P B f(y, \dot{y}) + 2z^T P B f_d. \end{aligned} \quad (4.21)$$

Note that  $\|f(y, \dot{y})\| \leq f_M$  and  $\|f_d\| \leq f_{dM}$ . Thus, it shows

$$-2z^T P B f(y, \dot{y}) \leq \eta z^T P B B^T P z + \frac{1}{\eta} f^2 \leq \eta z^T P B B^T P z + \frac{1}{\eta} f_M^2, \quad (4.22)$$

$$2z^T P B f_d \leq \eta z^T P B B^T P z + \frac{1}{\eta} f_d^2 \leq \eta z^T P B B^T P z + \frac{1}{\eta} f_{dM}^2, \quad (4.23)$$

where  $\eta$  is an arbitrary constant.

For the term  $d \int_0^t \text{sgn}(e) d\tau$  in  $D(t)$ , the assumption of a symmetric relay-induced oscillation is noted. Let us denote the relay switching number  $j$ . Then, if  $j = 2n$  (i.e., an even number of relay switches) for  $0 < \tau < t$ ,

$$\begin{aligned} d \int_0^t \text{sgn}(e) d\tau &= d \left[ \int_0^{t_1} \text{sgn}(e) d\tau + \int_{t_1}^{t_2} \text{sgn}(e) d\tau + \dots + \int_{t_{2n-1}}^{t_{2n}} \text{sgn}(e) d\tau \right] \\ &= 0; \end{aligned} \quad (4.24)$$

If  $j = 2n + 1$  (i.e., an odd number of relay switches) for  $0 < \tau < t$ ,

$$\begin{aligned} d \int_0^t \text{sgn}(e) d\tau &= d \left[ \int_0^{t_1} \text{sgn}(e) d\tau + \int_{t_1}^{t_2} \text{sgn}(e) d\tau + \dots + \int_{t_{2n-1}}^{t_{2n}} \text{sgn}(e) d\tau + \int_{t_{2n}}^{t_{2n+1}} \text{sgn}(e) d\tau \right] \\ &= d \int_{t_{2n}}^{t_{2n+1}} \text{sgn}(e) d\tau \leq d \int_{t_{2n}}^{t_{2n+1}} |\text{sgn}(e)| d\tau \leq d(t_{2n+1} - t_{2n}). \end{aligned} \quad (4.25)$$

In summary,  $d \int_0^t \text{sgn}(e) d\tau \leq d(t_{2n+1} - t_{2n})$ . Thus, it shows

$$\|D(t)\| \leq ck_p d + ck_i d(t_{2n+1} - t_{2n}) + ck_d d \|\dot{\text{sgn}}(e)\|. \quad (4.26)$$

Define

$$s = \text{sgn}(e).$$

Following [65], the function  $s$  has the following useful properties:

$$\dot{s} = 0; e > 0, \text{ or } e < 0.$$

Therefore, it follows that

$$\|D(t)\| \leq ck_p d + ck_i d(t_{2n+1} - t_{2n}) = D_M \text{ for } e > 0 \text{ or } e < 0. \quad (4.27)$$

Now the term  $2z^T PBD(t)$  can be expressed approximately as

$$2z^T PBD(t) \leq \eta z^T PBB^T Pz + \frac{1}{\eta} D^2(t) \leq \eta z^T PBB^T Pz + \frac{1}{\eta} D_M^2 \text{ for } e > 0 \text{ or } e < 0. \quad (4.28)$$

The following derivative of  $V$  is thus obtained for  $e > 0$  or  $e < 0$ .

$$\begin{aligned} \dot{V} &\leq -\|z\|^2 + 3\eta\lambda_{\max}(PBB^T P)\|z\|^2 + \frac{1}{\eta}f_M^2 + \frac{1}{\eta}f_{dM}^2 + \frac{1}{\eta}D_M^2 \\ &= -[1 - 3\eta\lambda_{\max}(PBB^T P)]\|z\|^2 + \frac{1}{\eta}f_M^2 + \frac{1}{\eta}f_{dM}^2 + \frac{1}{\eta}D_M^2. \end{aligned} \quad (4.29)$$

Let  $\rho = 1 - 3\eta\lambda_{\max}(PBB^T P)$  and choose  $\eta$  subject to  $0 < \eta < \frac{1}{3\lambda_{\max}(PBB^T P)}$ . Since  $\lambda_{\min}(P)\|z\|^2 \leq V \leq \lambda_{\max}(P)\|z\|^2$ , it follows that

$$\dot{V} \leq -\frac{\rho}{\lambda_{\max}(P)}V + \frac{1}{\eta}f_M^2 + \frac{1}{\eta}f_{dM}^2 + \frac{1}{\eta}D_M^2 = -\frac{\rho}{\lambda_{\max}(P)}V + \rho_0, \quad (4.30)$$

where  $\rho_0 = \frac{1}{\eta}f_M^2 + \frac{1}{\eta}f_{dM}^2 + \frac{1}{\eta}D_M^2$ .

Hence,

$$V(t) \leq \frac{\rho_0\lambda_{\max}(P)}{\rho} + \left[ V(0) - \frac{\rho_0\lambda_{\max}(P)}{\rho} \right] e^{-\frac{\rho}{\lambda_{\max}(P)}t}. \quad (4.31)$$

For state  $z$ , it thus follows that

$$\|z\| \leq \sqrt{\frac{\rho_0\lambda_{\max}(P)}{\lambda_{\min}(P)\rho} + \left[ V(0) - \frac{\rho_0\lambda_{\max}(P)}{\lambda_{\min}(P)\rho} \right] e^{-\frac{\rho}{\lambda_{\max}(P)}t}}. \quad (4.32)$$

This implies that

$$\lim_{t \rightarrow \infty} \|z(t)\| = \sqrt{\frac{\rho_0\lambda_{\max}(P)}{\lambda_{\min}(P)\rho}}, \quad (4.33)$$

i.e., state  $z$  is bounded under the conditions given in Theorem 4.1.

## 4.6 Simulation Study

To illustrate the performance attainable with the proposed control system, a simulation study is carried out on the level control of fluid in the classical spherical tank system. This

fluid level control problem is a common one associated with storage tanks, and blending and reaction vessels in the process industries. The spherical tank system is shown in Figure 4.4, it is essentially a system with nonlinear dynamics. The spherical tank has nonlinear dynamics described by the first-order differential equation;

$$Q_i(t - L) - Q_o = \pi R^2 \left[ 1 - \frac{(R - y)^2}{R^2} \right] \frac{dy}{dt},$$

where  $R$  is the radius of the spherical tank and the difference between the inflow  $Q_i$  and outflow  $Q_o$  causes the water level  $y$  to rise or fall in a manner described by the nonlinear first-order differential equation above.  $L$  represents the time delay due to the pipeline feeding the water from a reservoir into the spherical tank. From the expression, it can be seen that the rise time of the water level is fastest at the top and the bottom of the tank, but slowest at the middle, as befits intuition. The outflow of the tank is dependent on the water level in line with the Bernoulli equation which states that the outflow of a tank is proportional to the square root of the height of the fluid level:

$$Q_o = c_d \alpha \sqrt{2g(y - y_o)}.$$

In this simulation, the following parameters will respect to the spherical tank and P\_Relay are selected;  $R = 1$ ,  $c_d = 1$ ,  $\alpha = 1$ ,  $y_o = 0.1$ ,  $L = 0.05$  and  $d = 5$ .

#### 4.6.1 Performance with different gain settings

The first part of the simulation will illustrate the performance of the control system with different choice of  $K$ , resulting in different closed-loop amplitude margin. Three setpoint changes to different desired levels will be simulated, each followed by the simulation of a static load disturbance (with an amplitude roughly 10% of the setpoint change) seeping in. Figure 5.3 shows the closed-loop response for  $K = 0$ . In this case, the loop gain is

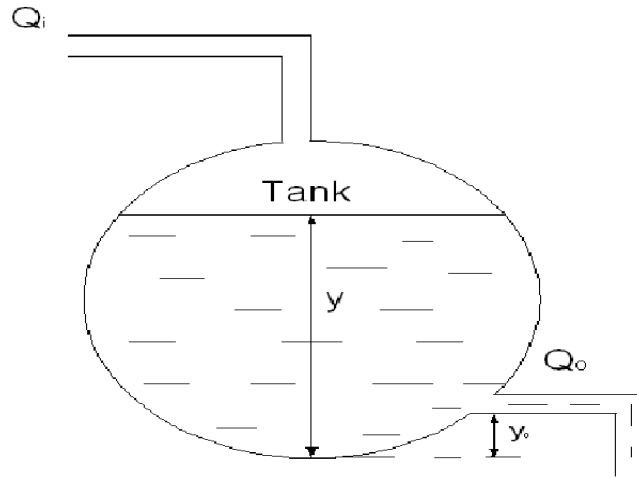


Figure 4.4: Spherical tank.

automatically adjusted to give an amplitude margin of two. Figure 4.6 shows an amplified portion of the first setpoint response, clearly illustrating the three phases during which different combinations of the control components are active. In the first phase, the P\_Relay is at work with the PID controller which is tuned to the previous operating point before the setpoint change. The P\_Relay ensures a robust transient response to the step change. In the second phase, the PID controller is tuned using the inherent limit cycle oscillations to the new setpoint. In the simulation study, the tuning is based on the parametric method presented in Section 4.3.2 with  $T_c = 0.34$ . In the third phase, the tuned PID controller resumes complete control responsibility and the P\_Relay is switched off. The steady state chattering phenomenon is thus only in force for a limited time span, during the second phase. This time duration can be as short as two or three limit cycle oscillations.

Figure 4.7 and 4.8 show the closed-loop response of the system with  $K = 2$  and  $K = -2$ . Clearly, the amplitude margin achieved is lower and higher than 2 respectively, in line with



our expectations. In the former case, the rise time is shortened with a larger overshoot. In the latter case, the rise time is longer with a reduction in the amplitude of overshoot.

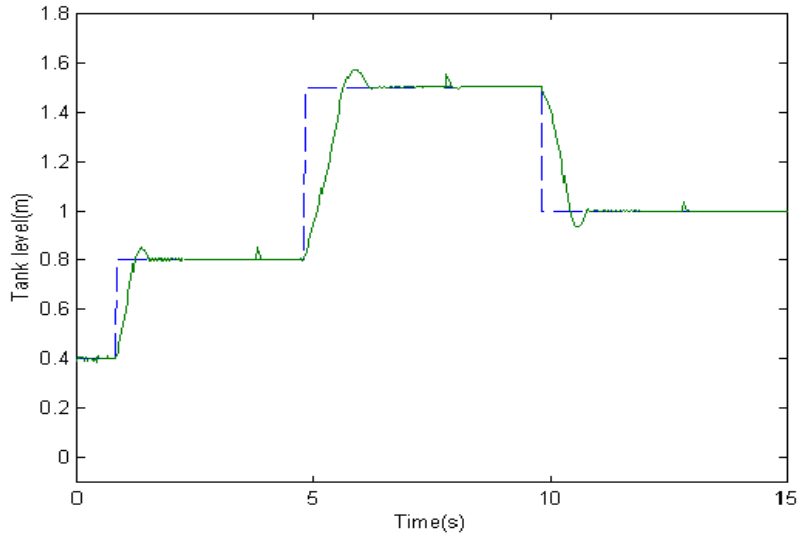


Figure 4.5: Closed-loop performance based on proposed control system with  $K = 0$ .

#### 4.6.2 Comparison with a fixed PID controller

The performance is compared to that achieved by a PID controller with fixed gains. This fixed PID controller is tuned also using [64] based on the model obtained at the midpoint of the spherical tank (i.e.,  $r = 1$ ).

Figure 4.9 shows the performance achieved with the fixed gains PID controller. For a clearer view, Figure 4.10 provides a magnified illustration of the response to the first setpoint change to show the improved performance of the proposed method, both in setpoint tracking and load regulation.

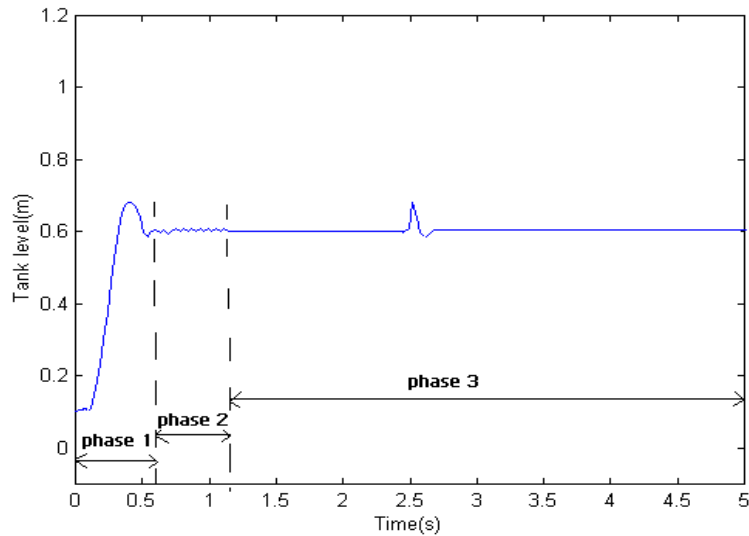


Figure 4.6: Amplified closed-loop performance based on proposed control system with  $K = 0$ .

## 4.7 Real-time Experiment

The proposed control scheme described above is applied to the water level control of a spherical tank system. A schematic of the experiment setup of the spherical tank system is shown in Figure 4.11, and a photograph of the experimental setup is given in Figure 4.12. The apparatus consists of one spherical tank (with a diameter of 25 cm) mounted above a reservoir which functions as the storage for the water. The inflow (control input) is supplied by a variable speed pump which pumps water from the reservoir into the spherical tank through two holes located at the bottom of the tank. A Transmitter series XT-800R type sensor is mounted inside into the tank to measure the water level. Depending on the water level or displacement, a magnet equipped float actuates some reed switches within the transmitter. The sensor can be moved from 20% to 80% of the tank level. The resulting signal will be converted into a current signal proportional to the float position. This signal can be converted to a voltage signal and fed into the computer through the signal

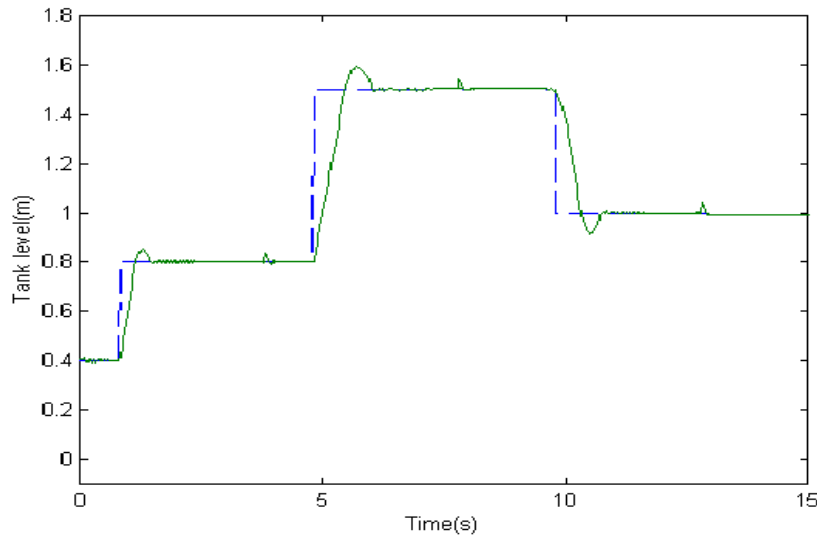


Figure 4.7: Closed-loop performance based on proposed control system with  $K = 2$ .

conditioning circuit. The output voltage varies between 0V to 10V and is proportional to the water level. In the experiment, the main interest is in controlling the process with the voltage to drive the pump as input and the water level in spherical tank as process output. The spherical tank apparatus is controlled from the PC via an A/D and D/A board. LabVIEW 7.0 from National Instruments is used as the control development platform.

The first part of the real-time experiment illustrates the performance of the control system with different choice of  $K$  (similar as Section 4.6.1), resulting in different closed-loop amplitude margin. Three setpoint changes to different desired levels is illustrated. Figure 4.13 shows the closed-loop response for  $K = 0$ . In this case, the loop gain is automatically adjusted and an amplitude margin of two is achieved. In the Figure, the PID controller is tuned using the inherent limit cycle oscillations to the new setpoint. The tuning is based on the parametric method presented in Section 4.3.2 and the tuned PID controller resumes complete control responsibility and the P\_Relay is switched off.

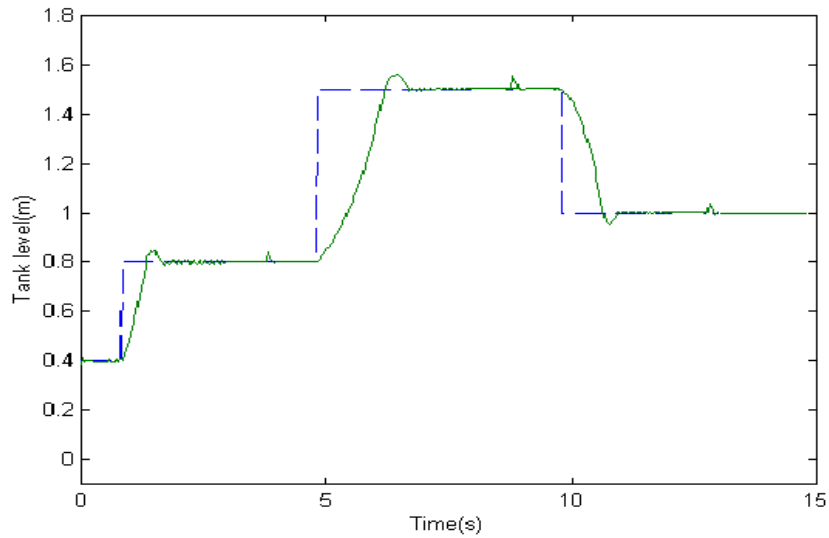


Figure 4.8: Closed-loop performance based on proposed control system with  $K = -2$ .

Figure 4.14 and Figure 4.15 show the closed-loop response with a positive and negative gain of  $K$  respectively. It is clearly observed that a faster response with a larger overshoot is achieved with a positive  $K$ , and a slower response with a reduction in the amplitude of overshoot is achieved with a negative  $K$  respectively.

The performance is compared to that achieved by a PID controller with fixed gains (similar as Section 4.6.2). This PID controller is tuned at the 40% level of the spherical tank using the proposed control scheme. The control performance is shown in Figure 4.16 with the fixed gains PID controller. If Figure 4.16 is compared to Figure 4.13, it is clearly observed that the improved performance of the proposed method. It is observed from all these Figures that the responses are slightly jittery in nature, this is due to the discrete nature of the transmitter of the sensor.

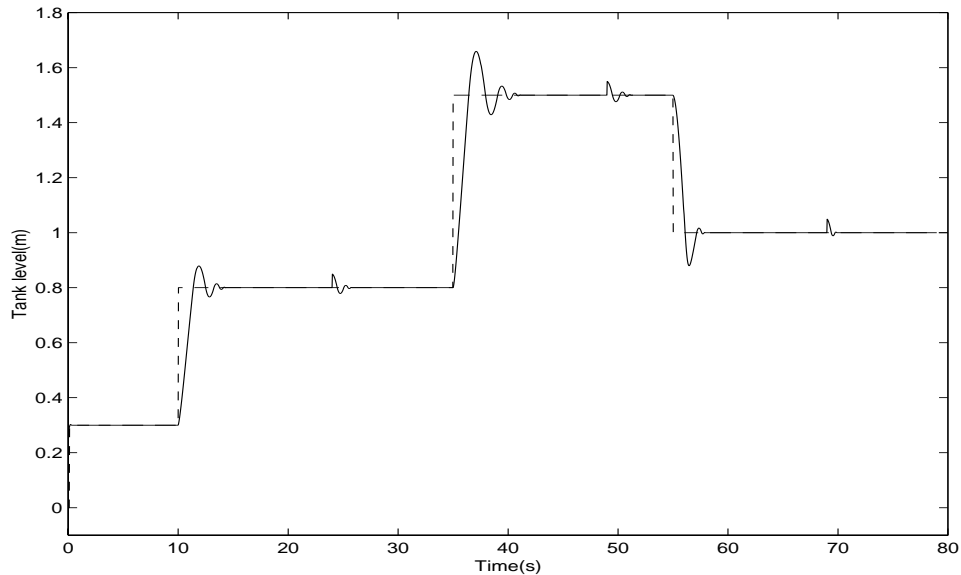


Figure 4.9: Closed-loop performance based on a fixed PID setting.

## 4.8 Conclusion

A robust self-tuning PID controller has been developed in this chapter which is suitable for nonlinear systems. The control system employs a preload relay (P\_Relay) in series with a PID controller. The P\_Relay ensures a high gain to yield a robust performance, and the chattering signal is used as a naturally occurring signal for tuning and re-tuning the PID controller as the operating regime digresses. No other explicit input signal is necessary. Once the PID controller is tuned for a particular operating point, the relay may be disabled and chattering ceases correspondingly. However, it is invoked when there is a subsequent change in operating level. In this way, the approach is also applicable to time-varying systems as the PID tuning will be continuous, based on the latest set of chattering characteristics. Analysis is done for closed-loop stability properties of the system. Simulation and experimental results for the level control of fluid in a spherical tank using the scheme are also provided which verify the good performance of the proposed control scheme.

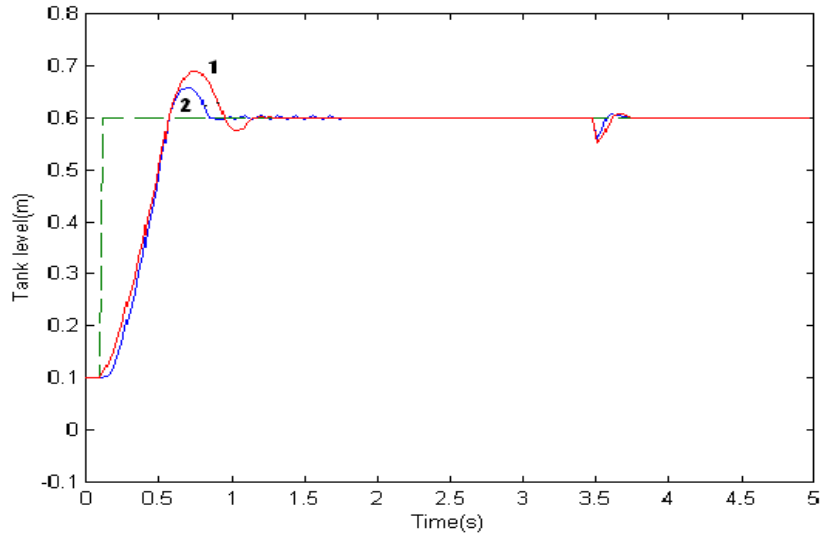


Figure 4.10: Comparison of closed-loop performance (1) fixed gains PID controller, (2) proposed control system.

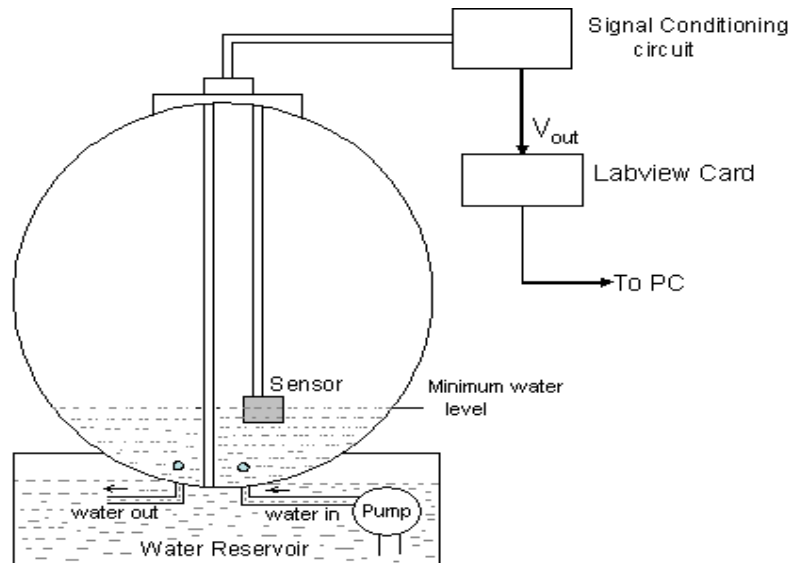


Figure 4.11: Schematic of the experiment setup of the spherical tank system.



Figure 4.12: Experimental setup.

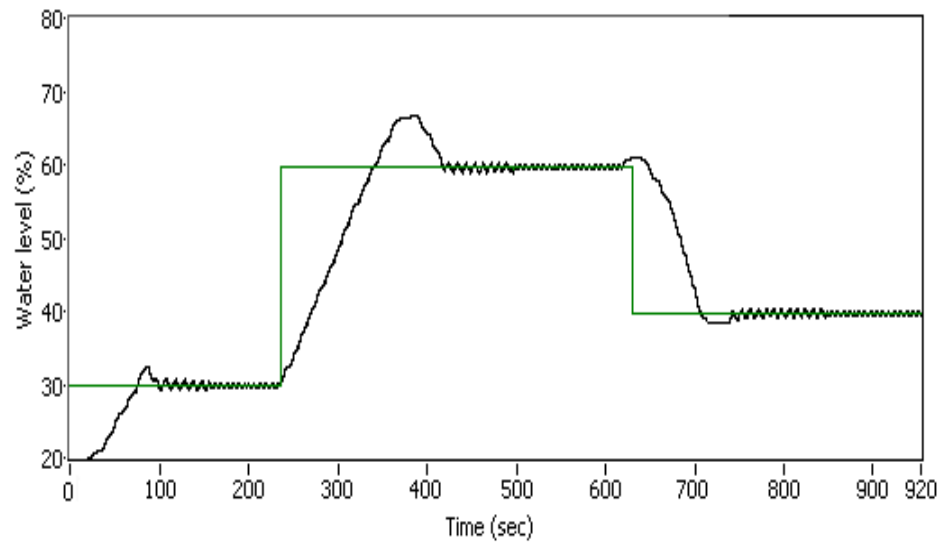


Figure 4.13: Experimental result based on proposed control system with  $K = 0$ .

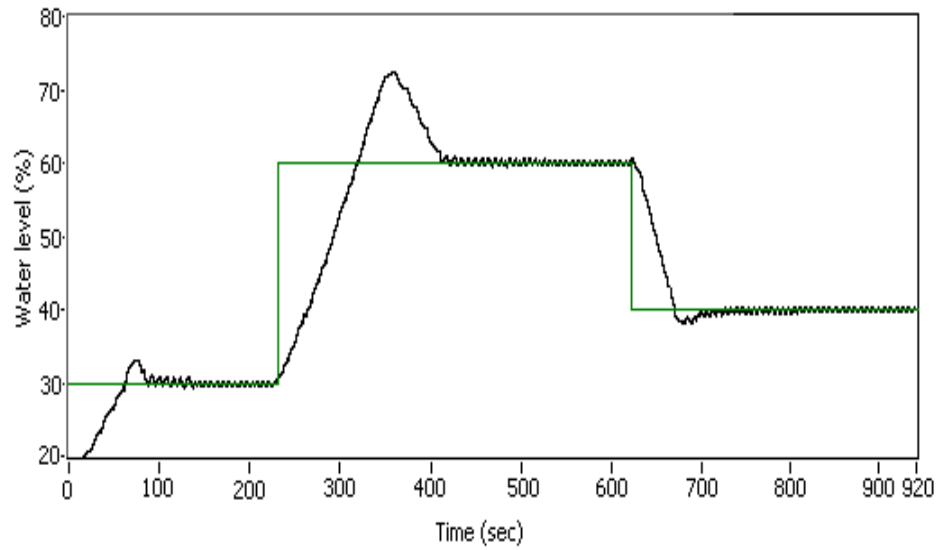


Figure 4.14: Experimental result based on proposed control system with  $K = 1$ .

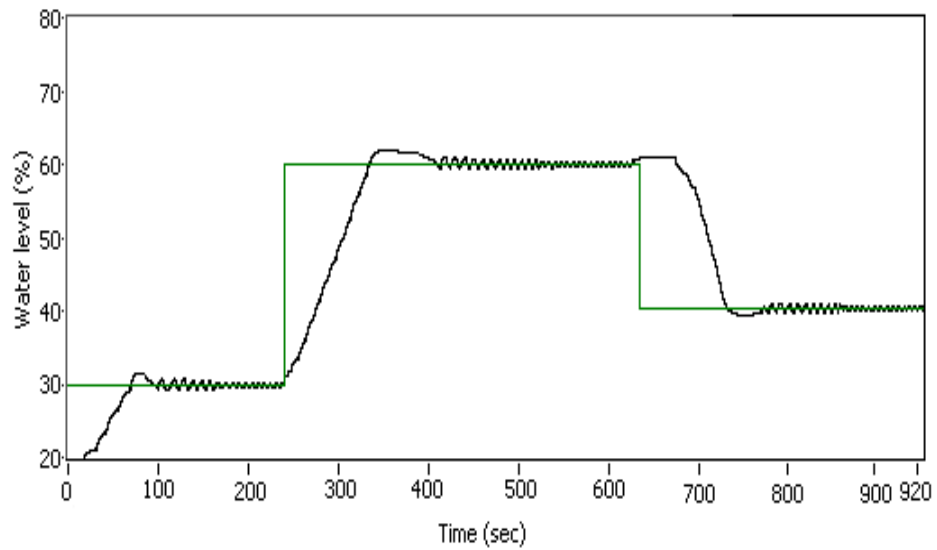


Figure 4.15: Experimental result based on proposed control system with  $K = -1$ .



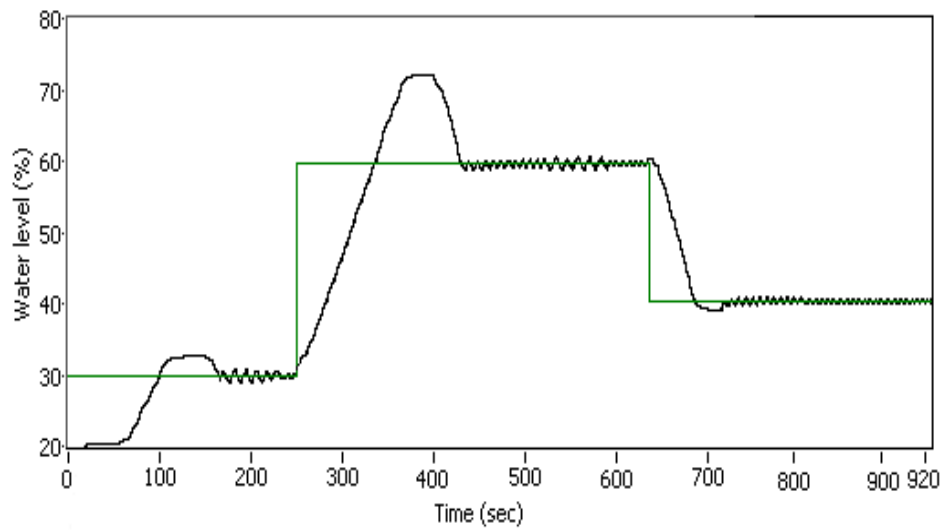


Figure 4.16: Experimental result based on a fixed PID setting

# Chapter 5

## Automatic Tuning of PID Controller for Nonlinear Systems

### 5.1 Introduction

All physical systems are nonlinear and have time-varying parameters to some degree. Whether the nonlinearity is undesirable or intended, the objective of nonlinear analysis is to predict the behaviour of the system. Linear analysis inherently cannot predict those features of behaviour that are characteristics of nonlinear systems [23]. It is already mentioned in the earlier chapters of the thesis that PI controller is a linear controller. Although it has several attractive features, it alone does not provide robust performance for nonlinear plants in some cases. Many approaches towards the design of PID control for linear systems has been proposed over the years [1], [23], [31]. For nonlinear systems, adaptive control methods are rampantly suggested [62], [63]. As a consequence of the nonlinearities of a real system, its dynamical behaviour and the parameters of the linearized model change with the operating conditions. Thus, a linear adaptive controller will adapt its parame-

ter everytime the process changes operating points, but this adaptive process takes some time to converge and in some situations can lead to an undesirable transient behaviour. Gain scheduling and robust high gain control are possible alternatives to adaptive control algorithms [29], [30]. Gain scheduling controller can cope better with a nonlinear process, because it changes its parameters according to the operating conditions, which are specified by the values of one or more exogenous variable requires a deep knowledge of the controlled process.

In this chapter, a robust control system is proposed first, involving the use of a relay in parallel with a PID controller, to provide a high gain feedback system which may be used for the robust control of nonlinear systems. The configuration may be viewed as PID control augmented with a sliding mode. The chattering signals, incurred as a consequence of the relay, are used in a recursive least squares (RLS) algorithm to autotune an equivalent robust PID controller which may then replace the parallel PID-Relay construct. The relay may be re-invoked for re-tuning purposes following changes in set-points or changes in the time-varying system dynamics, similar to the way an auto-tuning relay is used [23]. Robustness analysis will be provided in the chapter to illustrate the robust stability properties of the control scheme. Simulation and experimental results are provided to illustrate the effectiveness of the proposed control scheme when applied to the level control of fluid in a spherical tank.

## 5.2 Robustness Analysis

The configuration of the robust control scheme is shown in Figure 5.1, which comprises of a relay connected in parallel with a PID controller  $G_c$  (henceforth called the PID-Relay construct) for the robust control of a nonlinear system  $G_p$ . It may be viewed as a PID

controller augmented with a sliding mode, thus yielding a high gain feedback system which can ensure robust performance even in the face of modelling errors. The PID control may be tuned just based on a linear model, and the relay will compensate for possible inadequacy through its high gain incorporated into the feedback loop. The price to pay is the emergence of control chattering in the closed-loop, which in many cases should not be allowed to persist indefinitely due to potential damages caused to the final control elements. However, as will be illustrated in this section, the chattering signals can be used in the tuning of an equivalent robust PID controller which may subsequently replace the PID-Relay construct.

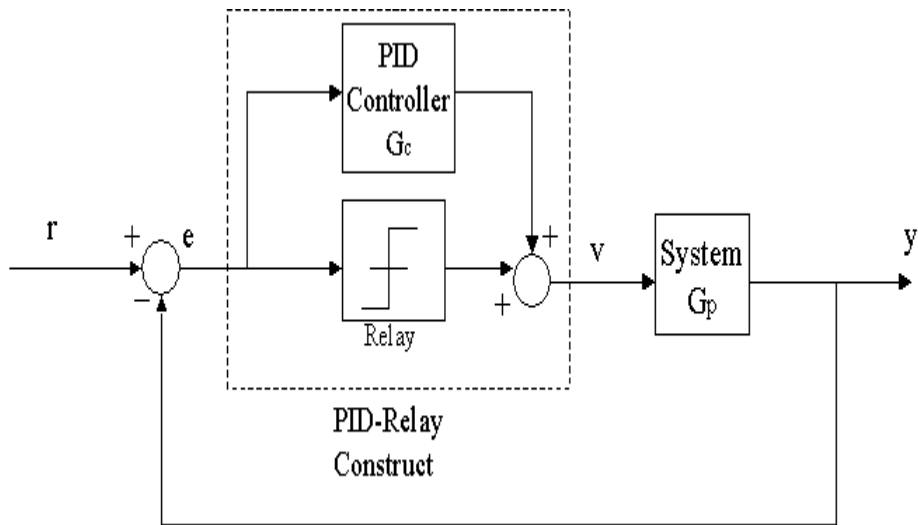


Figure 5.1: Configuration of the robust control scheme.

Consider a class of nonlinear systems described by:

$$\ddot{y} = a\dot{y} + by + cv + f(y, \dot{y}), \quad (5.1)$$

where  $y$  and  $\dot{y}$  are assumed to be limited, and therefore, the nonlinear part described by  $f(y, \dot{y})$  is assumed to be bounded, i.e.,  $\|f(y, \dot{y})\| \leq f_M$ .

Define the error between the desired trajectory  $r$  (which is twice differentiable) and the

system output  $y$

$$e = r - y. \quad (5.2)$$

Under the proposed structure of Figure 5.1, the control signal  $v$  is given by:

$$v = d \operatorname{sgn}(e) + k_p e + k_i \int_0^t e d\tau + k_d \dot{e}, \quad (5.3)$$

where  $\operatorname{sgn}(\cdot)$  is the usual sign operator,  $k_p$ ,  $k_i$  and  $k_d$  are the respective gains of the PID controller, and  $d$  denotes the relay amplitude.

For closed-loop control based on the model (5.1) under the control (5.3), it follows that

$$\ddot{e} = a\dot{e} + be - ck_p e - ck_i \int_0^t e d\tau - ck_d \dot{e} - cd \operatorname{sgn}(e) - f(x, \dot{x}) + f_d, \quad (5.4)$$

where  $f_d = \ddot{r} - a\dot{r} - br$ . Letting

$$z = \left[ \int_0^t e d\tau, e, \dot{e} \right]^T, \quad (5.5)$$

and formulating (4) into a matrix form, it shows

$$\dot{z} = Az + B[D(t) - f(x, \dot{x}) + f_d], \quad (5.6)$$

where

$$A = \begin{bmatrix} 0 & 1 & 0 \\ 0 & 0 & 1 \\ -ck_i & b - ck_p & a - ck_d \end{bmatrix}, \quad (5.7)$$

$$B = \begin{bmatrix} 0 \\ 0 \\ 1 \end{bmatrix}, \quad (5.8)$$

$$D(t) = -cd \operatorname{sgn}(e). \quad (5.9)$$

Assume that the PID parameters  $k_p, k_i, k_d$  and the relay amplitude  $d$  can be tuned to ensure the dominant system to be stable. This implies that  $A$  is a stable matrix. Thus, the following Lyapunov equation will hold:

$$A^T P + PA = -I, \quad (5.10)$$

where  $I$  is the unit matrix.

**Theorem 5.1.** Assume that system (5.1) admits a relay-induced oscillation under the setup proposed. Then, if the PID parameters are tuned properly, the state  $z$  is uniformly bounded.

**Proof.**

Define the Lyapunov function

$$V = z^T P z. \quad (5.11)$$

The derivative of  $V$  is given by:

$$\begin{aligned} \dot{V} &= z^T (A^T P + PA) z + 2z^T P B D(t) - 2z^T P B f(y, \dot{y}) + 2z^T P B f_d \\ &= -\|z\|^2 + 2z^T P B D(t) - 2z^T P B f(y, \dot{y}) + 2z^T P B f_d. \end{aligned} \quad (5.12)$$

Note that  $\|f(y, \dot{y})\| \leq f_M$  and  $\|f_d\| \leq f_{dM}$ . Thus, it can be written as

$$-2z^T P B f(y, \dot{y}) \leq \eta z^T P B B^T P z + \frac{1}{\eta} f^2 \leq \eta z^T P B B^T P z + \frac{1}{\eta} f_M^2, \quad (5.13)$$

$$2z^T P B f_d \leq \eta z^T P B B^T P z + \frac{1}{\eta} f_d^2 \leq \eta z^T P B B^T P z + \frac{1}{\eta} f_{dM}^2, \quad (5.14)$$

where  $\eta$  is an arbitrary constant.

Therefore, it follows that

$$\|D(t)\| \leq cd |\text{sgn}(e)| = cd = D_M; \quad \text{as } |\text{sgn}(e)| \leq 1. \quad (5.15)$$

Now the term  $2z^T PBD(t)$  can be expressed approximately as

$$2z^T PBD(t) \leq \eta z^T PBB^T Pz + \frac{1}{\eta} D^2(t) \leq \eta z^T PBB^T Pz + \frac{1}{\eta} D_M^2. \quad (5.16)$$

The following derivative of  $V$  is thus obtained.

$$\begin{aligned} \dot{V} &\leq -\|z\|^2 + 3\eta\lambda_{\max}(PBB^T P)\|z\|^2 + \frac{1}{\eta}f_M^2 + \frac{1}{\eta}f_{dM}^2 + \frac{1}{\eta}D_M^2 \\ &= -[1 - 3\eta\lambda_{\max}(PBB^T P)]\|z\|^2 + \frac{1}{\eta}f_M^2 + \frac{1}{\eta}f_{dM}^2 + \frac{1}{\eta}D_M^2. \end{aligned} \quad (5.17)$$

Let  $\rho = 1 - 3\eta\lambda_{\max}(PBB^T P)$  and choose  $\eta$  subject to  $0 < \eta < \frac{1}{3\lambda_{\max}(PBB^T P)}$ . Since  $\lambda_{\min}(P)\|z\|^2 \leq V \leq \lambda_{\max}(P)\|z\|^2$ , it follows that

$$\dot{V} \leq -\frac{\rho}{\lambda_{\max}(P)}V + \frac{1}{\eta}f_M^2 + \frac{1}{\eta}f_{dM}^2 + \frac{1}{\eta}D_M^2 = -\frac{\rho}{\lambda_{\max}(P)}V + \rho_0, \quad (5.18)$$

where  $\rho_0 = \frac{1}{\eta}f_M^2 + \frac{1}{\eta}f_{dM}^2 + \frac{1}{\eta}D_M^2$ .

Hence,

$$V(t) \leq \frac{\rho_0\lambda_{\max}(P)}{\rho} + [V(0) - \frac{\rho_0\lambda_{\max}(P)}{\rho}]e^{-\frac{\rho}{\lambda_{\max}(P)}t}. \quad (5.19)$$

For state  $z$ , it thus follows that

$$\|z\| \leq \sqrt{\frac{\rho_0\lambda_{\max}(P)}{\lambda_{\min}(P)\rho} + [V(0) - \frac{\rho_0\lambda_{\max}(P)}{\lambda_{\min}(P)\rho}]e^{-\frac{\rho}{\lambda_{\max}(P)}t}}. \quad (5.20)$$

This implies that

$$\lim_{t \rightarrow \infty} \|z(t)\| = \sqrt{\frac{\rho_0\lambda_{\max}(P)}{\lambda_{\min}(P)\rho}}, \quad (5.21)$$

i.e., state  $z$  is bounded under the condition of Theorem 5.1.

### 5.3 Automatic Tuning of an Equivalent PID Controller

The main idea, to be pursued in this section, is to approximate the parallel PID-Relay construct with an equivalently tuned PID controller  $\tilde{G}_c$  as shown in Figure 5.2.

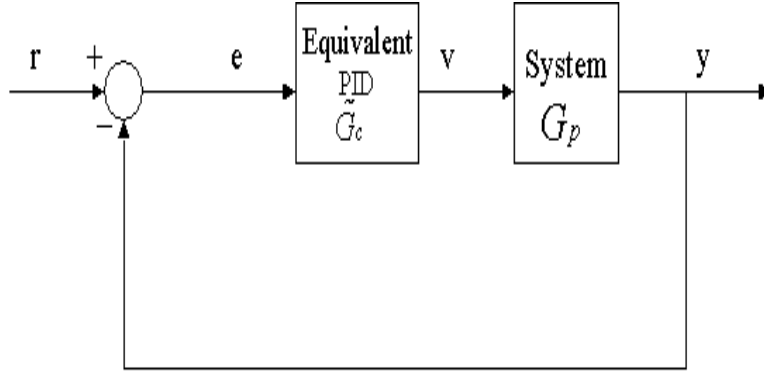


Figure 5.2: Equivalent PID controller.

The recursive least squares (RLS) fitting method is applied to the input and output chattering signals of the PID-Relay construct (directly in the time domain) to yield the gains of the equivalent PID controller.

The equivalent PID controller of this form is described by:

$$v(t) = K_p e + K_i \int_0^t e dt + K_d \frac{de}{dt}. \quad (5.22)$$

The equation can be written in a matrix form as:

$$v(t) = \begin{bmatrix} e & \int_0^t e dt & \frac{de}{dt} \end{bmatrix} \begin{bmatrix} K_p \\ K_i \\ K_d \end{bmatrix}. \quad (5.23)$$

(5.23) can be written in the linear-in-the parameters form as:

$$v(t) = \theta(t) \Phi^T,$$

where  $\theta(t) = \begin{bmatrix} K_p \\ K_i \\ K_d \end{bmatrix}$  and  $\Phi^T = \left[ e \quad \int_0^t e dt \quad \frac{de}{dt} \right]$ . The RLS algorithm with a time varying forgetting factor can be directly used here as  $v(t)$  and  $\Phi^T$  are available, the update of  $\theta(t)$



can be expressed as:

$$\theta(t) = \theta(t-1) + K(t)\epsilon(t), \quad (5.24)$$

where  $\theta(t-1)$  refers to the controller settings identified during the last cycle,  $\epsilon(t)$  and  $K(t)$  are the error signal and Kalman gain vector, where

$$\epsilon(t) = v(t) - \Phi^T\theta(t-1), \quad (5.25)$$

$$K(t) = P(t-1)\Phi(\lambda I + \Phi^T P(t-1)\Phi)^{-1}, \quad (5.26)$$

$$P(t) = (I - K(t)\Phi^T)P(t-1)/\lambda. \quad (5.27)$$

$\lambda$  is a forgetting factor ( $0 < \lambda < 1$ ). There are two matrices to be initialized for the recursive algorithm,  $P(0)$  and  $\theta(0)$ . It is usual to initialize  $P(0)$  such that  $P_0 = \alpha I$ , where  $\alpha$  is a large number ( $10^4 \sim 10^6$ ) and  $I$  is the identity matrix.  $\theta(0)$  may be set to be the gains of the PID controller before tuning.

## 5.4 Simulation Study

To illustrate the performance attainable with the proposed control system, a simulation study is carried out on the level control of fluid in the same classical spherical tank system described in Section 4.6. The spherical tank system is shown in Figure 4.4, it is essentially a system with nonlinear dynamics.

Figure 5.3 shows the closed-loop performance of the proposed control system for the two control schemes. The response (marked ‘1’) corresponds to the use of the PID-Relay construct, while the response (marked ‘2’) corresponds to the use of the equivalent PID controller, automatically tuned from the  $e$  and  $v$  signal based on the method presented in

Section 5.4.

Figure 5.4 shows the closed-loop performance based on the proposed equivalent PID controller, corresponding to different operating level of the spherical tank. Three setpoint changes to different desired level are simulated, each followed by the simulation of a static load disturbance (with an amplitude roughly 10% of the setpoint changes) is seaping in. Figure 5.5 shows the response to the same set of setpoint changes, but they now occur under the influence of significant measurement noise.

The performance is compared to that achieved by a PID controller with fixed gains. This PID controller is tuned at the mid level of the spherical tank. The control performance is shown in Figure 5.6. Figure 5.7 provides a magnified illustration of the response to a setpoint change to show the improved performance of the robust scheme, both in setpoint tracking and load regulation.

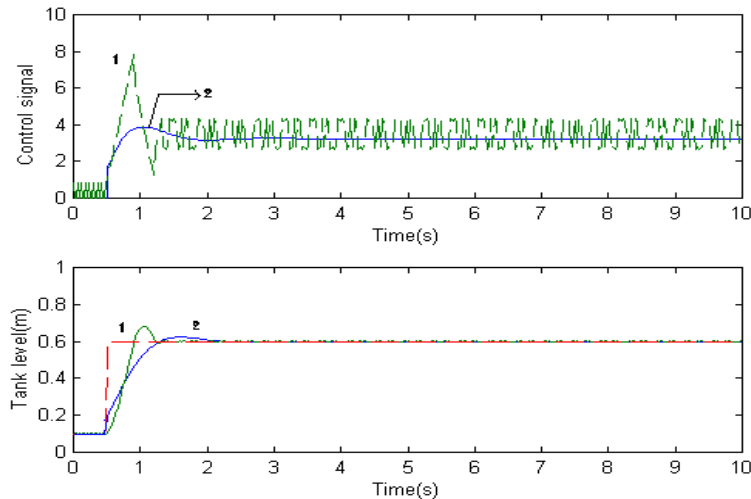


Figure 5.3: Simulation results (a) control signal and (b) closed-loop performance (1) PID-Relay controller, (2) equivalent PID controller.

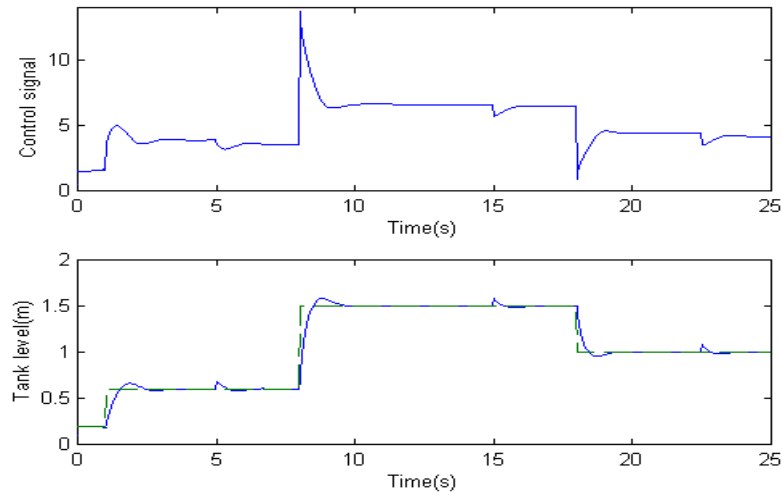


Figure 5.4: Simulation results (a) control signal (b)closed-loop performance at different operating level of the tank using the equivalent PID controller.

## 5.5 Real-time Experiment

The proposed control scheme described above is applied to the water level control of the same spherical tank system described in the previous chapter (Section 4.7). A schematic of the experiment setup of the spherical tank system is shown in the previous chapter (Figure 4.11), and a photograph of the experimental setup is also given in the previous chapter (Figure 4.12). The interested reader can refer to Section 4.7 for the description of the apparatus.

Figure 5.8 and Figure 5.9 show the closed-loop performance based on the proposed PID-relay controller and equivalent PID controller respectively, corresponding to different operating level of the spherical tank. The performance is compared to that achieved by a PID controller with fixed gains. This PID controller is tuned at the 40% level of the spherical tank. The control performance is shown in Figure 5.10 using the proposed control scheme. Figure 5.10 is compared to Figure 5.8 or Figure 5.9, and is clearly observed that the improved performance of the proposed method. It is observed from all these Figures that the

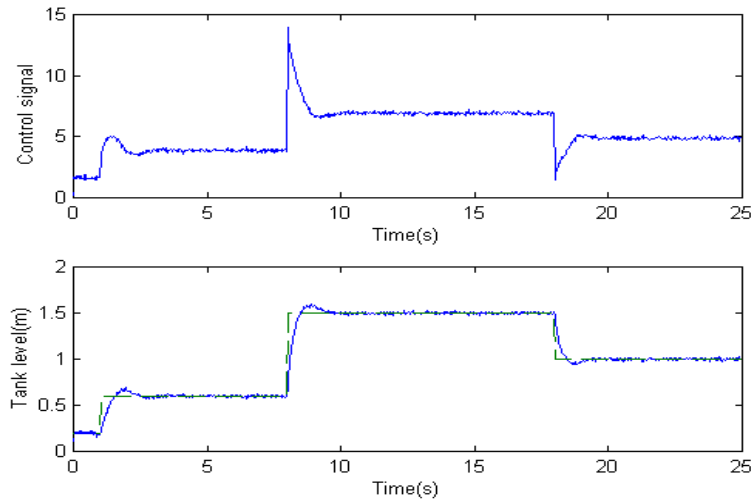


Figure 5.5: Closed-loop performance under the influence of measurement noise.

responses are slight jittery in nature, this is due to the discrete nature of the transmitter of the sensor.

## 5.6 Conclusion

A robust control system is proposed which is suitable for the control of nonlinear systems, comprising of a parallel connection of a relay to a PID controller. The relay ensures robust control by providing a high feedback gain, but it also induces a control chattering phenomenon. The chattering signals are used as a natural excitation signal for identifying an equivalent PID controller using the recursive least squares (RLS) algorithm. No other explicit input signal is required. Analysis shows the robust stability properties of the control scheme. Simulation and experimental results on a spherical tank level control further illustrate the practical applicability

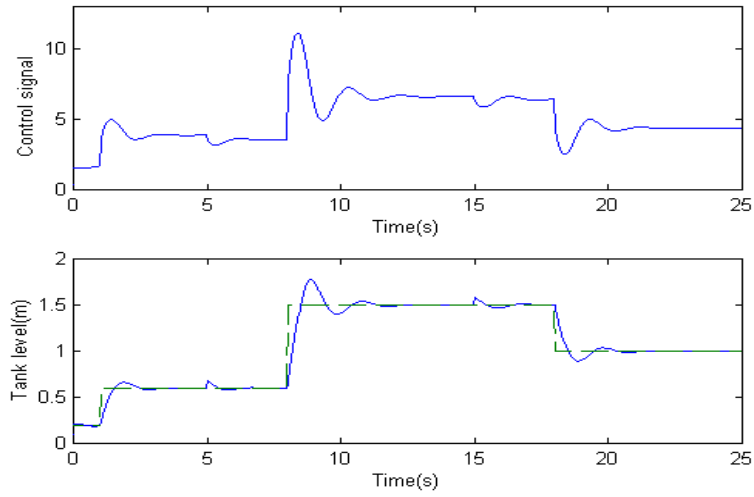


Figure 5.6: Closed-loop performance based on a fixed PID setting.

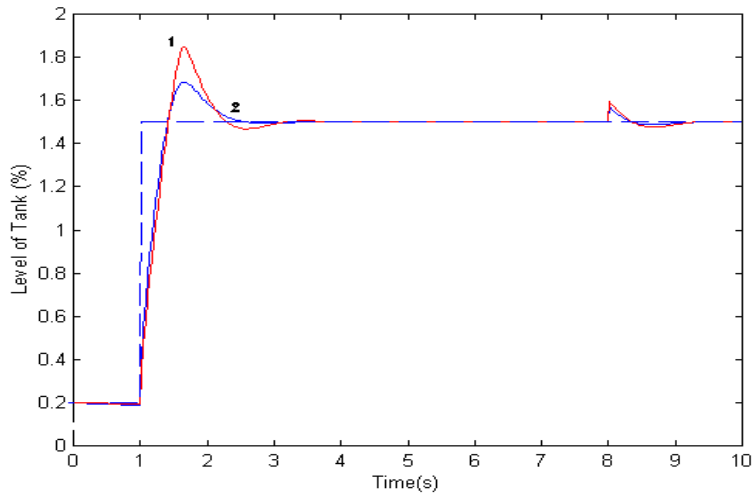


Figure 5.7: Comparison of closed-loop performance (1) fixed PID controller, (2) proposed control system.

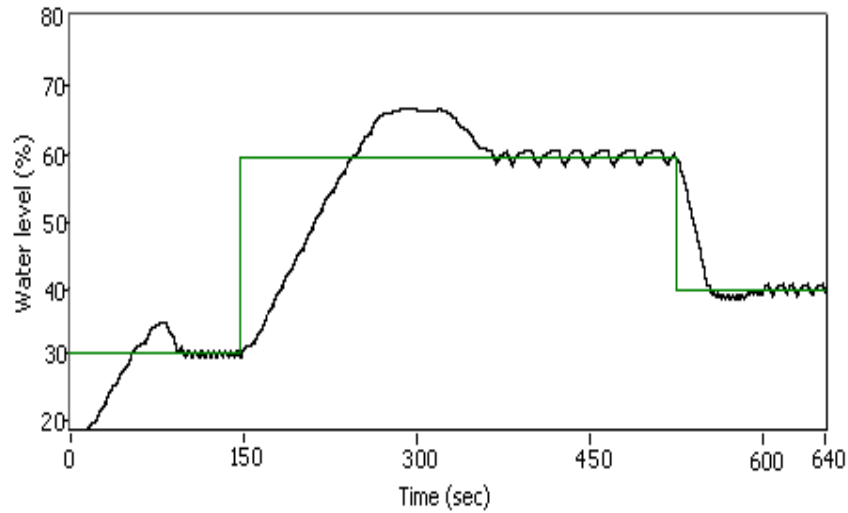


Figure 5.8: Experimental result at different operating level of the tank using the PID-relay controller.

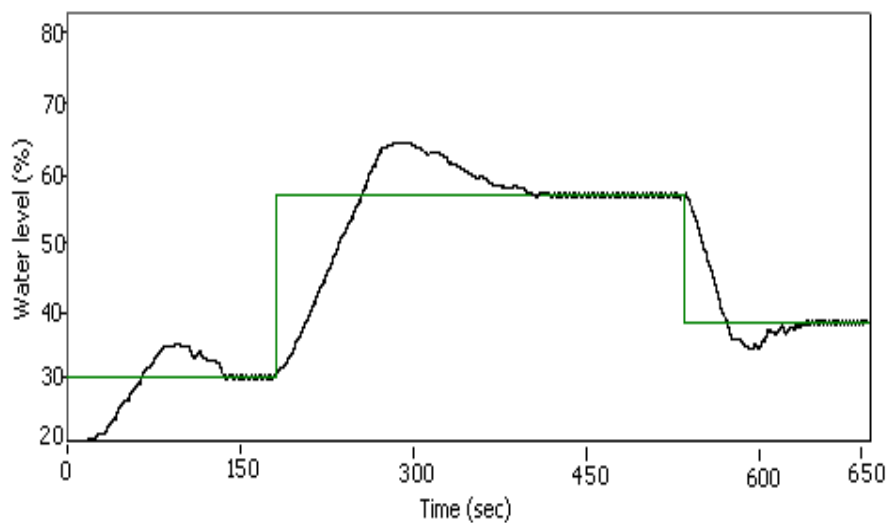


Figure 5.9: Experimental result at different operating level of the tank using the proposed equivalent PID controller.

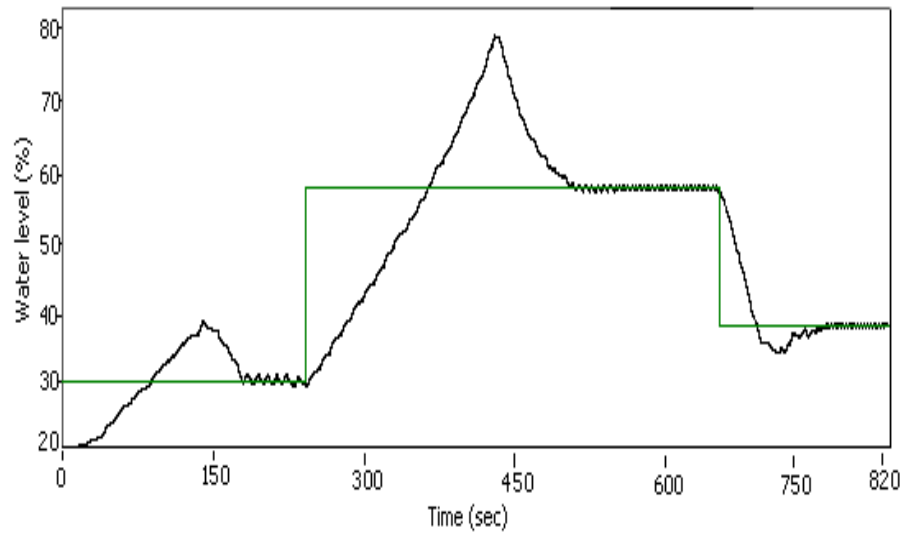


Figure 5.10: Experimental result based on a fixed PID setting.

# Chapter 6

## Conclusions

### 6.1 General Conclusions

Relay feedback has attracted considerable research attention for more than a century. The classical work of Tsypikin [3] on analysis of relay summarizes the progress till 1960s. Early applications of relay systems ranged from stationary control of industrial processes to control of mobile objects. It was in 1980s that Astrom and Hagglund successfully applied the relay feedback method to auto-tune PID controllers for process control, and triggered a resurgence of interest in relay methods, including extensions of the method to more complex systems. Since then, new tools and powerful results have emerged. This thesis presents some recent developments of relay feedback those are applicable to advanced process control applications. Several useful results are obtained in the thesis which are suitable for automatic control design for industrial controllers, including petro-chemical, food and pharmaceutical, semiconductor, and general automation industries.

The thesis has presented a modified relay feedback method named as P\_Relay feedback



method that serves primarily to achieve consistent and significant improved frequency estimation accuracy without incurring significant and additional complexities over the relay feedback method that is being practiced now in the industries. The improved estimation accuracy will lead to improved control and assessment performance when the estimated point is used for these primary purposes. Apart from this primary objective, there are other benefits which can be achieved with regards to applicability to other classes of processes when the present relay method fails, a shortened time to achieve stationary oscillations, and versatility to identify other points of the process frequency response.

Apart from control tuning, the relay feedback approach can also be used for control performance assessment purposes. In this thesis, one such application of the relay feedback method towards assessment of sensitivity has been illustrated. The method is based on deriving sensitivity parameters (maximum sensitivity and stability margins) from the non-parametric frequency response of the compensated system. Based on the derived sensitivity parameters, this thesis presents an approach for the design of PI control based on specifications of maximum sensitivity and stability margins.

Motivated by Astrom [34], the thesis presents two methods for the tuning of PID controller for nonlinear system using relay feedback approach. In the first method, a robust self-tuning PID controller has been developed which is suitable for nonlinear systems. The control system employs a preload relay (P\_Relay) in series with a PID controller, where the P\_Relay ensures a high gain to yield a robust performance. For the second method, a parallel connection of a relay to a PID controller collectively forms the robust controller. Relay induces a control chattering phenomenon in both cases and instead of viewing chattering as an undesirable yet inevitable feature, the chattering signals are used as natural excitation signals.

The results obtained in the thesis have both useful practical implications and sound theoret-

ical contributions. The effectiveness of these results have been demonstrated in simulation and successful real-time implementations documented in the main body of the thesis. For a more detailed summary on the results, the reader may refer to Section 1.4.

## 6.2 Suggestions for Further Work

This thesis presents some recent developments of relay feedback method for advance process control system. As mentioned in Chapter 2, the preload relay method improves the estimation accuracy of critical point without incurring significant and additional complexities. There are still some cases left where the preload relay does not show a significant improvement, specially for the processes with high time delay. Like the conventional relay feedback method, the preload relay method is also not applicable to double integrator plant, as it yields unstable limit cycle oscillations which increase in amplitude beyond bound. The double integrator is a feature present in several kinds of system, one of which is the classical ball on the beam apparatus. The new preload relay feedback technique developed in this thesis can be extended to overcome such limitations.

In Chapter 3, a relay feedback approach for the assessment of robustness in control systems is proposed. The results achieved in the simulations and real-time experiment are satisfactory using the proposed method. Nevertheless, there is room for future improvements. There are two proposals here for future development towards the improvement of the performance and accuracy of the proposed modified relay feedback method. Firstly, the relay can be used with a hysteresis. There are advantages of having a relay with hysteresis instead of a pure relay. With an ordinary relay, a small amount of noise can make the relay switch randomly. By introducing hysteresis, the noise must be larger than the hysteresis width to make the relay switch. The describing function approach will be used

to investigate the oscillations obtained. By choosing the relation between width and amplitude of relay, it is therefore possible to determine a point on the Nyquist curve with a specified imaginary part. Several points on the Nyquist curve are easily obtained by repeating the experiment with different relations between relay amplitude and width. It is easy to control the oscillation amplitude to a desired level by a proper choice of the relay amplitude. Secondly, to improve the accuracy of the results, a low-pass filtering circuitry at the output of the modified relay can be added. The filter output will be a sinusoidal wave if the low-pass filter is able to filter out the higher harmonics other than the fundamental frequency component. However, the challenge of this proposal is in the designing of the low-pass filter. Since the oscillations take place in different frequencies, the low-pass filter must be design in such a way that it is able to effectively filter out the higher harmonics, and yet does not attenuate the fundamental frequencies components. These two areas are left open to be developed in the future if very accurate results are desired.

The robust control configuration, comprising of the relay and the PID controller in Chapter 5, puts a high gain in the loop and ensures satisfactory closed-loop performance. Although it incurs a chattering phenomenon, the chattering signals have been used as naturally arising signals to automatically tune an equivalent PID controller. No other explicit and deliberate excitation signals are needed, sparing the usual tedious identification exercise necessary for control tuning. However, it should be acknowledged that the equivalent PID controller chosen remains a linear controller. It is only tuned to the closest equivalence to the original relay-plus-PID controller in the least squares sense. As such, in terms of actual performance and robustness, a degradation is expected with the equivalent controller. The favorable trade-off is the chattering phenomenon will be eliminated with the equivalent PID controller. The interested researchers can consider to extend the work by choosing a nonlinear PID controller in place of the equivalent controller to reap further performance improvement.

# Bibliography

- [1] Astrom, K. J. and T. Hagglund., (1988), *Automatic tuning of PID controllers*, Instrument Society of America, Research Triangle park, NC.
- [2] Weiss, H. K., (1946), *Analysis of relay servomechanisms*, J. Aeronautical Sciences, 13, 364-376.
- [3] Tsympkin, Y. Z., (1984), *Relay control systems*, Cambridge University Press, Cambridge, UK.
- [4] Hang, C. C., A. P. Loh and V. U. Vasani, (1994), *Relay feedback auto-tuning of cascade controllers*, IEEE transaction on control system technology, 2(1), 42.
- [5] Smith, O. J. M., (1957), *Closer control of loops with dead time*, Chem. Eng. Progr, 53, 217.
- [6] Tan, K. K., Wang, Q. G. and Lee, T. H., (1998), *Finite Spectrum Assignment Control of Unstable Time delay Processes with Relay Tuning*, Ind. Eng. Chem. Res., 37, 1351.
- [7] Loh, A. P., C. C. Hang, C. K. Quek and V. U. Vasani, (1993) *Autotuning of Multi loop PI controllers using relay feedback*, Industrial Engineering and Chemical Research, 32, 1102.
- [8] Wang Q. G., Bao Zou, T. H. Lee and Qing Bi, (1997), *Auto-tuning of Multivariable PID controllers from Decentralized Relay Feedback*, Automatica, 33(3), 319-330.

- [9] Astrom, K. J., C. C. Hang, P. Person, W. K. Ho, (1992), *Towards intelligent PID control*, Automatica, 28(1),1.
- [10] Lee, T. H., Q. G. Wang, K. K. Tan, (1995), *Knowledge-based process identification using relay feedback*, Journal of process control, 5(6), 387.
- [11] Astrom, K. J., and T. Hagglund, (1984), *Automatic Tuning of Simple Regulators with specification on phase and amplitude margins*, Automatica, 20(5), 645.
- [12] Tan, K. K., Q. G. Wang, C. C. Hang and T. Hagglund, (1999), *Advances in PID control*, Springer.
- [13] Hang, C. C., K. J. Astrom, W. K. Ho, (1993), *Relay auto-tuning in the presence of static load disturbance*, Automatica, 29(2), 563-564.
- [14] Lee, T. H., Q. G. Wang, K. K. Tan, (1995), *A modified relay-based technique for improved critical point estimation in process control*, IEEE Trans. Control Systems Tech. 3(3), 330.
- [15] Sung, S. W., J. H. Park, I. Lee, (1995), *Modified relay feedback method*, Ind. Eng. Chem. Res. 34, 4133.
- [16] Shen, S., H. Yu, C. Yu, (1996), *Use of saturation -relay feedback for autotune identification*, Chem. Eng. Sci., 51, 1187.
- [17] Tan, K. K., T. H. Lee, Q. G. Wang, (1996), *An enhanced automatic tuning procedure for PI/PID controllers for process control*, AIChE Journal, 42(9), 2555.
- [18] Ho, W. K., C. C. Hang, L. S. Cao, (1993), *Tuning of PID controllers based on gain and phase margin specifications*, Proceedings of 12th IFAC World Congress, 5, 267.
- [19] Harris, T., (1989), *Assessment of closed loop performance*, Canadian Journal of Chemical Engineering, 67, 856.

- [20] Harris, T., Boudreau, F., MacGregor, J., (1996), *Performance assessment of multi-variable feedback controllers*, *Automatica*, 32, 1505.
- [21] Sheng, W., B. Huang., (2002), *Robust performance assessment of feedback control systems*, *Automatica*, 38, 33.
- [22] Huang, B., Shah, S. L. (1999), *Performance assessment of control loops: Theory and Applications*, London: Springer, ISBN 1-85233-639-0.
- [23] Astrom, K. J. and T. Hagglund., (1995), *PID Controllers: Theory, Design and Tuning*, Instrument Society of America, Research Triangle Park, NC.
- [24] Wang, Y. G., and Cai, W. J., (2001), *PID Tuning for Integrating Processes with Sensitivity Specification*, Proceedings of the 40th Conference on Decision and Control, Orlando, Florida, USA, 4087-4091.
- [25] Wang, Q. G. and H. Ru., (2002), *PI Tuning under Performance Constraints*, *Asian Journal of Control*, 4(4), 397-402.
- [26] O'Dwyer, Aidan. (2003), *Handbook of PI and PID Controller Tuning Rules*, Imperial College Press, London, 375pp. ISBN 1-86094-342-X.
- [27] Ho, W. K., Hang, C. C. and L. S. Cao., (1995), *Tuning of PID Controllers Based on Gain and Phase Margins Specifications*, *Automatica*, 31, 497-502.
- [28] Marlin, T. E., (1995), *Process control, designing processes and control systems for dynamic performance*, McGraw-Hill, Inc, USA.
- [29] Jiawen, D. and C. B. Brosilow., (1998), *Nonlinear PI and gain-scheduling*, American Control Conference, Proceedings of the 1998, Vol 1, 323-327.

- [30] Kuang-Hsuan, T. and J. S. Shamma., (1998), *Nonlinear gain-scheduled control design using set-valued methods*, Proceedings of the 1998 American Control Conference, Vol. 2, 1195-1199.
- [31] Gawthrop, P. J., (1986), *Self-tuning PID Controllers: Algorithms and Implementations*, IEEE Transaction on Automatic Control, 31(3), 201.
- [32] Glad, T. and L. Ljung., (2000), *Control Theory: Multivariable and Nonlinear Methods*, Taylor & Francis Book Company, UK.
- [33] Liu, H., (1997), *Self-oscillating adaptive systems (SOAS) without limit cycles*, Proceedings of the 1997 American Control Conference, Albuquerque, New Mexico, June 1997.
- [34] Astrom, K. J., and B. Wittenmark, (1995), *Adaptive Control*, 2nd ed. Addison-Wesley, Reading Mass.
- [35] Eykhoff, P., (1974), *System Identification*, Wiley, New York.
- [36] Ljung, L., (1987), *System Identification—Theory for the User*, Prentice-Hall, Englewoods-Cliff.
- [37] Ziegler, J. G., and N. B. Nichols, (1943), *Optimum Settings for Automatic Controllers*, Trans. ASME, 65, 433.
- [38] Astrom, K. J. and T. Hagglund, (1988), *A New Auto-Tuning Design*, Preprints IFAC Int. Symposium on Adaptive Control of Chemical Processes, ADCHEM '88, Lyngby, Denmark.
- [39] Palmor, Z.J. and M. Blau, (1992), *An Auto-tuner for Smith Dead-time Compensators*, Internal Report, Faculty of Mechanical Engineering, Technion - I.I.T. Haifa 32000, Israel.

- [40] Satt Control Instruments, (1986), *Controller ECA40 Technical Description Manual*, Sweden.
- [41] Fisher Controls International, (1992), *DPR900 Instruction Manual*, Austin, Texas, USA.
- [42] Hang, C. C., Astrom, K. J., and Wang, Q. G., (2002), *Relay-feedback auto-tuning of process controllers - a tutorial review*, Journal of Process Control, 12, 143.
- [43] Goncalves, J. M., Megretski, A. and Dahleh, M. A., (2001), *Global stability of relay feedback systems*, IEEE Transaction on Automatic control, 46(4), 550.
- [44] Friman, M., and Waller, K. V., (1997), *A Two-Channel Relay for Autotuning*, Ind. Eng. Chem. Res., 36, 2662.
- [45] Wang, Q. G., Hang, C. C. and Zou, B., (1997), *Low-order modeling from relay feedback*, Industrial and Engineering Chemistry Research, 36(2), 375.
- [46] Sung, S. W., Park, J. H., Lee, I., (1995), *Modified relay feedback method*, Ind. Eng. Chem. Res., 34, 4133.
- [47] Gelb, A., and W. E. Vander Velde, (1968), *Multiple-Input Describing Functions and Nonlinear System Design*, McGraw-Hill, New York, USA.
- [48] Atherton, D. P., (1975), *Nonlinear Control Engineering — Describing function analysis and design*, Van Nostrand Reinhold Company Limited, Workingham, Berks, UK.
- [49] Leonardo, F., R. Oubrahim, (1998), *Two steps relay auto-tuning in the presence of static load disturbance*, UKACC International Conference on Control'98, 1339.
- [50] Tan, K. K., T. H. Lee, D. Huifang and H. Sunan., (2001), *Precision Motion Control*, Advances in Industrial Control, Springer, UK.



- [51] Tan, K. K., Wang, Q. G. and Lee, T. H., (1998), *Finite Spectrum Assignment Control of Unstable Time delay Processes with Relay Tuning*, Ind. Eng. Chem. Res., 37, 1351.
- [52] Luyben, W. L., Luyben, M. L., (1997), *Essentials of Process Control*, McGraw-Hill. New York.
- [53] Instrument Society of America, (1985), *Process Control Package — PID Module*, Research Triangle Park, NC, USA.
- [54] Corless, M.,G.Leitmann, “Deterministic control of uncertain systems”, in *Modelling and Adaptive Control* Edited by Ch.I. Byrnes and A.Kurzanski, Springer. New York,pp108-133, 1988
- [55] Ioannou, P.A. and J. Sun, *Stable and Robust Adaptive Control*, Englewood Cliffs, NJ: Prentice-Hall, 1995.
- [56] Astrom, K. J., H. Panagopoulos and T. Hagglund., (1998), *Design of PI controllers based on non-convex optimization*, Automatica, 35(5), 585.
- [57] Panagopoulos, H., K. J. Astrom and T. Hagglund., (1999), *Design of PID controllers based on constrained optimization*, In Proc. 1999 American Control Conference (ACC'99). San Diego, California. Invited Paper.
- [58] Morari, M. and Zafiriou, E., (1989), *Robust process control*, Englewood Cliffs, Prentice Hall.
- [59] Davison, D. E., Kabamba, P. T., Meerkov, S. M., (1999), *Limitations of disturbance rejection in feedback system with finite bandwidth*, IEEE Transactions on Automatic Control, 44(6), 1132 -1144.
- [60] Crowe, J., and M. A. Johnson., (2002), *Automated Maximum Sensitivity and Phase Margin Specification Attainment in PI Control*, Asian Journal of Control, 4(4), 388.

- [61] Middleton, R. H., Freudenberg, J. S. and McClamroch, N. H., (2001), *Sensitivity and robustness properties in the preview control of linear non-minimum phase plants*, Proceedings of the American Control Conference (ACC'2001), 4, 2957.
- [62] Zhang, T., Ge, S. S. and Hang, C. C., (2000), *Stable adaptive control for a class of nonlinear systems using a modified Lyapunov function*, IEEE Transactions on Automatic Control., 45(1), 129-132.
- [63] Ordonez, R. and K. M. Passino., (2001), *Adaptive control for a class of nonlinear systems with a Time varying structure*, IEEE Transactions on Automatic Control., 46(1), 152.
- [64] Smith, C. A. and A. B. Corripio., (1997), *Principles and Practice of Automatic Process Control*, John Wiley & Sons.
- [65] Slotine, J-J.E. and Li, W. P. (1991), *Applied nonlinear control*, Prentice Hall, Englewoods Cliffs, NJ, USA.

# Appendix A

## AUTHOR'S PUBLICATIONS

### Journal:

- [1] K. K. Tan, S. Huang and R. Ferdous, "Robust Self-tuning PID Controller for Nonlinear Systems", *Journal of Process Control*, **12(7)**, 753-761 (2002).
- [2] K. K. Tan, R. Ferdous and S. Huang, "Closed-loop Automatic Tuning of PID Controller for Nonlinear Systems", *Chemical Engineering Science*, **57(15)**, 3005-3011 (2002).
- [3] K. K. Tan, R. Ferdous, "Assessment of Control Robustness Using a Relay Feedback Approach", *IEE Computing and Control Engineering Journal*, *accepted for publication*.
- [4] K. K. Tan, T. H. Lee, K. Y. Chua and R. Ferdous, "Improved Critical Point Estimation Using a Preload Relay", *Automatica - submitted*, (2004).
- [5] K. K. Tan, R. Ferdous, "PI Control Design Based on Specifications of Maximum Sensitivity and Stability Margins", *IECR Journal - submitted*, (2005).

### Conference:

- [1] K. K. Tan, S. Huang and R. Ferdous, "Robust Self-tuning PID Controller for Nonlinear Systems", *Industrial Electronic Society, IECON'01, The 27th Annual Conference of the*

*IEEE* (1), 758-763 (2001).

[2] K. K. Tan, R. Ferdous and S. Huang, "Closed-loop Automatic Tuning of PID Controller for Nonlinear Systems", *Proceedings of Asian Control Conference, ASCC2002*, 25-27 September'2002, Singapore, (2002).

[3] K. K. Tan, S. Huang, R. Ferdous and T. S. Giam, "Nonlinear PID for process control applications", Proc. of International Symposium on Design, Operation and Control of Chemical Plants, *PSEA Asia 2002, Taipei, Taiwan, (2002)*.

[4] Tong Heng Lee, Kok Kiong Tan and Raihana Ferdous, "Intelligent PI Control Design for Maximum Sensitivity and Stability Margins", *ISIC 2004, Taipei, Taiwan, (2004)*.

**Book Chapter:**

[1] Tan, K K, T H Lee and R Ferdous, "Automatic PID controller tuning - the non-parametric approach", *PID Control - New Identification and Design Methods*, edited by M.A. Johnson and M.H.Moradi, pp.147-182. London: Springer Verlag, Publication\_no : 0209529, (2005).

[2] K. K. Tan and R. Ferdous, "Pressure Sensors", *Industrial Sensors, Vol 2*, submitted. (2004).